Dimerization of the prion protein studied by site specific mutagenesis to *p*-benzoyl-L-phenylalanine

Ph.D. Thesis

Sudheer Babu Sangeetham

Supervisors:

Dr. Ervin Welker

Dr. Elfrieda Fodor

Faculty of Medicine

Doctoral School of Multidisciplinary Medical Sciences

University of Szeged

Institute of Biochemistry

Biological Research Centre

Szeged

2021

Table of Contents

LIST OF PUBLICATIONS AND CONFERENCE ABSTRACTS

Publications related to Ph.D. thesis:

I. **Sangeetham, S. B.**, Huszár, K., Bencsura, P., Nyeste, A., Hunyadi-Gulyás, É., Fodor, E., Welker, E. (2018). Interrogating the dimerization interface of the prion protein via site-specific mutations to *p*-benzoyl-L-phenylalanine. *J. Mol. Biol.*, 430, 17, pp. 2784-2801.

II. **Sangeetham, S. B.**, Engelke, A, D., Fodor, E., Krausz, S. L., Tatzelt, J., Welker, E. (2021). The G127V variant of the prion protein interferes with dimer formation *in vitro* but not *in cellulo. Sci. Rep.,* 11, 3116.

Conference abstracts:

I. **Sangeetham, S. B.**, Huszár, K., Bencsura, P., Nyeste, A., Hunyadi-Gulyás, É., Fodor, E., Welker, E. Prion protein variants containing genetically coded, site-specifically incorporated *p*-benzoyl-L-phenylalanine; interrogating the dimerization interface of an alpha helical mPrP dimer, (2017, Edinburgh, Scotland).

II. **Sangeetham, S. B.**, Huszár, K., Bencsura, P., Nyeste, A., Fodor, E., Welker, E. Dimerization of the recombinant mouse prion protein: site-specific crosslinking of dimers *in vitro*, (2016, Gothenburg, Sweden).

III. **Sangeetham, S. B.**, Huszár, K., Bencsura, P., Fodor, E., Welker, E. Mapping the dimerization interface of the prion protein *in vitro* by site specific photocrosslinking, (2015, Szeged, Hungary).

IV. **Sangeetham, S. B.**, Huszár, K., Bencsura, P., Fodor, E., Welker, E. Mapping the dimerization interface of the prion protein *in vitro* by site specific crosslinking, (2015, Timisoara, Romania).

ACKNOWLEDGEMENTS

This thesis would not have been possible without the support of many people in many aspects, notably those at the Institute of Biochemistry, Biological Research Centre, Szeged, Hungary.

I am forever grateful to Dr. Ervin Welker, my supervisor who introduced me to the subject of conformational diseases and prion research. His constant patience, guidance and efforts were essential throughout my Ph.D. work. He went beyond the call of a thesis advisor and made an effort to not only explain the concepts of the different aspects of that thesis, but also create a stimulating atmosphere and give interesting feedback and invaluable discussions.

I would like to convey my heartfelt gratitude and sincere appreciation to my supervisor, Dr. Elfrieda Fodor for her timely support, significant discussions, suggestions and guidance during the doctoral period. Without her help and orientation, this thesis would not have been possible. In addition, her extensive advice helped develop my experimental skills and our lab discussions on the projects broadened my knowledge and made my work easier. During the study, her extraordinary care and assistance led me to complete this thesis.

I would also like to express my deepest gratitude to my colleagues, Krisztina Huszár, Petra Bencsura, Antal Nyeste and Sarah Laura Krausz for preparing the plasmids during these studies. Special thanks to Erika Zukic, Mária Ádámné Meszlényi and Gergely Fenyvesi for the technical assistance. I want to thank the former lab members of the conformational diseases research group, Dr. Pradeepkumar Reddy Cingaram and Andrea Papdiné-Morovicz for their support during my doctoral studies. I would like to extend my thanks to Dr. Zoltán Asztalos, Lenke Asztalos, Dr. Tamás Szlanka, Dr. Eszter Erika Virágh and all members of the laboratory of conformational diseases for their help.

I want to express my appreciation to Anna D. Engelke and Prof. Jörg Tatzelt from Department Biochemistry of Neurodegenerative Diseases, Institute of Biochemistry and Pathobiochemistry, Ruhr University Bochum, Bochum, Germany for collaborative research during my studies.

I would like to thank the Laboratory of proteomics research at the Biological Research Centre, Szeged, specially Dr. Éva Hunyadi-Gulyás, for their help in validating the proteins by MALDI-TOF mass spectrometry.

I would like to convey special thanks to Dr. Győző Garab and Dr. Ottó Zsiros for their help with carrying out the CD-spectrometry analysis of the protein samples during my Ph.D. timeline.

I am also grateful to the administrative staff, Olga Miklós, Katalin Bozóné Tóth, Dr. Mónika Bali, Tímea Varga and Anita Kiss for their aid during my studies.

I would like to thank my International training course program and Ph.D. friends, Dr. Jayapalreddy Mallareddy, Dr. Badri Aekbote, Dr. Mary Prathiba Joseph, Dr. Vamsikrishna Gali, Dr. Yathish J. Achar, Sai Divya Kanna, Sandeesha Kodru, Surya Regis, Dr. Sasha Vaz, Dr. Ashutosh Sharma, Dr. Sangita Giri, Dr. Phani Babu, Raghu Ram, Jyothi Jampana and Anna Pelka for their tremendous care and precious support during the studies.

I am also grateful to my family members, Sowjanya, Suresh, Sanjay, Rishi Koduru, Suvarna, Kirthi Kirit and Krissi Donato Dondapati for their great support during my studies. The achievement of this thesis could not have been happened without the consistent support, motivation and incredible care of my parents, Sulochanamma, Subrahmanyam Sangeetham and in-laws, Vijaya Kumari and Chandra Shekar Dondapati. I particularly want to thank a loving and supportive spouse, Divya Teja Dondapati for her daily scientific encouragement and prayers that culminated in the completion of my doctoral thesis and lastly to my beloved son Saadhik Nirvaantej Sangeetham, who provided new hope and joy to complete this thesis.

ABBREVIATIONS IN ALPHABETICAL ORDER

aa.: amino acid

BSE: bovine spongiform encephalopathy

CJD: Creutzfeldt-Jacob disease

CNS: central nervous system

CWD: chronic wasting disease

DTT: dithiothreitol

Dpl: Doppel protein

FFI: fatal familial insomnia

GPI: glycosylphosphatidylinositol

GSS: Gerstmann–Sträussler–Scheinker syndrome

HD: hydrophobic domain

mPrP: mouse prion protein

mPrP-mCh: mouse prion protein in fusion with mCherry

ncAAs: noncanonical amino acids

NEM: N-ethyl maleimide

*p*Bpa: p-benzoyl-L-phenylalanine

PrP: prion protein

PrP^{C}: cellular isoform of PrP

PrP^{Sc}: abnormal, scrapie isoform of PrP

Sho: Shadoo protein

TSE: transmissible spongiform encephalopathy

SUMMARY OF THE THESIS

Transmissible spongiform encephalopathies (TSEs) or prion diseases, are a group of devastating neurological diseases of humans and animals caused by the conformational conversion of the normal cellular prion protein (PrP^{C}) into an abnormal misfolded pathological form (PrP^{Sc}). Despite several investigations, the exact structure of PrP^{Sc} or of the intermediate forms and the mechanism leading to its formation, are not yet known. Formation of a dimeric PrP may be a crucial step and may play a key role in the conformational transition of PrP^{C} to PrP^{Sc}.

Kuru is one of the human TSEs, which originated as a result of cannibalistic rituals and became an epidemic in the Fore tribe of Papua New Guinea at the middle of the twentieth century. Studies found that a group of the tribe presented resistance to kuru. Subsequent genomic analysis studies reported that these individuals possessed a mutation encoding the novel prion protein variant, G127V, which appeared to provide strong protection against the disease in the heterozygous state and on an M129 allele background. Transgenic mice studies validated the protective effect of the newly found mutation, G126V (correspondent of the human G127V), moreover, in mice PrP(G126V) confers complete resistance to all kinds of prion_diseases when in homozygous state. Recently, NMR and molecular dynamics studies indicated that the mutation G127V weakens the main-chain H-bond interactions and prevents the formation of dimers and stable fibrils of PrP. However, this has not yet been confirmed in more native conditions for the protein and it is not known whether this is the mechanism also *in vivo* or not?.

As major aims in the presented studies, firstly, we set forward to investigate and identify the amino acid (aa.) positions present in the dimerization interface of the full length recombinant mouse prion protein (mPrP) by using site specific crosslinking with a genetically incorporated photoreactive amino acid, p-benzoyl-L-phenylalanine (*p*Bpa). Secondly, our aim was to test the effect of G126V mutation on the dimer formation ability of mPrP experimentally, by using two different approaches. One is in an *in vitro* system employing recombinant mPrP proteins containing *p*Bpa or G126V mutations in the sequence of prion protein, and untagged or C-terminally tagged by an mCherry, and using covalent crosslinking of the dimers by UV irradiation. Second is a mammalian cell culture based approach that follows the formation of prion dimers through expression of cysteine prion mutants, which are able to form intermolecular disulfide bonds.

The most important results obtained during these studies are as follows.

We created a set of 44 DNA constructs encoding wild type-, *p*Bpa- and G126V-mutant variants of mPrP with and without an mCherry fusion tag, and expressed and purified the recombinant proteins using BL21(DE3) *Escherichia coli (E. coli)* bacteria for expression, followed by purification using Ni-NTA chromatography. Testing selected proteins, MALDI-TOF mass spectrometry analysis confirmed that the *p*Bpa is correctly incorporated at the desired positionin in at least of ~90% of protein molecules expressed. Urea gradient assay revealed that conformational stabilities of wild type and of *p*Bpa mutant PrP-s are similar in case of both untagged and tagged proteins, indicating that the presence of *p*Bpa did not disturb the protein's stabilities.

We utilized the set of proteins created and the method established to investigate the dimerization interface of mPrP. Analysis of the photocrosslinked proteins in conditions favoring dimerization of PrP, indicate that *p*Bpa-s at few positions that are part of the hydrophobic domain- and also few from N-terminal domain of PrP, yield significant amounts of crosslinked dimers.The far-UV CD spectra of the wild type and *p*Bpa-variant monomers and of the crosslinked dimers of untagged mPrPs confirmed that upon dimer formation only slight variations in the secondary structural elements of the proteins occur, and that the predominantly helical structure of mPrP is preserved during dimerization. Taken together, we demonstrate here that beside the hydrophobic domain the N-terminal part of the prion protein, specifically the regions around position 127 and 107, is also integral part of the dimerization interface of the full length mPrP, and that the formed dimers are alpha helical.

By applying the same method and selected *p*Bpa-variants (at aa. positions 127, 128 and 131) and/or G126V mutant variants of mPrP (untagged and mCherry tagged), we studied the effect of the disease-protective mutation G127V (HuPrP), (corresponding to G126V in mPrP sequence), upon the dimerization ability of mPrP. By crosslinking studies, we found that wild type G126 mPrPs, are able to form both hetero- and homodimers when detected by *p*Bpas at either 127^{th} or 131^{th} positions. However, when the G126V mutation is present in the sequence of mPrP, both hetero- and homodimerization significantly diminish. To test whether a similar diminishing effect can also be observed in a more natural environment, we used transiently transfected HeLa cells to express mPrP constructs corresponding to wild type sequence with G126 and/or the G126V, mutation referred to as the G127V-mutant, for cell culture studies. We employed protein constructs containing a serine or cysteine at aa. 132 to enable detecting dimers through disulphide bond formation and applied also fusion tags (hemagglutinin (HA) and V5) for native co-immunoprecipitation and/or identification by

Western blotting. These experiments revealed that the G127V mutant variant could form homodimers and also heterodimers with the wild type counterpart PrP, and showed that the mutation did not have an effect on the interaction. Taken together, we demonstrated that the disease protective valine mutation exerts a diminishing effect on prion dimerization *in vitro*, which is consistent with NMR and molecular dynamics studies, however, this effect is not apparent *in cellulo*, indicating that the disease protection mechanism *in vivo* may be more complex than perturbing the dimer formation propensity of the protein.

Overall, our results also demonstrate that the mutant prion variants developed here are suitable to gain site-specific insights into the dimerization process of prion and indicate that these proteins may also facilitate to gain structural insights into oligomeric and fibrillar prion protein species formation, including the pathological variants of prion, and also could be used for identification of true binding partners of PrP.

ÖSSZEFOGLALÁS

A fertőző szivacsos agysorvadás (angolul, Transmissible Spongiform Encephalopathy, TSE) betegségei, másnéven prionbetegségek, az ember- és állatokban egyaránt előforduló, halálos kimenetelű idegrendszeri betegségek azon csoportja, melyeket a sejtekben természetesen előforduló prion fehérje (PrP^{C}) egy kóros konformációs állapotba (PrP^{Sc}) való átalakulása eredményez. Számos vizsgálat ellenére a PrP^{Sc} állapot kialakulási mechanizmusa és a folyamat során keletkező átmeneti fehérjekonformációs állapotok napjainkban még ismeretlenek. A prion fehérje dimer állapotának képződése kulcsfontosságú lépés lehet, és döntő szerepet játszhat a PrP^{C}, PrP^{Sc}-vé való konformációs átmenetében.

A humán prion betegségek egyik formája a kuru, amely a Pápua Új-Guineában élő fore törzsben kannibalizmus nyomán alakult ki, majd vált járvánnyá a huszadik század közepére. Későbbi vizsgálatok felfedték, hogy a törzs egy csoportja rezisztenciát szerzett a kuru betegséggel szemben. Genetikai elemzések később kimutatták, hogy a rezisztens egyének egy mutációval és így egy új prionfehérje-variánssal, a G127V-mutánssal rendelkeznek, amely heterozigóta állapotban és M129 allélú háttéren erős védelmet nyújt a betegséggel szemben. Transzgenikus egérvizsgálatok validálták az újonnan talált mutáció, G126V (az emberi G127V megfelelője egérben) protektív hatását, ráadásul, az egerek esetében, homozigóta állapotban is teljes ellenállást biztosított minden fajta prionbetegséggel szemben. A közelmúltban mag mágneses rezonancia (NMR) és molekuladinamikai (MD) vizsgálatok azt mutatták, hogy a G127V mutáció jelenléte gyengíti a polipeptid lánc által létrehozott hidrogén-kötéseket, és megakadályozza PrP dimerek és stabil fibrillumok képződését. Azonban, natív körülményekhez közelebb álló feltételek mellett, oldatban, ezt kísérletesen eddig nem igazolták. Valamint, arra vonatkozólag sem állnak adatok a rendelkezésünkre, hogy vajon ez-e a protektív hatás kifejtésének mechanizmusa *in vivo* körülmények között?.

A jelen tanulmány egyik fő célkitűzése, a teljes szekvenciahosszúságú rekombináns egér prionfehérje (mPrP) dimerizációs felszínében résztvevő aminosavak feltérképezésére irányul. Ezt egy olyan módszer felhasználásával terveztük megvalósítani, amelyben genetikailag helyspecifikusan építünk egy fotoreaktív aminosavat, *p*-benzoil-L-fenilalanint (*p*Bpa), a prion fehérje szekvenciájába, majd UV-fény alkalmazásával, keresztkötjük a segítségével az esetleges kölcsönhatásban résztvevő fehérje felületeket. A másik fő célkitűzésünk az volt, hogy kísérletileg teszteljük a G126V mutáció hatását az mPrP dimerképző képességére. Ezt két különböző megközelítés alkalmazásával céloztuk

megvizsgálni. Elsőként, *in vitro* rendszerben, amelyben *p*Bpa- és G126V mutációkat tartalmazó rekombináns mPrP fehérjéket önmagukban vagy fúziós fehérjeként C-terminálison egy mCherry fehérjével alkalmaztunk, és a hetero- valmaint homodimerek képződését vizsgáltuk UV besugárzás hatására képződött keresztkötés segítségével. Másodszor, egy emlős sejtkultúra modellrendszert alkalmaztunk, amelyben a prion dimerek képződését cisztein prion mutánsok tranziens expresszióján keresztül vizsgáltuk, amelyek képesek intermolekuláris diszulfidkötések létrehozására.

Főbb eredményeink közé tartoznak az alábbiak.

Létrehoztunk egy 44 DNS konstrukcióból álló fehérje-expressziós plazmid sorozatot melyek az mPrP vad típusú-, *p*Bpa beépítésére alkalmas- és G126V-mutáns variánsait kódolják, önmagukban vagy C-terminálison mCherry fúziós fehérjével ellátva. A kódolt fehérjéket BL21 (DE3) *Escherichia coli (E. coli)* törzsben sikeresen expresszáltuk, majd Ni-affinitás kromatográfiával tisztítottuk. Kiválasztott fehérjéken végzett MALDI-TOF tömegspektrometriás elemzés során igazoltuk, hogy a *p*Bpa az expresszált fehérje populáció legalább ~ 90% -ában helyesen, a kívánt pozícióba épült be. Urea-gradiens elemzéssel kimutattuk, hogy a vad típusú és a *p*Bpa-mutáns PrP-k konformációs stabilitása hasonló, azaz, a *p*Bpa jelenléte nem befolyásolta azt.

A létrehozott fehérjerendszert alkalmaztuk a fehérje dimerizációs felületének feltérképezésére: a különböző pozícióba épített *p*Bpa-t tartalmazó prion fehérjék keresztkötése során, a PrP dimerizációját elősegítő körülmények között, azt tapasztaltuk, hogy jelentős mennyiségű dimer mutatható ki akkor amikor a fotoreaktív aminosav a prion hidrofób doménjének részét képezi, valamint, amikor az N-terminális flexibilis doménje bizonyos pozícióiban van jelen. A fúziós fehérje nélküli mPrP *p*Bpa-variánsainak monomer- és keresztkötött dimer- állapotaiban felvett távoli-UV cirkuláris dikroikus (CD) spektruma megerősítette, hogy a fehérjék másodlagos szerkezeti elemeiben nincs jelentős eltérés, és hogy az mPrP helikális szerkezete megmaradt a dimerizáció során. Összefoglalva, módszerünkkel, tehát, kimutattuk, hogy a teljes hosszúságú prionfehérje hidrofób régiója és N-terminális doménje, elsősorban a 127- és 107-es pozíciók körüli régiók, az mPrP dimerizációs felületének szerves részét képezik, és hogy a képződött dimerek a-helikálisak.

A protektív mutáció (G126V) fehérje-dimerizációra gyakorolt hatásának vizsgálatát, *in vitro* megközelítéssel, szintén helyspecifikusan (a 127-, 128- vagy a 131-es pozíciókban) beépített *p*Bpa-mutánsokkal és az egér mPrP variánsok (*p*Bpa- és/vagy G126V és/vagy mCherry fúziós prion fehérje mutánsok) kombinációinak keresztkötése segítségével végeztük. Kísérleteinkben azt tapasztaltuk, hogy a vad típusú G126 aminosavval rendelkező mPrP-k

képesek hetero- és homodimereket alkotni. Azonban, amikor a G126V mutáció jelen van az mPrP szekvenciájában, a fehérje hetero- és homodimerizációja egyaránt jelentősen lecsökken. Sejtkultúrás környezetben való vizsgálatra, tranziensen transzfektált HeLa-sejteket használtunk melyek a vad típusnak megfelelő G126 és a G126V mutáns (továbbiakban, a „G127V protektív-mutáns" -ként hivatozva a sejtes kísérletekben) egér prion fehérjéket expresszálták, Cys 132 pontmutációval a dimerizáció diszulfid hidon keresztüli detektálásához, valamint, különböző fúziós toldalékokkal ellátva immunoprecipitációhoz. A ko-immunprecipitációs kísérletek azt mutatták, hogy a G127V-mutáns képes homodimerként- és heterodimerként is, vad típusú megfelelőjével, diszulfid kötést létrehozni, valamint, hogy a mutáció nem befolyásolja a kölcsönhatást. Összegezve, így kimutattuk, hogy a betegségtől-védő valin-mutáció ugyan csökkenti a prion fehérje dimerizációs képességét *in vitro* körülmények között, ami összhangban van az NMR és a molekuladinamikai vizsgálatokkal, azonban, ez a hatás nem mutatható ki *in cellulo* körülmények között. Ez azt jelzi, hogy a betegséggel szembeni védő hatás mechanizmusa, *in vivo*, összetettebb lehet, a pusztán fehérje dimer képző képességének csökkentésénél.

Eredményeink igazolják továbbá azt is, hogy az itt kifejlesztett *p*Bpa-mutáns prion fehérje-készlet és módszer alkalmas a prion fehérje dimerizációs felszínének részletes, helyspecifikus tesztelésére. Mindez jelezi, hogy az itt kifejlesztett rendszer szintén alkalmassá válhat és jelentősen megkönnyítheti az oligomer- és fibrilláris- prionfehérje-struktúrák vizsgálatát is, beleértve a patológiás prion forma kialakulását. E mellett, elősegítheti a PrP egyéb fehérjékkel történő kölcsönhatásának a részletes vizsgálatát is.

1. INTRODUCTION

1.1. Prion diseases

Prion diseases, also known as transmissible spongiform encephalopathies (TSEs), are a group of rare, progressive and inevitably fatal neurodegenerative disorders that affect both humans and animals. They include, Creutzfeldt-Jacob disease (CJD), Gerstmann–Straussler–Scheinker disease (GSS), fatal familial insomnia (FFI) and kuru in humans, scrapie in sheep, bovine spongiform encephalopathy (BSE) or mad cow disease in cattle, chronic wasting disease (CWD) in mule deer and elk, transmissible mink encephalopathy (TME) [1–3] and others, as summarized in Table 1 [4]. TSEs are classified into three categories based on their etiology: sporadic, hereditary, and acquired. Approximately 85–90% of CJD cases are sporadic, affecting 1–2 people per million per year [5], 15% of Familial CJD (fCJD), GSS and FFI are hereditary diseases associated with specific mutations of the PrP gene [3], and 2-5% are being acquired through transmission of infectious prion, such as in the case of kuru, iatrogenic CJD (iCJD) and variant CJD (vCJD) [6]. The pathogenesis of these diseases is caused by the conformational conversion of the normal, host-encoded prion protein (PrP^{C}) to an altered state [1] in which it becomes infectious and forms the so called scrapie (Sc) prion (PrP^{Sc}) – termed based on analogy to scrapie of sheep, the prototypic prion disease.

Table 1. Various types of TSEs among host species and the mechanism of pathogenesis are described* [4]**.**

Disease	Host	Mechanism of Pathogenesis
kuru	Fore people	Infection through ritualistic cannibalism
iCJD	Humans	Infection from prion-contaminated HGH, dura mater grafts, etc.
vCJD	Humans	Infection from bovine prions
fCJD	Humans	Germline mutations in PrP gene
GSS	Humans	Germline mutations in PrP gene
FFI	Humans	Germline mutation in PrP gene (D178N, M129)
sCJD	Humans	Somatic mutation or spontaneous conversion of PrP^{C} into PrP^{Sc}?
FSI	Humans	Somatic mutation or spontaneous conversion of PrP^{C} into PrP^{Sc}?

Scrapie	Sheep	Infection in genetically susceptible sheep
BSE	Cattle	Infection with prion-contaminated MBM
TME	Mink	Infection with prions from sheep or cattle
CWD	Mule deer, elk	Unknown
FSE	Cats	Infection with prion-contaminated beef
Exotic ungulate encephalopathy	Greater kudu, nyala, oryx	Infection with prion-contaminated MBM

*Abbreviations: FSE, feline spongiform encephalopathy; FSI, fatal sporadic insomnia; HGH, human growth hormone; MBM, meat and bone meal.

According to the 'protein-only' hypothesis [7], TSEs are caused solely by the abnormal form of the prion protein and lacking the presence of nucleic acid. Misfolded prion is the major constituent of the infective material, PrP^{Sc}, and it is capable of forming amyloid plaques in the diseased brain. The accumulation of misfolded protein deposits in prion disease affected individuals leads to phenotypic characteristics, such as, dementia, ataxia (usually gait), extrapyramidal features, myoclonus, astrogliosis and spongiform neurodegeneration [3]. The brain images of healthy and CJD affected individuals are presented on Figure 1, showing the typical spongiform lesions associated to prion disease. TSEs are currently not treatable, they usually possess lengthy incubation periods ranging from months to decades, which eventually lead to death of the affected host [8].

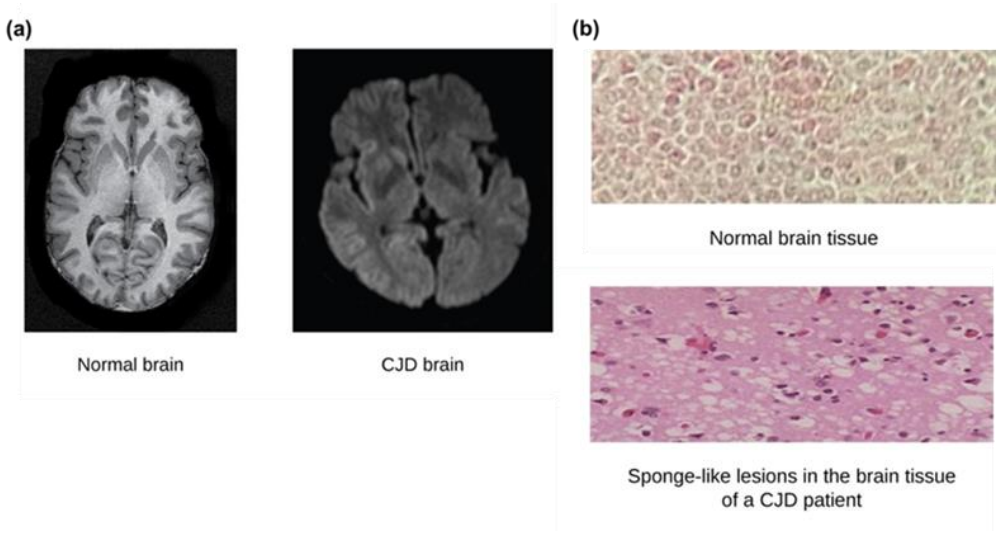

Figure 1. Comparison between healthy and CJD brains. (a) The brain scans contrast the images of a healthy brain with a brain affected by CJD. **(b)** When compared to a normal

brain, the brain tissue of a CJD patient is full of sponge-like lesions caused by abnormal prion protein formation, (Source: https://opentextbc.ca/microbiologyopenstax/chapter/viroids-virusoids-and-prions/#return-footnote-62-1).

In addition to TSEs, there are other neurodegenerative diseases caused by protein aggregation that lead to degradation of normal tissue topology in affected hosts. Alzhemier's disease is the most common such neurodegenerative disease, which is associated with the accumulation of β-amyloid peptide (Aβ) plaques, as a result of the cleavage of the β-amyloid precursor protein [9]. Parkinson's disease is another type of neurodegenerative disorder linked to the formation of Lewy bodies produced by α-synuclein [10]. Huntington's disease is a rare inherited neurodegenerative disease caused by a mutation in the huntingtin gene, which results in the formation of multiple recurrences of the triplet nucleotide CAG, that eventually leads to the formation of huntingtin protein deposits [11]. The major difference between TSEsand other neurodegenerative diseases is that they can be transmitted from one host to another, while for the other diseases this had not been observed so far.

1.2. The cellular prion protein and its structure

The cellular prion protein (PrP^C) is primarily expressed in the central nervous system, particularly in the synaptic regions of the neurons, and although at lower levels, it is also present in extraneuronal tissues, including lymphoid cells, lungs, heart, kidneys, gastrointestinal tract, muscle and mammary glands [12]. The protein is a sialoglycoprotein that is attached to the outer leaflet of the plasma membrane of cells by a glycosylphosphatidylinositol (GPI) anchor, which usually localizes proteins to lipid rafts, [13]. Accordingly, PrP^C is synthesized as a precursor protein (pre-pro-PrP), containing 253 amino acids (human numbering) with a signal peptide at the N-terminus (aa. 1-22) and a GPI anchor peptide signaling sequence (GPI-PSS) at the C-terminus (aa. 231-253). The signal peptide guides pre-pro-PrP to the endoplasmic reticulum, where it is cleaved and pro-PrP is formed. Pro-PrP is then transferred to the Golgi complex, where it is further processed by addition of N-linked glycans, removal of the GPI-PSS, and addition of the pre-assembled GPI anchor. Subsequently, the mature PrP^C consisting of 208 amino acids is translocated to the outer membrane leaflet of the cells. However, not all PrP^Cs are found on the cell surface, but they are continuously internalized and transported back through endosome recycling. PrP^Cs are also found in the Golgi complex, nucleus and mitochondria as a result of this recycling process [14]. The protein's primary structure is highly conserved among mammals. The major

regions and elments of the sequence (Figure 2a) [15], are as follows. Proceeding the signal sequence there is a short positively charged N-terminal patch, which plays role in various functions of PrP. This is followed by five glycine-rich octarepeat segments with the sequence PHGGGWGQ, forming together the so called octarepeat region (OR) of the protein, which posesses affinity to several divalent cations, such as copper, zinc, nickel, iron and manganese and is highly conserved from fish to mammals [16]. The next highly conserved region of the sequence is the hydrophobic domain (HD), through which several of PrP interactions with other protiens occur. The HD is situated at about the middle of the sequence and marks the transition between the two major domains, the N-terminal and the C-terminal domain of the PrP.

The three dimensional structure of recombinant PrP, as determined by nuclear magnetic resonance (NMR) spectroscopy shows that the N-terminal domain (aa. residues 23–124) posesses a disordered, flexible structure, while the C-terminal domain (aa. residues 125–231) is globular, as it is depicted on Figure 2b [17], and contains three α-helices [between aa. residues 144–154 (α1), 175–194 (α2) and 200–226 (α3)] and two β-strands [between aa. residues 128–131 (β1) and 161–164 (β2)] [18–20]. The C-terminal domain also possesses one intramolecular disulfide-bridge, which enhances protein stability, and two N-glycolisation sites [21].

The precise physiological function of PrP^C is difficult to determine because in various animals, the PrP-encoding gene knockout (*PRNP*$^{0/0}$) did not result in significant developmental phenotype changes [22–24]. However, PrP^C participates in several physiological functions in cells, such as stress protection, cellular differentiation, neuronal excitability, myelin maintenance, regulation of circidian rhythm, metal ion homeostasis, mitochondrial homeostasis, amyloid-β peptide and tau regulation, and immune system modulation, exerting its effects either directly or through interacting with different protein partners [14].

The mammalian PrP gene family consists of three genes: prion protein gene *(Prnp)*, which encodes PrP^C, prion protein doppel gene *(Prnd)*, which encodes Doppel (Dpl), and shadoo of prion protein gene *(Sprn)*, which encodes the Shadoo (Sho) protein. All three proteins are GPI-anchored and while structurally Dpl resembles the C-terminal glogular domain, and Sho the N-terminal unstructured domain of PrP, the two proteins have very little sequence homology to PrP.

Dpl consists of a short, unstructured N-terminal tail and a globular C-terminal domain similarly to C-terminal domain of PrP, composed of three α-helices and two β-sheets, contains

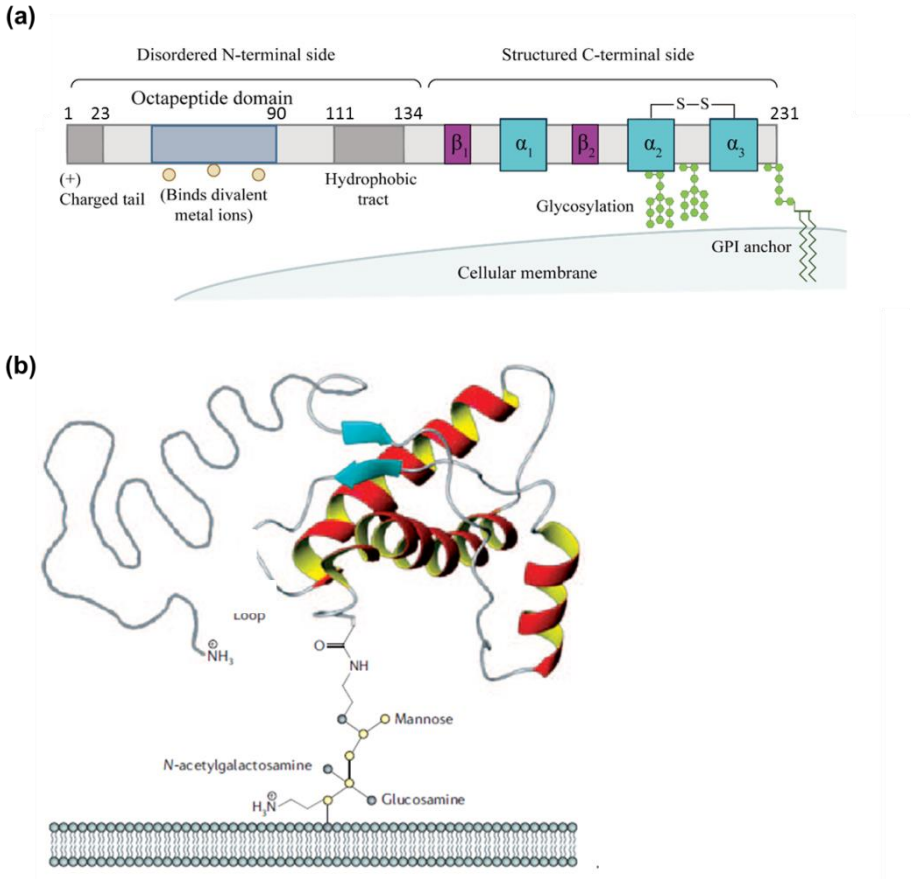

Figure 2. Structural features of the cellular prion protein. (a) A schematic representation of the primary structure of the nascent PrP^C with the most important regions and attributes marked, as follows. A secretory signal peptide at the extreme N-terminal end (aa. 1-23), followed by a short, positively charged segment, the octapeptide domain, which allows PrP^C to bind divalent metal ions, and a hydrophobic tract that is highly conserved from fish to humans. Following is the C-terminal domain of PrP, consisting of the three α-helices and two short β-strands. It is also the site of the post-translational modifications of PrP^C: up to two N-glycans are added within the α-helical domain, a single disulfide bridge links helices 2 and 3, and a GPI anchor addition occurs, as a response to a signal peptide at the C-terminus, before PrP^C is transported to the outer surface of the plasma membrane [15]. **(b)** Schematic visualization of the tertiary structure of the protein. NMR spectroscopy revealed that PrP^C consists of an unstructured N-terminal and ordered C-terminal domain, this structure is depicted as connected to a GPI-anchor, which in turn it is embedded into a lipid bilayer [17].

two (instead of one as for PrP) disulphide bonds, and two N-glycosylation sites. Dpl expression is highest in the testis, where it is mainly involved in the male reproductive functions and its mRNA has also been found in the spleen, bone marrow, skeletal muscles, and heart [25]. Doppel is not expressed in the CNS, so it is unlikely to play a role in TSE pathogenesis [26].

Contrary to Dpl, Sho is found highly expressed in brain tissues and CNS, where PrP is most prevalent [27]. Sho protein exhibits some features that resemble similarities to the PrP^C's N-terminal domain, although it lacks sequence homology to PrP^C. These include:

being intrisically unstructured, having a highly conserved N-terminal signal sequence, and also a highly conserved HD (which is the only portion showing some sequence homology to PrP). In between the two segments, Sho lacks PrP's copper binding octarepeat domain, instead it contains an Arg-rich tetrarepeat segment, typical of nucleic acid binding domains. The C-terminal region of Sho also possesses one (instead of two for PrP) N-glycosylation site and a GPI anchor signal peptide.

Sho had been reported to have also some functional similarities to wild type PrP. Sho, like WT-PrP, protects cells from glutamate-induced excitotoxicity [28] and prevents neuronal cell death [29] in cell cultures, emphasizing that Sho and PrP^{C} may act on similar signaling pathways. Studies on the brains of prion-infected mice and on infected neuroblastoma cells, revealed that Sho protein levels profoundly declined, while PrP^{Sc} accumulated [30]. Taking these findings together, Sho seems to display some functional links with PrP and could be contributive to the process of prion biology and/or prion diseases, however, a direct link of Sho to PrP^{Sc} formation could not be demonstrated.

1.3. Conversion of the cellular prion protein to the scrapie-prion

Prion diseases are caused by the conversion of a monomeric, α-helical, protease-sensitive, native cellular prion protein, PrP^{C} to an oligomeric, ß-sheet rich, misfolded, pathogenic form, PrP^{Sc}, which is rapidly polymerized to form aggregates or fibrils and possess a protease resistant core [1]. The structural conformation of PrP^{Sc} varies from that of PrP^{C}, but not the amino acid sequence. According to the biophysical studies the secondary structure of PrP^{C} possesses an α-helical content of 42% and a ß-sheet content of 3%, whereas, PrP^{Sc} an α-helical content of 30% and a ß-sheet content of 43%, implying that conformational transition is a fundamental event of PrP^{Sc} formation [31]. In addition, the large unstructerd N-terminal domain of PrP^{C} conferes an inherently flexible structure to the protein that may render it to be prone to form PrP^{Sc} [32].

Currently, there are two different models for describing the mechanism of scrapie replication [33]: the template assistance model and the nucleated (seed) polymerization model. The template assistance model rarely occurs when PrP^{Sc} acts as pre-existing template and PrP^{Sc} is formed from PrP^{C}, i.e., $PrP^{C} + PrP^{Sc} \rightarrow PrP^{Sc} * PrP^{C} \rightarrow 2PrP^{Sc}$. The conformational transition is an autocatalytic mechanism that occurs when PrP^{C} interacts transiently with PrP^{Sc}, transforming PrP^{C} to PrP^{Sc} and forming a PrP^{Sc} homodimer, which then divides into

two PrP^{Sc} monomers. Thermodynamically PrP^{Sc} is considered to be more stable than PrP^{C} (Figure 3a) [33].

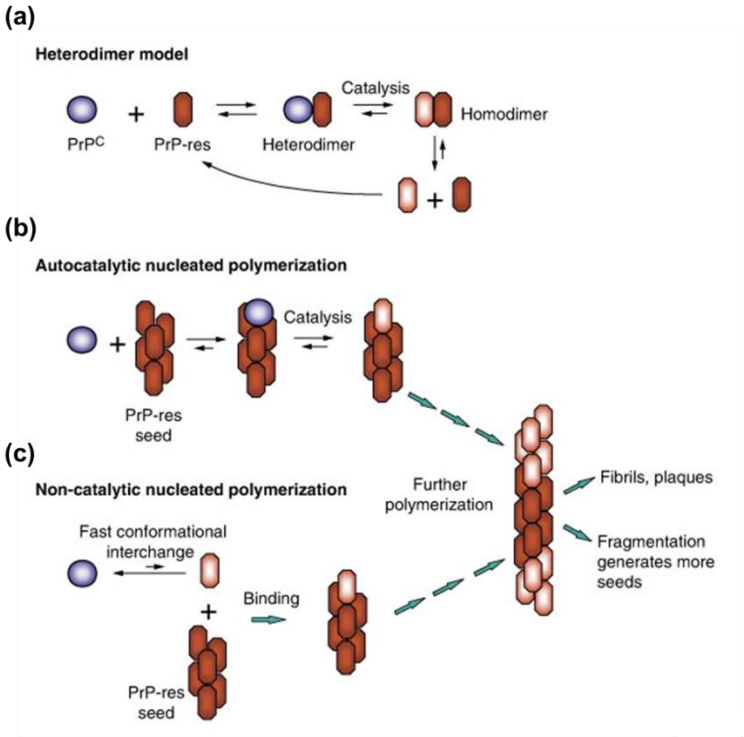

Figure 3. Presumed models for the formation of proteinase-k resistant (PrP-res) or PrP^{Sc} forms from PrP^{C}. The conformational conversion of PrP^{C} to PrP^{Sc} is presumed to be extremely rare in the template assisted **(a)** and autocatalytic nucleated polymerization **(b)** models unless catalyzed by contact with monomeric or polymeric PrP^{Sc}, respectively. The conformational interchange is relatively faster in the non-catalytic nucleated polymerization model **(c)**, but the PrP^{Sc} conformer is sparsely populated unless stabilized by binding to a preformed, stable PrP^{Sc} polymer. PrP^{Sc} that has newly formed is depicted in a lighter shade of red than the original [33].

In the nucleated polymerization model, oligomerization or polymerization of PrP is required to stabilize PrP^{Sc}, which is the most fundamental aspect of this model of prion propagation. This model consists of two subcategories, (i) autocatalytic nuleated polymerization, in which the initial formation of nuclei or seeds of PrP^{Sc} encompasses weaker monovalent interactions between PrP^{C} and/or PrP^{Sc} molecules. Subsequently, the oligomeric or polymeric seeds are stabilized through multivalent interactions (Figure 3b) [33]; (ii) non-catalytic nuleated polymerization, in which PrP^{C} rapidly interchanges between the high α-helix and high ß-sheet conformers, with the latter being poorly populated until stabilized by binding to a pre-existing polymeric seed of PrP-res (Figure 3c) [33]. The latter is based on the assumption that

intermolecular disulfide bonds link the prion polymer [34], implying that disulfide reorganization is necessary for PrP^{Sc} generation.

1.4. Dimerization of the prion protein

A PrP dimer may be one of the intermediate forms leading to the formation of oligomers and amyloid fibrils. Transgenic studies in mice demonstrated that propagation of prions involve the formation of a PrP^{C}/PrP^{Sc} heterodimer complexes and that this is an initial and critical step [35]. It was also proposed that under physiological conditions, PrP^{C} exists as a dimer that must dissociate before monomeric PrP^{C} can bind to and be converted by PrP^{Sc} [35,36]. In another study it has been proposed that PrP^{C} dimerization is mediated by its internal hydrophobic domain, which is required for dimerization and subsequent stress-induced signaling [37]. Prion replication involves the interaction of PrP^{C} and PrP^{Sc} where the formation the heterodimer (PrP^{C}-PrP^{Sc}) requires similar amino acid sequences between the two possibly reflecting also the natural tendency of PrP^{C} for homodimerization [35]. Subsequently, a low resolution model of the homodimer [38] and later of the heterodimer has been generated based on ß-stacking [39]. This model was further extended to explain prion propagation by assuming the addition of dimers through hairpin stacking [40]. Molecular simulation studies produced a simple low-resolution lattice model of prion protein folding, revealing that prion proteins are less stable in the monomeric state and are susceptible to the formation of alternative native states such as homodimers [41].

In addition to indirect evidence gathered from model systems and calculations, there is also substantial direct evidence for PrP dimerization under physiological conditions. A 54 kDa PrP^{C} dimer was identified in uninfected hamster and murine brains with antibodies raised against the hamster infectious PrP^{Sc}, indicating not only that dimers of PrP exists in natural conditions but also that they present similar epitopes to antibodies as the infectious form [42]. Despite vast studies, prion propagation and the mode of interaction of PrP^{C} to prP^{Sc} has not been elucidated yet. In 1995 an as-yet unidentified accessory protein was proposed to may be involved in linking the two forms of PrP [43,44]. A spontaneous monomer-dimer equillibrium of cellular PrP^{C} was found to exist in bovine brain homogenate by using various methods, but this was not present in case of recombinant bovine PrP, which presented only monomeric states [45]. This difference in behavior between native PrP^{C} and recombinant PrP was suggested to be the result of glycosylation of PrP^{C}. In contrast, recombinant PrP (aa. residues 90–231) of Syrian hamster forms dimers as detected by multidimensional heteronuclear NMR

studies [46]. A crystallographic study reported a structure for the human PrP (aa. 90-231), which consisted of a domain-swapped dimer configuration in which the disulfide bonds were rearranged [47]. Furthermore, a 60 kDa PrP dimer could be covalently crosslinked in case of hamster PrP expressed in murine neuroblastoma cells, which comprised characteristics of both the normal and disease associated forms of PrP [48]. The dimer was sensitive to proteinase-K and formed larger aggregates in presence of chaotropic agent, Gn-HCl, moreover, in a cell-free conversion system, it could be converted to a protease-resistant form resembling PrP^{Sc} [49]. This latter system is considered to be an appropriate *in vitro* model for generation of PrP^{Sc} from PrP^{C}. Since this dimer displayed both normal and disease-associated characteristics, indicated that a dimeric form might represent an intermediate state in prion formation. Protease-resistant PrP dimers were also found in the hamster brain following large-scale purification conditions [50]. Recent findings indicate that PrP^{C} monomers are the most important substrates for PrP^{Sc} propagation and that stabilizing PrP^{C} dimers may be a plausible way to inhibit infectious prion formation [51]. Despite numerous investigations, the mechanism of transition of PrP^{C} from monomeric to oligomeric forms and/or to infectious, PrP^{Sc} form is still elusive. The dimeric state of the cellular PrP^{C} could lie as an important intermediate form on the pathway of formation of PrP^{Sc} from PrP^{C}, however, the exact role played by PrP^{C} dimers in PrP^{Sc} formation is not yet clear.

1.5. The G127V variant of the prion protein confers resistance to kuru

The prion disease kuru emerged in the Fore linguistic group of the Eastern Highlands of Papua New Guinea as a result of ritualistic anthropophagy of mostly CNS-derived tissues of dead, and become the major cause of death in the region by 1950 [52]. Kuru primarily affected women and children and only 2% of adult men, as boys older than 7 years were exempt of mortuary feasts, and the disease was associated with long incubation periods of up to five decades [53]. Analysis of the *PRNP* gene from individuals who had been exposed to but did not contract kuru, revealed the presence of a novel mutation, G127V in heterozygous state, in association with the 129M allele of PrP, in homo- or heterozygous condition, resulted in an extension of incubation periods or complete protection against the kuru, respectively [54].

Further, transgenic mice experiments validated the protective effect of G127V, moreover in mice V127PrP in homozygous state, rendered mice intrinsically resistant to prion propagation, exhibiting protective effect against various types of prion infections, such as,

kuru, classical and variant CJDs [55]. The extensive study of aggregation kinetics explicit the differences between the wild type and G126V mPrP as the critical concentration is higher, the lag phase is longer and fibril growth is diminished for the new protective mutant variant [56]. Based on these findings, it is an intriguing question to investigate the molecular basis for this resistance. *In silico* studies revealed that HuPrP(G127V) not only prevents the dimer formation by reducing the main-chain H-bond interactions, but also is unfavourable for prion fibril formation due to resulting weaker interaction energies between fibril layers and reduced number of H-bonds [57]. Another study using solution-NMR and molecular dynamics (MD) simulations demonstrated considerable structural and dynamic differences between the wild type and mutant HuPrP (residues 91–231 with G127M129). While WT forms stable β-sheet with two strands (β1: Tyr128-Gly131; β2: Val161-Arg164) the G127V mutant forms a stretch-strand (SS) pattern with two segments (SS1: Tyr128-Gly131; SS2: Val161-Arg164) and a considerable conformational rearrangement of Tyr128, Gly131 and Tyr163 side chains, resulting to higher flexibility for this region and to altered α1- and α2-helices, which in turn give rise to a more packed structure for the three helices. MD simulations of this study suggested that HuPrP(G127V) prevents the formation of stable β-sheets and dimers, which together with the unique structural and dynamic features were inferred to potentially inhibit the conformational conversion of the G127V mutant [58]. However, whether such effects are also at play in more physiological conditions, and/or whether or not they form the key mechanism of the rescue effect of G127V mutation observed *in vivo*, remains to be elucidated.

1.6. Expanded genetic code and the utility of noncanonical amino acids in the determination of the protein-protein interactions, protein structure and function

The genetic code is made up of 64 triplet codons that specify 20 canonical amino acids and three stop codons called, ochre (TAA), opal (TGA), and amber (TAG). Selenocysteine and pyrrolysine are the 21st and 22nd amino acids, respectively, that are incorporated into proteins encoded by stop codons [59]. The methods for the engineering proteins possessing noncanonical amino acids (ncAAs) have advanced rapidly in the last few years. The expansion of the genetic code by utilization and incorporation of ncAAs into proteins in a site specific manner is a powerful tool for probing not only protein-protein interactions (PPIs), but also protein physical and chemical behavior and mechanistic questions in atomic detail. It allowed researchers to incorporate a wide range of structurally and functionally diverse ncAAs into

recombinant proteins with no or minimal structural pertubation, in order to investigate a wide range of protein structural and functional questions. Amber suppression is well established in *E. coli*, *Saccharomyces cerevisiae*, *Pichia pastoris* and mammalian cells [59]. For instance, suppression of the amber stop codon (TAG) is widely used to site-specifically incorporate ncAAs into proteins of interest. In this method, the endogenous codon of the target amino acid residue is replaced by a TAG stop codon. When the cellular biosynthetic machinery is supplemented with a complementary tRNA (CUA) and an orthogonal aminoacyl tRNA synthetase that recognizes both the tRNA (CUA) and the ncAA, the ribosome can decode the stop codon as a new sense codon and precisely incorporate the ncAA into a protein at the targeted position (Figure 4a) [60].

More than 230 ncAAs have been incorporated into proteins by *in vivo* or *in vitro* methods. In addition, bio-orthogonal ncAAs tagging with bicyclononynes and trans-cyclooctenes has also been reported to monitor the biological processes via protein imaging [61]. UV light has been used to convert aromatic azides, benzophenones, diazirines, and a wide range of other types of ncAAs into a short-lived reactive intermediate [62]. The most widely used photolabile moiety is p-benzoyl-L-phenylalanine (*p*Bpa) because of its reportedly high site specificity, reduced reactivity to water and light, photokinetics, and ease of incorporation into proteins during synthesis [63]. The structure of *p*Bpa is shown in Figure 4b. No laborious chemical synthesis is needed and the length of the polypeptide is not restricted. When irradiated with long-wavelength UV light, *p*Bpa can crosslink to aliphatic side chains of other amino acids. Alternatively, the activated chromophore can sequentially abstract two hydrogen atoms from nearby amino acids (Figure 4c).

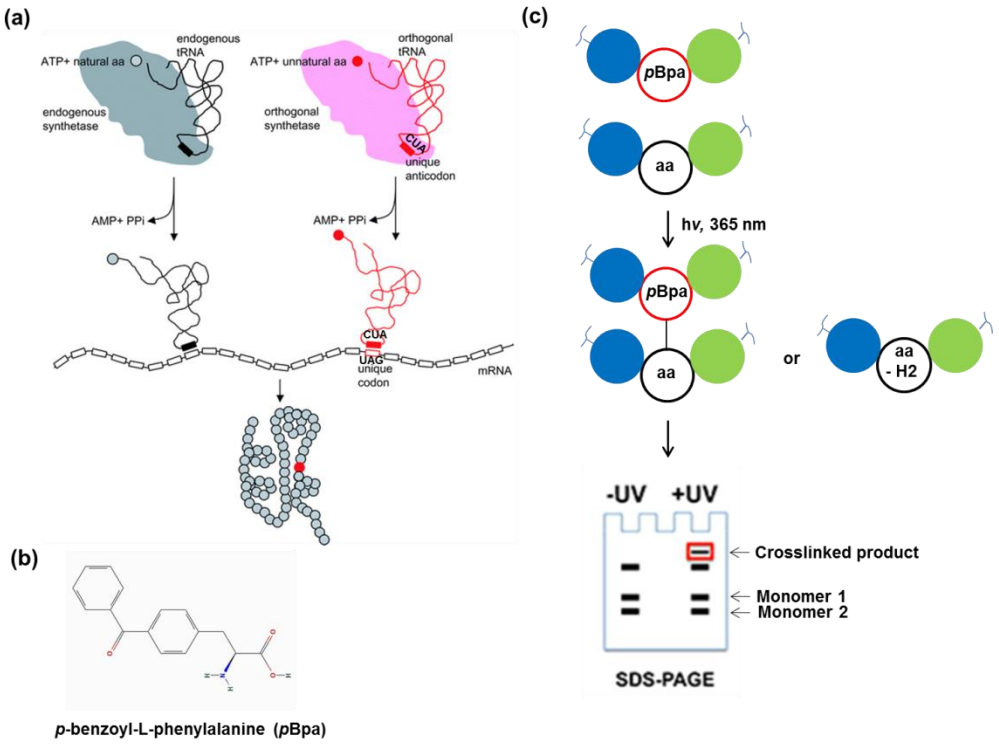

Figure 4. A general approach for the site-specific incorporation of unnatural amino acids into proteins *in vivo* and analyze the protein-protein interaction. (a) The formation of acylated orthogonal tRNA by orthogonal aminoacyl-tRNA synthetase incorporates the unnatural amino acid at the position specified by the amber codon UAG, which is introduced into the gene encoding the protein of interest to study [60]. **(b)** The chemical structure of ncAA, *p*Bpa and **(c)** depiction of protein of interest comprising the site specfic insertion of *p*Bpa that is photo activated by UV light (365 nm) can result in radical-mediated crosslinking to a nearby amino acid (aa.) within 3.1 Å distance or in hydrogen elimination (-H2) without formation of a crosslink [64]. When the protein harboring a *p*Bpa is exposed to UV light, transient dimer (hetero- or homodimer depending on the actual experiment) can be crosslinked and visualised on SDS-PA gel.

The knowledge of the prion protein's numerous protein-protein interactions (PPIs) or of its oligomeric self-interactions (homodimers or higher order oligomers) is still limited. Understanding these interactions in detail, will provide insights into both physiological and pathological events.

2. AIMS OF THE THESIS

The main goal of the thesis is to address current questions related to the dimerization of the prion protein, such as: "Which are the residues that participate in forming the dimerization interface?" and "What is the effect of a novel disease-protective mutation on

dimerization?", by employing an *in vitro* approach that allows studying the process at single amino acid level resolution along the sequence of the prion protein. In line with this goal, the specific aims set are as follows.

2.1. To interrogate the dimerization interface of full length recombinant mPrP by site specific incorporation of the crosslinkable amino acid *p*Bpa.

2.1.1. To develop an *in vitro* model system consisting of a set of purified, recombinant full length (aa. 23–230) mouse prion proteins (mPrPs) that bear genetically coded single-substitutions of selected residues to the photocrosslinkable amino acid, *p*Bpa, placed strategically at various positions along the sequence in order to allow testing of the sites involved in the formation of a dimer.

2.1.2. To test whether site specific insertion of *p*Bpa into the mPrP sequence occurred correctly and whether *p*Bpa insertion has any disruptive effect on the structure or conformational stabilities of the mPrP variants.

2.1.3. To use the system to study the sites involved in the homodimerization of mPrP, by evaluating the efficiency of homodimer formation of each *p*Bpa-mutant variant, using photocrosslinking, and identification of covalently crosslinked dimers by sodium dodecyl sulphate polyacrylamide gel electrophoresis (SDS-PAGE) and densitometry analysis of protein bands.

2.2. To investigate the effects of the novel disease-protective mutation, G127V, on the dimerization of the prion protein.

2.2.1. We aimed to develop further mutants, including G126V mutants and site-specific *p*Bpa mutants of full length recombinant mPrP, untagged and mCherry tagged variants, to have an appropriate set of proteins by which the effect of G126V mutation upon the dimerization of the mPrP can be studied.

2.2.2. Using the produced set of mPrP mutant variants, to test the efficiency of dimerization of mPrP in the presence and absence of the disease-protective G126V mutation, by using protocrosslinking and densitometry analysis after SDS-PAGE and by assessing both hetero- and homodimerization.

2.2.3. To compare the results obtained in the *in vitro* approach to results obtained *in cellulo* in experiments conducted in parallel on a model cell culture system using HeLa cells transfected

by various mutant mPrP constructs designed to test the dimerization efficiency of mPrP in the presence and absence of the disease-protective mutation G126V.

3. EXPERIMENTAL METHODS

3.1. Materials and reagents used in the studies

E. coli BL21(DE3) competent cells were purchased from Novagen (Cat. No.: 69450) and the bacterial expression vector pRSET-B was obtained from Thermo Fisher Scientific (Cat. No.: V35120). *p*Bpa was purchased from BACHEM (Cat. No.: F-2800.0005). Dithiothreitol (DTT) (Cat. No.: D0632), L-Glutathione oxidized (GSSG) (Cat. No.: G6654), L-Glutathione reduced (GSH) (Cat. No.: G4251), Phenylmethylsulfonyl fluoride (PMSF) (Cat. No.: P7626), Protease Inhibitor Cocktail (Cat. No.: P2714), L(+)-Arabinose (Cat. No.: A3256), selection antibiotics kanamycin (Cat. No.: K400) chloramphenicol (Cat. No.: C0378) and ampicillin (Cat. No.: A9518), Urea (Cat. No.: 51456), N-ethyl maleimide (NEM) (Cat. No.: 04259) were from Merck/Sigma-Aldrich. ProSieve QuadColor prestained protein marker was purchased from Lonza (Cat. No.: 00193837). Guanidine hydrochloride (Gn-HCl) (Cat. No.: A13543), isopropyl-ß-D-thiogalactopyranoside (IPTG) (Cat. No.: R0392) and all restriction enzymes (unless otherwise specified) were from Thermo Fisher Scientific., Protino Ni-NTA Agarose (Cat. No.: 745400.100), Nucleospin Gel PCR Clean-up Kit and NucleoSpin DNA purification kit (Cat. No.: 740952.50) were from Macherey-Nagel NgoMIV (Cat. No.: R0564) enzyme was from New England Biolabs. Sodium dodecyl sulphate (SDS) (Cat. No.: 151-21-3) was from SERVA. All other common reagents and chemicals were from Molar Chemicals.

3.2. Plasmid constructs and DNA cloning

3.2.1. Preparation of DNA plasmid constructs for bacterial expression and purification of prion proteins designed to study the dimerization interface of mouse prion protein

The cDNA of the full length mouse PrP (mPrP) (Uniprot entry P04925) was obtained from the laboratory of Dr. Byron Caughey (Laboratory of persistent viral diseases, National institutes of Health, Hamilton, USA) [65]. The bacterial expression plasmid vector pRSET-B was used as the base vector for cloning to generate protein expression plasmids for producing

recombinant mPrPs in *E. coli*. Two sets of constructs were prepared for the prion protein: one set where the encoded mPrP was present as untagged, and another set, where an mCherry coding DNA sequence (CDS) was inserted downstream of the CDS of mPrP as a fusion tag, to result a fusion protein for mPrP with mCherry at its C-terminal. The two sets comprised each a plasmid coding for the corresponding wild type (WT) protein (reffered to as WT mPrP for untagged and WT mPrP-mCh for mCherry-tagged), and several other plasmids coding for various *p*Bpa-mutants of the mPrP (untagged or mCherry tagged). The nucleic acid sequences of the bacterial expression plasmids generated for the two wild type proteins, pRSET-B-mPrP and pRSET-B-mPrP-mCh plasmids, and the amino acid sequences of the proteins encoded by them are presented in the Appendix I and Appendix II, respectively. The sequences of the oligonucleotides used for PCR and linker ligation are presented in Appendix III, Table 1.

The pRSET-B-mPrP and pRSET-B-mPrP-mCh plasmids were used also as parental plasmid vectors for generating the amber stop codon mutants: pRSET-B-mPrP(S131X), pRSET-B-mPrP(E206X), pRSET-B-mPrP(E210X), where numbers denote the positions of amino acids where mutations to a *p*Bpa (noted as X) is initiated by placement of the amber stop-codon TAG to encoding for this amino acid positions in the DNA sequence of the full length mPrP. The numbering nomenclature corresponds to the numbering of the mammalian, translated mouse PrP, which begins with the signal sequence (aa. 1-22). Mutations were carried out by QuikChange site directed mutagenesis with the following primers: *mPrPS131Ambfwd, mPrPS131Ambrev, PrP-E206X-fw, PrP-E206X-rev, PrP-E210X-fw* and *PrP-E210X-rev*, respectively (for sequence see Appendix III, Table.1).

Further, two vectors pRSET-B-mPrP-RE and pRSET-B-mPrP-mCh-RE were generated from pRSET-B-mPrP and pRSET-B-mPrP-mCh plasmids for cloning purposes, by the introduction of the unique restriction enzyme sites EagI, BsmBI and MluI at strategic positions into the prion protein coding sequence using QuikChange site directed mutagenesis. The DNA oligonucleotide primers used for the silent mutagenesis were, in the order of the introduced restriction sites listed above, *EagIfwd, EagIrev, BsmBIfwd, BsmBIrev, MluIfwd, MluIrev*, possessing the sequences listed in Table III-1 (Appendix III).

The following mutations were introduced, individually, into the sequence of mPrP encoded by these pRSET-B-mPrP-RE and pRSET-B-mPrP-mCh-RE vectors: W80X, G89X, Q90X, N107X, K109X, V111X, G113X, A116X, A117X, G118X, A119X, V120X, V121X, L124X, G125X, G126X, Y127X, M128X, L129X, M133X or R135X, where X denotes the amber-mutation where a *p*Bpa will be incorporated. Each of the mutations were introduced to both plasmids by linker ligations using the linkers presented in Table III-1 and -2 (Appendix

III). The procedure was carried out briefly, as follows. The pRSET-B-mPrP-RE and pRSET-B-mPrP-mCh-RE plasmids were digested with the appropriate restriction endonulease pairs for each mutant, as presented in Table III-2 (Appendix III), after which they were purified with NucleoSpin DNA purification kit and the appropriate DNA linker (or linkers) were ligated between the two sticky ends of the plasmids. The sequences of the oligonucleotides used as the DNA linkers are presented in TableIII-1 (Appendix III). When a fragment of the prion protein coding sequence was reconstituted from two or more linkers, all 5' termini of the oligonucleotides at the linker junctions were phosphorylated.

3.2.2. Preparation of DNA plasmid constructs for expression and purification of prion protein variants for the study of the effect of disease protective mutation G126V on dimerization of mouse prion protein

To produce the untagged and mCherry tagged wild type mPrP and the *p*Bpa-mutant variants Y127*p*Bpa, M128*p*Bpa and S131*p*Bpa of the untagged mPrP, the same DNA-plasmids were used as mentioned previously, named as pRSET-B-mPrP, pRSET-B-mPrP-mCh, pRSET-B-mPrP(Y127X), pRSET-B-mPrP(M128X) and pRSET-B-mPrP(S131X), respectively. Each of the plasmid constructs encoding for a G126V mutant mPrP (that corresponds to the G127V mutation of the human PrP sequence) was generated from the corresponding pRSET-B plasmids of either untagged mPrP or the mCherry tagged mPrP-mCh encoding plasmids by using standard molecular biology techniques. Briefly, the plasmids were digested with NgoMIV and AfeI restriction enzymes and the oligonucleotides were inserted as indicated in Table III-3 (Appendix III).

3.3. Bacterial overexpression and production of recombinant mouse prion protein variants

Recombinant wild type, *p*Bpa-, G126V-, and G126V- and *p*Bpa-mutant prion proteins with and without an mCherry fusion tag were produced in *E. coli* BL21(DE3) protein expression strain, based on published protocols for wild type [66] and for site-specific incorporation of *p*Bpa into proteins for the *p*Bpa-mutants [67], as follows. For the wild type proteins the pRSET-B expression plasmids carrying the mPrP or mPrP-mCherry genes (pRSET-B-mPrP and pRSET-B-mPrP-mCh) were transfected into competent *E. coli* BL21(DE3) cells, and transformant cells were selected on Luria-Bertani (LB) agar plates in presence of

100 μg/ml ampicillin. In case of the *p*Bpa-mutant proteins, first the pEVOL-pBpF plasmid [68] encoding the cognate tRNA and the amino acyl transferase and possessing also a chloramphenicol resistance gene, was transfected into competent *E. coli* BL21(DE3) cells. This plasmid was kindly provided by the laboratory of P. Schultz (The Scripps Research Institute, San Diego, California, USA). Transformant cells were selected on LB-agar plates in presence of 34 μg/ml chloramphenicol and competent cells were prepared by $CaCl_2$ method [69]. These pre-transformed cells were used in the second step to transfect the pRSET-B-expression plasmids harboring the amber codon mutant-prion genes of interest and possessing an ampicillin resistance gene. Successful transformants were selected on LB-agar plates in presence of both of the antibiotics, ampicillin: 100 μg/ml and chloramphenicol: 34 μg/ml, and were used to produce the recombinant proteins, typically as follows. Single colonies were picked from the agar plates to inoculate 16 ml starter cultures, which were then grown overnight in the presence of the appropriate selection antibiotics. Using the starter cultures, usually, 800 ml volumes of LB media with corresponding antibiotics (ampicillin 50 μg/ml for wild-type or both ampicillin and chloramphenicol 50 μg/ml and 17 μg/ml for *p*Bpa mutant variants). were inoculated the next day by using 1:1000 volume/volume ratio of inoculum to culture media (or the starting OD_{600} = 0.01-0.03 range, and were cultured further at 37 °C and 200 rpm in an incubator shaker (Labtech, LSI-2005RL). Usually, within the OD_{600} = 0.5-0.6 range the cultures were induced for protein expression: by adding either 1 mM IPTG alone (for protein expressions without *p*Bpa) or together with 0.02% arabinosefor the expression of *p*Bpa-mutant PrPs, in this latter case 1 mM *p*Bpa was also supplemented to the culture media at this stage. The cultures were further grown, usually for at least 4 h at 37 °C and 200 rpm, before harvesting by centrifugation.

3.4. Purification of recombinant mouse prion protein variants

Harvested bacterial pellets were resuspended in 100 mM NaCl solution and the suspension was supplemented with protease inhibitors: 0.5 mM PMSF and 1x concentration of Protease Inhibitor Cocktail after which cells were disrupted by pulse-sonication (30 s on- and 30 s off-pulse repeated for seven times) (Sonifier Cell Disruptor B-30, Branson Sonic Power Co, USA). The disrupted cell suspension was centrifuged (60,480 x g for 50 min at 4 °C), and the pellet containing the inclusion bodies were collected and were solubilized in 30 ml of buffer A (6 M Gn-HCl, 10 mM Tris, 100 mM Na_2HPO_4-$2H_2O$, pH 8.0) for 1 h at RT while continuously stirred. The dissolved inclusion body suspension was centrifuged (60,480

x g, 50 min, 4 °C) and the supernatant, containing the solubilized proteins, was applied to Ni-NTA agarose beads (3 ml bed-volume was used per an 800 ml culture) pre-equilibrated by buffer A. The suspension of sample and beads was gently mixed on a rocker for 30 min at RT to allow for portien binding. Next, the suspension was sedimented by centrifugation (750 x g, 3 min, 4 °C) and the pelleted beads were washed two times using buffer B (1 M Gn-HCl, 10 mM Tris, 100 mM $Na_2HPO_4.2H_2O$, pH 8.0) and centrifugation at 750 x g for 3 min at 4 °C. Then, the prion protein was allowed to correctly refold by adding a redox buffer (1 M GnHCl, 10 mM Tris, 100 mM $Na_2HPO_4.2H_2O$, 0.5 mM PMSF, 1x concentration of Protease Inhibitor Cocktail, 5 mM GSSG, 10 mM GSH, pH 8.0) to resuspend the pelleted beads and keeping the suspension on ice, while gently mixing on a rocker, for ~16 h [70,71]. The refolded protein-bead suspension was poured onto an empty column. The flow through was kept to test for the presence of unbound proteins, and the beads were washed by using 75 ml of washing buffer (10 mM Tris, 100 mM $Na_2HPO_4.2H_2O$, 20 mM imidazole, pH 5.8). The proteins were eluted from the beads by elution buffer (10 mM Tris, 100 mM $Na_2HPO_4.2H_2O$, 500 mM imidazole, pH 5.8), collecting about six fractions of 1 ml. The collected fractions were subjected to dialysis, which was performed initially against 20 mM sodium acetate, pH 5.5, 1 mM EDTA and 1 mM EGTA, at a protein to buffer ratio of 1:1000 vol:vol, at 4 °C for 6 h, followed by two changes of 20 mM sodium acetate, pH 5.5 buffer at 4 °C for 6 h and 12 h, respectively. Dialyzed protein concentrations were measured by Bradford method [72], aliquots of 1 ml were flash-frozen by liquid nitrogen and were stored at -80 °C for later use.

3.5. Mass spectrometry analysis of the correct insertion of *p*Bpa into proteins

For mass spectrometry analysis all protein samples were run on 10% polyacrylamide (PA) SDS gels at reducing conditions. Protein bands were excised from gels and were in-gel digested for mass spectrometry analysis according to the UCSF In-Gel Digestion Protocol, available at http://msf.ucsf.edu/protocols.html. Briefly: the excised gel bands were cut into little pieces, were washed twice by 25 mM NH_4HCO_3/50% acetonitrile. The gel pieces were then dried. Disulfide-bridges were reduced with DTT, free sulphydrils were alkylated with iodoacetamide and proteins were digested with trypsin (sequencing grade modified porocine trypsin, Promega) at 37 °C for 4 h. Tryptic peptides were extracted and analysed by MALDI-TOF (Bruker Reflex III) using DHB (2,5 dihydroxybenzoic acid) as matrix, in positive reflectron mode. Peptide sequences were confirmed by MS/MS analysis acquired on a nanoLC coupled LCQ-Fleet (Thermo Fisher Scientific) ion trap mass spectrometer. To test for

correct insertion of the *p*Bpa amino acid into a desired amber codon coded position, we chose position 131 of mPrP and generated two mutants for this position: one coding for a tyrosine, mPrP(S131Y)-mCh and another for an amber stop codon to initiate insertion of *p*Bpa, mPrP(S131*p*Bpa)-mCh. The tyrosine mutant serves as a control, given that the tRNA-RNA synthetase pair may preserve some potency for being charged by tyrosine over *p*Bpa. The tyrosine mutant was expressed in two conditions: in LB culture media (-*p*Bpa) or in LB media supplemented with *p*Bpa amino acid (+*p*Bpa). In parallel, the amber codon mutant was expressed in *p*Bpa-supplemented LB media.

To provide a comprehensive verification of *p*Bpa vs. tyrosine incorporation, mass spectrometry analysis was performed not only on these three protein samples but also on mixtures of purified *p*Bpa- and Tyr-mutants [mPrP(S131Y)-mCh and mPrP(S131*p*Bpa)-mCh, respectively] grown in presence of *p*Bpa, containing the two proteins at various percentages, such as: 75:25, 88:12 and 94:6% of *p*Bpa- to Tyr-mutant (Mixture 1-3, respectively).

3.6. Conformational stability analysis of purified prion proteins by urea denaturation assay

Conformational stabilities of the wild type and *p*Bpa-mutant prion proteins were compared by employing an urea-gradient assay, described eariler [73] and briefly, as follows. An urea concentration gradient treatment was applied to the proteins in presence of reducing agent (20 mM DTT), that can reduce the single disulfide bond present in the structure of the prion protein upon unfolding. Samples of 7.44 μM protein were treated by increasing concentrations of urea, starting from 0 to 5 M, in steps of one molar increment, in presence of 20 mM DTT in phosphate buffer saline (PBS), (137 mM NaCl, 2.7 mM KCl, 10 mM $Na_2HPO_4.2H_2O$, 2 mM KH_2PO_4, pH 7.4). Treatments were applied for 2.5 h while samples were kept at RT and on a mini-rotator (Bio RS-24 from BioSan). Further, 50 mM of N-Ethylmaleimide was added and the samples were incubated for 1 h to block the reduced thiol groups of the unfolded protein population as well as DTT. Using Laemmli SDS sample uffer with no reducing agent the samples were analyzed on 10% PA-SDS-PAGE followed by RAMA staining [74] to visualize the non-reduced and reduced populations present in the protein samples. Since we found that the width of the transition region and midpoint were sensitive to the actual experiment/condition of the protein preparation, for the stability comparisons we performed the assay side-by-side for those samples, which were to be

compared. Also, we have repeated the unfolding experiments at least on three separate protein preparations.

3.7. *In vitro* photocrosslinking

Photocrosslinking of *p*Bpa-mutant PrP homodimers or heterodimers were performed on samples of 6 μM protein concentration in PBS (137 mM NaCl, 2.7 mM KCl, 6 mM $Na_2HPO_4.2H_2O$, 1.4 mM KH_2PO_4, pH 7.4), containing 0.06% SDS that favored homo or heterodimerization and crosslinking of dimers at highest amounts. Volumes of 200 μl sample in 1.5 ml microfuge tubes were placed on ice at a distance of 5 cm from the light bulbs [75] and were irradiated by 365 nm UV light for 2 h to give highest amounts of crosslinked proteins [67] using a Crosslinker CL-1 (Herolab Gmbh Laborgeräte) apparatus, producing a total UV energy of 18.598 J/cm^2. As negative controls, the wild type proteins containing no *p*Bpa were also included in the experiment and were irradiated similarly. For each sample non-irradiated control pairs were also prepared that were incubated in similar conditions but at dark.

To estimate the amount of the background, non-specifically associated and crosslinked dimers similar experiments were performed with each protein at higher, 2% SDS condition that favors a monomeric form of the prion protein [76].

3.8. Quantification and statistical analysis

Crosslinked samples were tested on either 10% or 12% PA-SDS gels, in case of the mCherry-tagged or untagged mPrP proteins, respectively. The percentage of photocrosslinked dimer to monomer ratios were assessed by gel-densitometry and using the ImageJ 1.48v program [77]. As reported earlier, in case of the mCherry tagged protiens, the mCherry fusion tag presents cleavage products when incubated/boiled in the sample-buffer [78] that results additional bands below dimer- and monomer-levels on the gel. Assuming that the mCherry split occurs the same way in a monomeric or a dimeric (or multimeric) species, the dimer percentage can be calculated as the area corresponding to the dimer band divided by the sum of the monomer and the dimer area (similarly as for the untagged mPrP protein variants). Performing such evaluations for both irradiated and control, non-irradiated (-) samples that were kept at dark and using these latest values for subtractions (for both types of proteins), the crosslinked dimer percentages can be corrected for the “background” fraction of dimers not

attributable to UV-crosslinking. The wild type protein samples treated the same way also provide a non-zero value (perhaps representing dimer products crosslinked at some non-*p*Bpa positions) that was also considered to interpret the *p*Bpa-specific values obtained for the mutants. Similar evaluation of samples at 2% SDS condition was also performed to have an estimate of a (maximum possible) nonspecifically crosslinked dimer amount.

All crosslinking experiments were carried out on at least three independent protein samples ($n \geq 3$) derived from different expressions. The mean ± SD (standard deviation) of these values is used for data representation. The significance of differences in values obtained at 0.06% and 2% SDS conditions for each protein examined was determined using an unpaired Student's t-test with GraphPad Prism software. Asterisks denote the following: *: $p<0.05$, **: $p<0.01$ and ***: $p<0.001$.

The hetero- or homodimers of mPrP(G126V) variants were analyzed on 10% PA-SDS gels. The efficiency of heterodimer or homodimer formation of mPrP variants were measured densitometrically as described above. To determine the percentages of the crosslinked heterodimer PrPs, the area corresponding to the heterodimer band on the intensity plot was divided by the total area corresponding to the sum of areas of all protein bands in the lane. The percentage of the homodimers formed was calculated as presented above: The area corresponding to the homodimer band was divided by the sum of the monomer and the dimer area. All crosslinking experiments were performed three times, using independent protein samples ($n = 3$) obtained from different expressions. For data representations the mean ± SD of these values are used. The significance of the difference obtained for valine mutant and control was tested using unpaired Student's t-test. Asterisks represent as follows, *: $p\leq0.05$ and **: $p\leq0.01$.

3.9. Circular dichroism spectroscopy

Far-UV circular dichroic (CD) spectra of samples of the untagged wild type and *p*Bpa-mutant mPrP proteins, typically of 0.1 to 0.2 mg/ml concentrations, were recorded at room temperature using a Jasco J-810 Spectropolarimeter (Jasco Co.), using a 1 mm path length quartz cuvette as the sample holder. CD spectra were recorded between 180 to 260 nm, at 100 nm/min speed, using 2 nm bandwidth and 4 s integration time, sensitivity standard, 1 nm data pitch, and accumulating three spectra for each sample. Spectra were recorded in three conditions for each type of protein variant: in the originalal monomeric-state (in MilliQ water) and in dimer-state favoring conditions of 0.06% SDS, PBS, pH 7.4, following either

UV light crosslinking for 2 h or without crosslinking (on parallel samples kept at dark for 2 h). For each condition and sample, the corresponding buffer-only spectra were recorded in the same way as the sample spectra and were used to subtract from sample spectrum before calculating the mean residue molar ellipticities (degrees square centimeter per decimole). The program BeStSel (http://bestsel.elte.hu) was used to evaluate spectra for secondary structure composition based on Micsonai et al. [79]. Samples originating from at least two to three distinct crosslinking experiments were measured.

4. RESULTS

4.1. Study of the dimerization interface of the mouse prion protein

4.1.1. Wild type and various pBpa-mutant variants of untagged or mCherry tagged recombinant mouse prion proteins are succesfully produced and purified from E. coli

We adapted the system developed by the P. Schultz laboratory [80] for genetic incorporation of ncAAs into protein sequences in *E. coli*, in order to generate *p*Bpa-mutants of the mPrP. The key step of the method is the use of an amino-acyl tRNA synthetase/tRNA (aaRS/tRNA) pair that is orthogonal to the *E. coli* and which selectively recognizes and inserts *p*Bpa into positions where the amino acid's codon is mutated to an amber stop codon, TAG.

We established new unique restriction sites to the coding sequence of PrP by silent mutations, in order to be able to generate *p*Bpa-point mutants sweeping through regions of interest in the sequence, that allowed for the introduction of amber codon mutations by using simple linker ligation along the almost entire coding region of mPrP (see Materials and methods). Using this method, we were able to quickly access the large number of mutant PrPs we produced (approximately 45, of which 38 were used here).

We selected a set of 24 aa. positions of mPrP tagged with mCherry to site specific insertion of *p*Bpa, along the sequence of PrP based on previous studies suggest that certain regions of PrP, such as the hydrophobic domain (HD, aa. 111 to 134) [37,81] or the central region (HD, aa. 105 to 125) [82] or the N-terminal 90-120 segment [83] participate in dimerization/oligomerization and also few positions that are not involved in formation of dimerization. Using this strategy, we had selected 22 aa. positions falling in the N-terminal

domain and HD and additional two positions in the C-terminal domain of the protein (Figure 5a). We generated amber stop codon mutants of mPrP in fusion with an mCherry fluorescent protein expression cassette at the C-terminus using pRSET-B vectors for expression. The tag allowed on the one hand, visual monitoring and tracking of the protein during purification steps, assisting with optimization of the conditions, and on the other hand, it may have increased the protein's solubility and made it easier to handle. The purified wild type and *p*Bpa-mutant mPrP-mCherry fusion proteins appear at about the same position on SDS polyacrylamide gels and at around their expected molecular weights of 52 kDa, constituted by the MW of PrP (23.1 kDa) and of the mCherry tag (29 kDa) (Figure 5b).

We further generated also untagged mPrP constructs with *p*Bpa substitutions at specific positions and evaluated their crosslinking efficienciesto verify whether the tag had any significant influence on the results obtained.

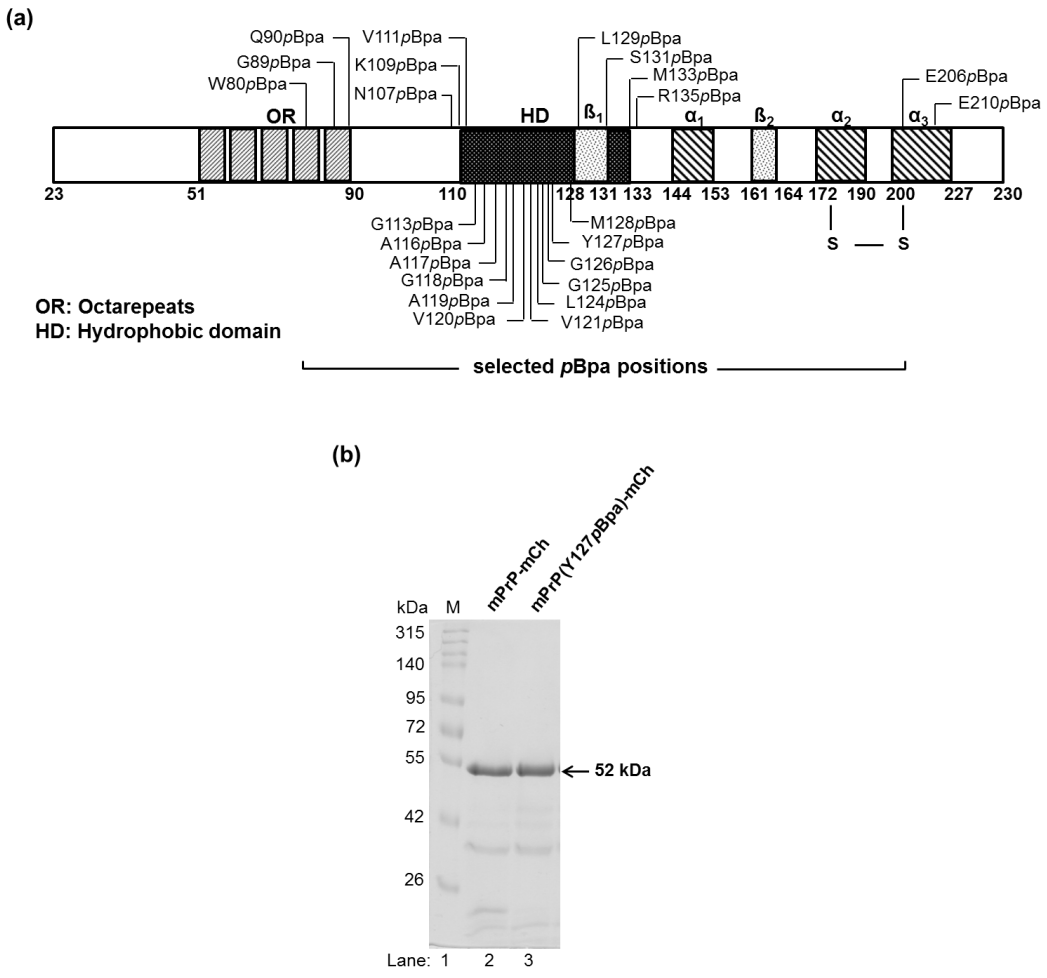

Figure 5. The series of site specific single-*p*Bpa-mutant PrPs generated to investigate the dimerization interface. (a) Schematic presentation of the mPrP sequence (aa. 23-230)

depicting the residues chosen for *p*Bpa-mutation to generate a series of individual-*p*Bpa-mutant mPrPs. β_1 *and* β_2, beta sheets; $\alpha_{1\text{-}3}$, alpha helices; *S-S*, disulfide bond. **(b)** Representative SDS-PAGE gel picture of purified mCherry tagged wild type (lane 2, mPrP-mCh) and a *p*Bpa-mutant [lane 3, mPrP(Y127*p*Bpa)-mCh] prion protein. Proteins resolve at about their expected weights, sum of wild type PrP and mCherry (~52 kDa). Additional bands can be noticed below the full length protein, which is common for mCherry tagged proteins, due to the hydrolysis of the acylimine linkage of the chromophore of mCherry upon sample-treatment such as SDS-denaturing and boiling, as well as fragmentation of the mCherry during SDS-PAGE analysis [78].

In comparison to minimal media for culturing, we found that LB media yielded the highest protein yields. The amino acyl synthetase has been reported to retain some of its ability to charge its cognate tRNA with tyrosine, particularly when the protein is expressed in LB medium.

4.1.2. The correct site specific insertion of pBpa into the prion protein sequence is validated by MALDI-TOF mass spectrometry

To determine whether *p*Bpa was indeed inserted selectively, we cultured and induced in parallel cells transfected with the wild type mPrP protein gene containing the amber codon at a selected position (in this case, codon 131) and a mutant protein coding for a tyrosine at that position. All three cultures were either supplemented by *p*Bpa or grown in the absence of *p*Bpa and then induced for protein expression. The purified proteins were excised from SDS gels and subjected to MALDI-TOF mass spectrometry. The findings revealed that a correctly inserted *p*Bpa is present in at least ~90% of the protein molecules of the *p*Bpa-mutant protein sample, and that insertion only occurred at the expected position (Figure 6).

MALDI-TOF mass spectrometry analysis of the six samples revealed that both tyrosine-mutant proteins contained only Tyr at position 131, regardless of whether the culture media contained *p*Bpa or not, whereas only *p*Bpa was detected at position 131 in the *p*Bpa-mutant protein sample. In the mixtures of the two proteins, both Tyr and *p*Bpa containing corresponding fragments could be identified with the exception of the third mixture, which was mixed as to contain 94% *p*Bpa-mutant and 6% of Tyr-mutant, only *p*Bpa-containing corresponding fragments were detected.

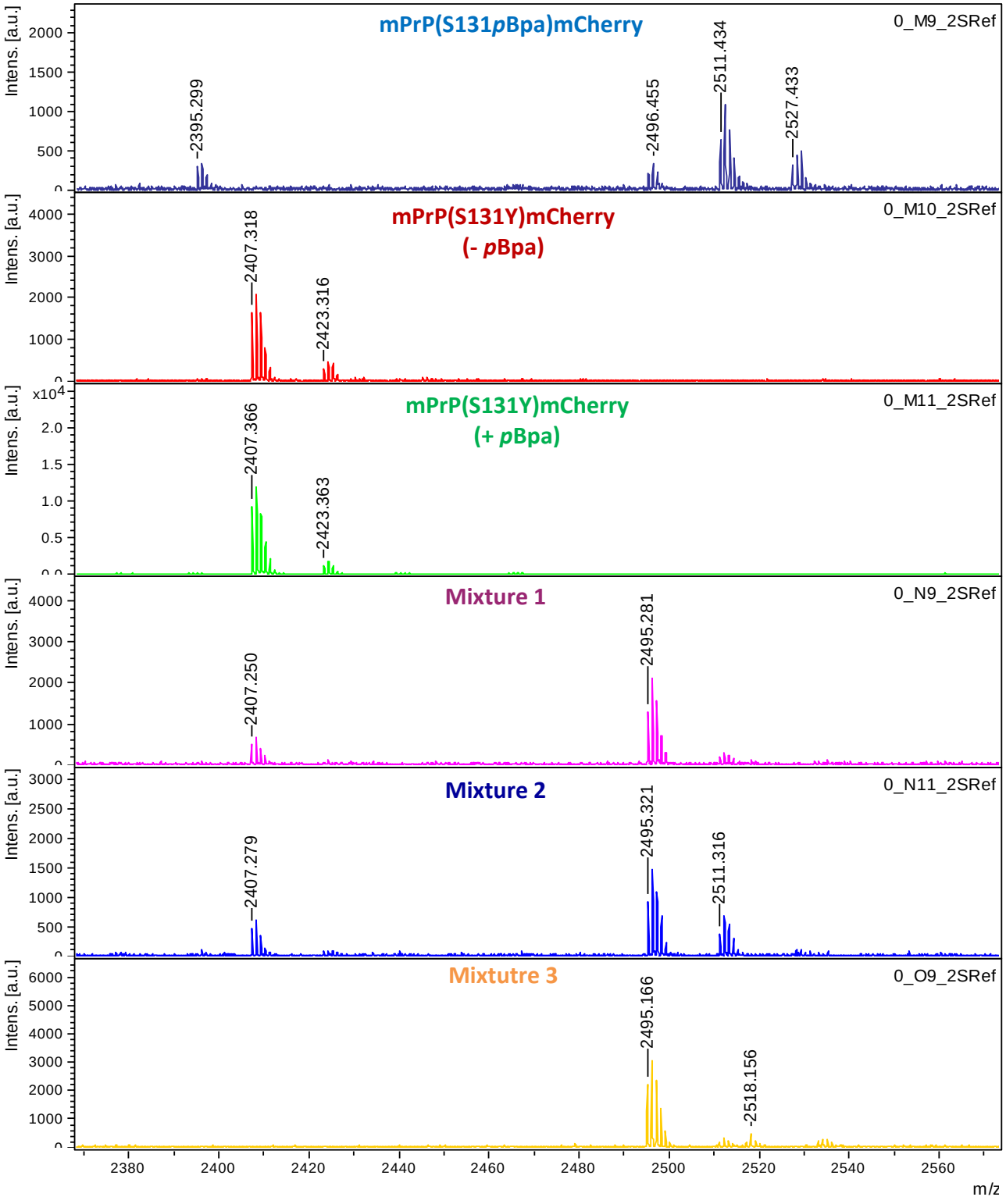

Figure 6. The insertion of *p*Bpa into the prion protein sequence isconfirmed by mass spectrometry. The following six samples were used for MALDI-TOF mass spectrometry analysis and validation of proper *p*Bpa insertions into the sequence: a *p*Bpa-mutant mPrP(S131*p*Bpa)-mCh and a tyrosine mutant for the same position mPrP(S131Y)-mCh (control) produced with (+ *p*Bpa) or without (- *p*Bpa) supplementing *p*Bpa to the culture

media, and three mixtures (Mixture 1, 2 and 3) made of the two types of mutants, S131*p*Bpa and S131Y (+ *p*Bpa), by mixing them at different ratios (75:25, 88:12 and 94:6%, respectively). The calculated m/z for the Tyr and for the *p*Bpa containing shortest tryptic peptides, are 2407.27 Da and 2497.23 Da, respectively, which corresponds to the (89-114) fragment of the prion protein: (K)HVAGAAAAGAVVGGLGGYMLGXAMSR(P) where X refers to the modified amino acid, that is either Tyr or *p*Bpa.

4.1.3. Presence of pBpa does not affect the prion protein's conformational stability

We incorporated most of the *p*Bpa substitutions in the conformationally disordered part of the prion protein, and a few in the globular domian, but only in positions were they are unlikely to cause structural changes of the folded protein or to alter its stability. To test this, we employed a urea gradient assay developed for monitoring the stability and unfolding of disulfide bond containing proteins [73] and performed stability experiments on selected *p*Bpa-mutants and the wild type protein. In this assay, the disulfide-containing protein is being treated with increasing concentrations of urea in the presence of a low concentration of reducing agent, 20 mM DTT. When the protein is unfolded by the urea, the disulfide bonds become available to the reducing agent and can be reduced, whereas, this can not occur if the protein is still folded. The reducing agent and the protein thiols at this time can be blocked by addition of NEM in excess (here, 50 mM), to fix the amount of the folded (disulfide-intact) and unfolded (reduced) protein populations, which later can be visualized on non-reducing SDS-PA gel, based on the differing mobilities of the disulfide-intact and reduced forms.

The mPrP comprises a single disulfide bond linking the Cys residues at aa. positions 178 and 213 within the C-terminal globular half of the protein, stabilizing its structure. Since, the mCherry does not possess internal cysteines, the approach can be used to examine not only the untagged PrP, but also the prion protein-mCherry fusion constructs because the unfolding of mCherry will be "silent" to this assay without showing mobility change on a denaturing gel. Furthermore, without a functional interaction between PrP and mCherry, the unfolding of mCherry is unlikely to alter the stability of the prion protein's structure/unfolding process. In accordance with this, the gradual appearance of the unfolded prion proteins at increasing urea concentrations can be clearly detected on the gels (Figure 8).

Along with the wild type, we tested several of the *p*Bpa-mutant variants. Among them we chose those with *p*Bpa at aa. positions 127, 128 and 129. These positions are part of the hydrophobic domain, HD, where most of PrP's interactions occur, and were reported to be either part of or adjacent to interaction sites [84]. This region is also the interconnecting segment between the unstructured and the globular part of the protein and these positions

were reported to become part of the globular domain when a truncated version aa. 121-227 of recombinant human PrP was analyzed by NMR [85] We also chose to test two variants with *p*Bpa substitutions at positions Glu206 and Glu210, both of which are located on PrP's α-helix III. We found that these proteins with *p*Bpa substitutions unfold in the same way as the wild type protein; their transition regions are within 2 to 4 M urea, and midpoints at 3 ± 0.5 M urea concentration (Figure 7). These indicate that substitutions of amino acids at these positions to *p*Bpa did not perturb the stability of the protein and also suggest that *p*Bpa can be well-tolerated in these protein structures.

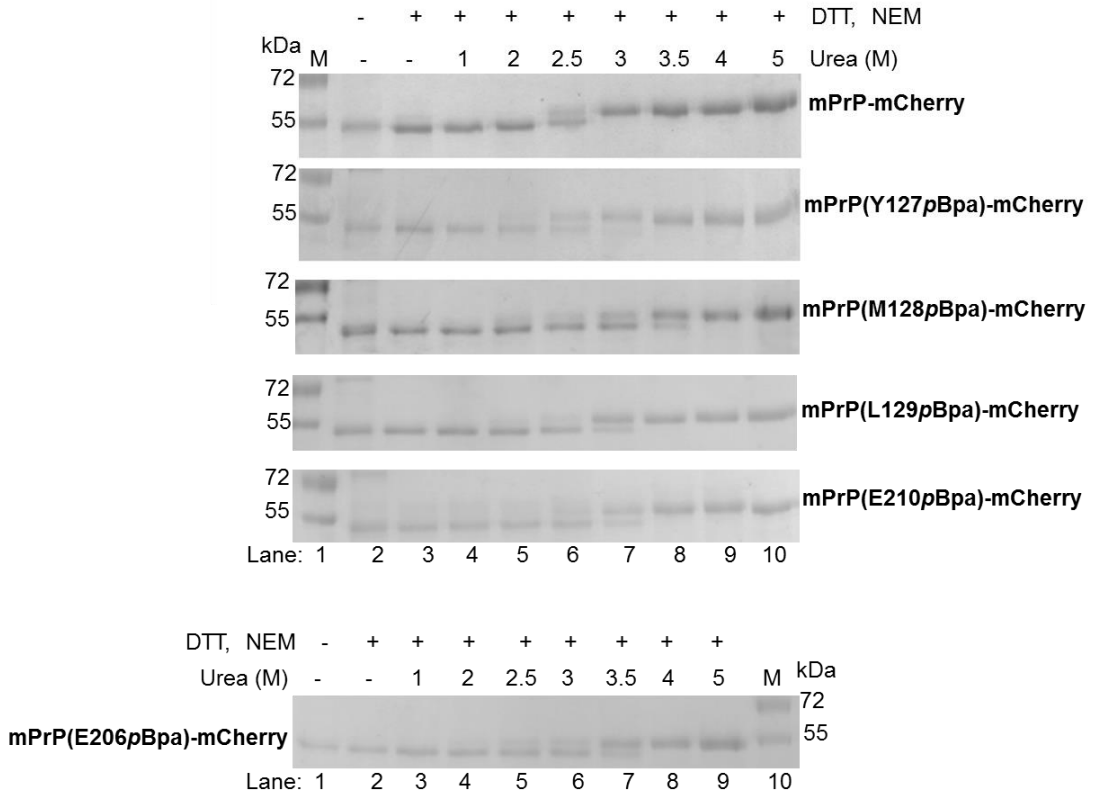

Figure 7: The conformational stability of wild type and *p*Bpa-mutant prion-mCherry proteins is similar. Representative gel pictures of the urea gradient assay for wild type and *p*Bpa mutants at 127, 128, 129, 206 and 210 aa. positions, as indicated on the figure.

The purified recombinant mPrP is known to be prone to oligomerization in solutions around physiological pH [86,87], a phenomenon that is also concentration dependent [88,89] Kaimann et al. [76] had shown that by using various submicellar concentrations of SDS in the buffer, the recombinant hamster PrP (haPrP 90-231) could be kept in specific oligomeric states, dimeric or higher oligomeric, depending on the amount of SDS applied. An SDS

concentration lower than 0.1% does not act as a denaturant but mimics some membrane-like features and a concentration as low as of 0.06% promotes formation of an α-helical structure for PrP [90]. Based on the findings of Kaimann et al. [76] we optimized the conditions of photocrosslinking reactions for sample condition, SDS concentration and the UV-crosslinking parameters (Figure IV-1 and Figure IV-2, Appendix IV). We were able to achieve successful crosslinks of dimeric proteins as confirmed by reducing SDS-polyacrylamide gels of samples irradiated in conditions of 0.06% SDS in PBS buffer of pH 7.4 and a protein concentration of 6 μM. To rule out the possibility of crosslinking dimers through a non-*p*Bpa residue (a process the prion protein is prone to) two types of controls were used in all experiments: non-irradiated samples incubated in dark and the wild type protein irradiated in the same conditions and for the same amount of time as the experimental samples. The appearance of non-*p*Bpa crosslinked protein species on the SDS gels could be kept to a minimum by careful handling and timely processing of the samples. Each purified *p*Bpa-mutant prion-mCherry fusion protein, a total of 24 and the wild type, were irradiated and SDS-PAGE was used to check for the formation of covalently photocrosslinked dimers (Figure 8).

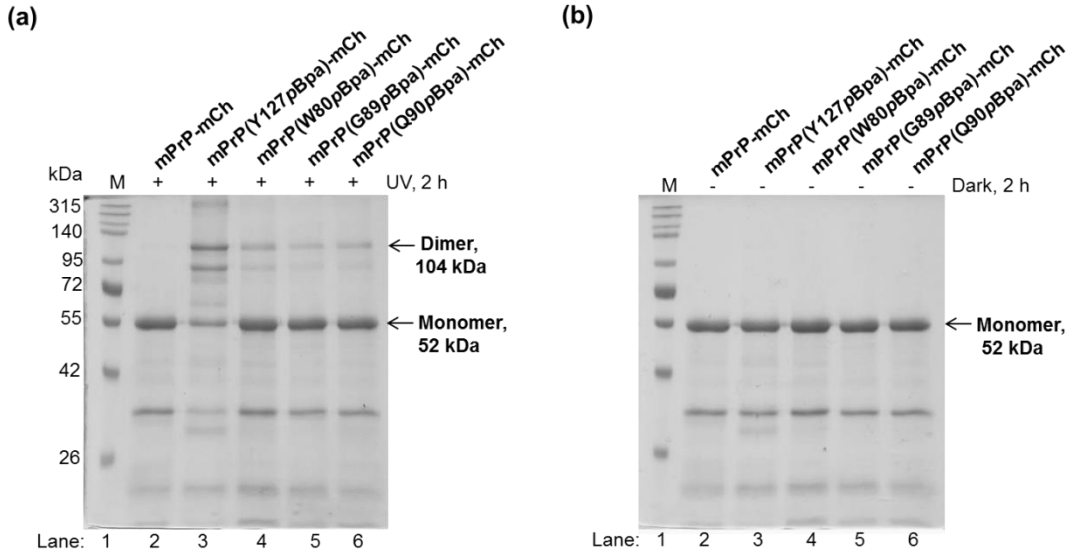

Figure 8. Photocrosslinking of dimers of distinct prion-mCherry proteins harboring one site specific *p*Bpa-mutation in the sequence of prion. Representative images of reducing 10% polyacrylamide gels of wild type and selected *p*Bpa-mutants **(a)** irradiated at 365 nm for 2 h and **(b)** non-irradiated, but incubated in similar conditions at dark, as specified on the figure. Proteins are crosslinked at 6 μM concentration in the presence of 0.06% SDS (in PBS, pH 7.4), which promotes dimerization.

The crosslinked dimers can be observed on SDS-PAGE at the expected molecular weight of around 104 kDa, which is double of the monomeric protein weight of 52 kDa, as indicated by arrows (lanes 3 through 6 on Figure 8a). There are no bands present at above the level for the monomeric size in case of the wild type (no *p*Bpa-containing) and for the non-irradiated (Figure 8b, respectively) samples, implying that all bands in this upper region for the irradiated samples are crosslinked proteins. The two satellite bands observed in crosslinked samples between the levels corresponding to dimeric and monomeric forms, as well as, those observed below the monomeric form in case of all samples, are not the consequence of proteolytic degradation but rather of the specific cleavage of mCherry taking place in the sample buffer as previously discussed (Figure 5, legend). Since the crosslinking of 127*p*Bpa mutant resulted strong dimer bands, we decided to use this protein as a positive control in all further experiments, as well as, included it on all gels to aid in identification of the dimer band of other samples. It can be observed that, the amount of crosslinked dimers varies depending on where *p*Bpa is located, with highest level being found for the variant containing *p*Bpa at position 127. However, we can not entirely exclude the possibility that some amount of dimers or oligomers visible on the gels of irradiated samples originate from nonspecific interaction of protein molecules, which had been covalently crosslinked by *p*Bpa during irradiation.

In order to measure the real dimer-crosslinking efficiency, we need to account for any nonspecific dimers that occur from random, temporary interaction of the two protein molecules that may be crosslinked by *p*Bpa during irradiation. To solve this, we chose to look for conditions by varying the SDS concentration in the solution, that would move the system away from the dimer specific equilibrium and successfully disrupt the specific interactions that lead to dimer formation. Using the 127*p*Bpa-mutant mPrP-mCh and performing crosslinking at a series of increasing urea concentrations we found that above a 2% SDS the amount of dimer visible on the gels after crosslinking, can not be reduced (Figure IV-3, Appendix IV). Therefore, we chose this condition for measuring the background, originating from the temporary non-specific interactions. Further, we included the 2% SDS condition-samples in all of the crosslinking experiments performed, placing side-by-side the two samples, in 0.06% and 2% SDS conditions, for each particular *p*Bpa-mutant (Figure 9 and Figure IV-4, Appendix IV).

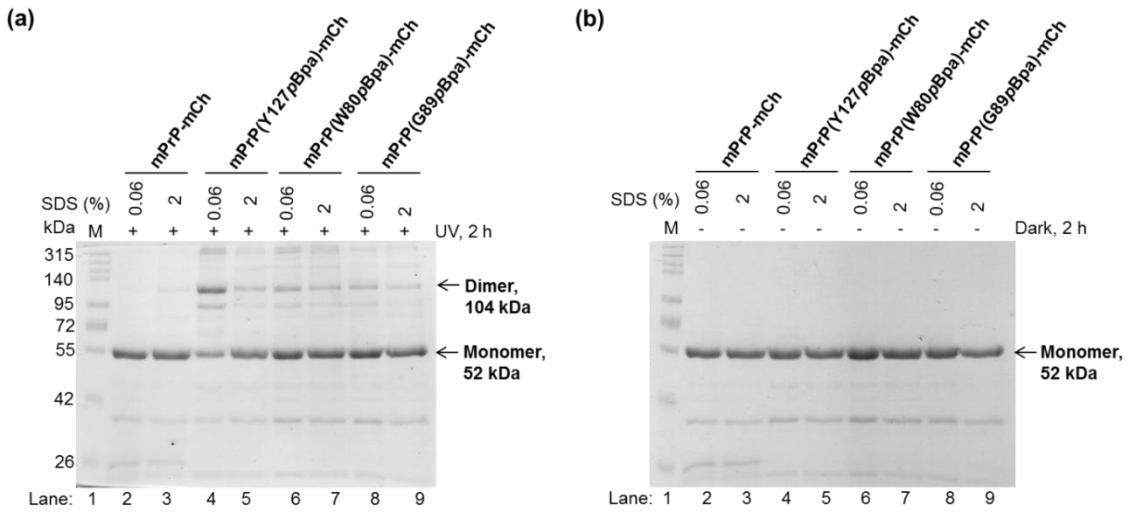

Figure 9. Assessing the specific and nonspecific dimers crosslinked. Representative SDS-PAGE gel images of wild type and selected *p*Bpa-mutant prion-mCherry proteins, as indicated on top of each gel, irradiated at 365 nm **(a)** or kept in the dark **(b)** for 2 h, at dimer (0.06%) or monomer (2%) favoring SDS conditions. For the rest of the 24 positional *p*Bpa-mutants see Figure IV-4, Appendix IV.

4.1.4. Comparison of crosslinking efficiencies permit identification of the residue positions involved in the dimerization interface of prion protein

The efficiencies of various positional *p*Bpa-mutants to crosslink PrP dimers at 0.06% SDS were calculated using gel-densitometry analysis of the SDS-PA gels of crosslinked proteins (presented on Figures 9 and Figure IV-4, Appendix IV) as described in the Experimental methods. The obtained results are indicated on Figure 10.

The highest efficiency of crosslinking the dimer was found for the mutant with *p*Bpa at position 127, which resulted about 40% crosslinked protein amount. This was followed by the positional *p*Bpa mutants 131, 107 and 128, respectively, yielding between 10% and 20% crosslinked products. In total, 10 of the 24 positions examined yielded crosslinked dimers at levels that were significantly higher than those corresponding to non-specific association in 2% SDS.

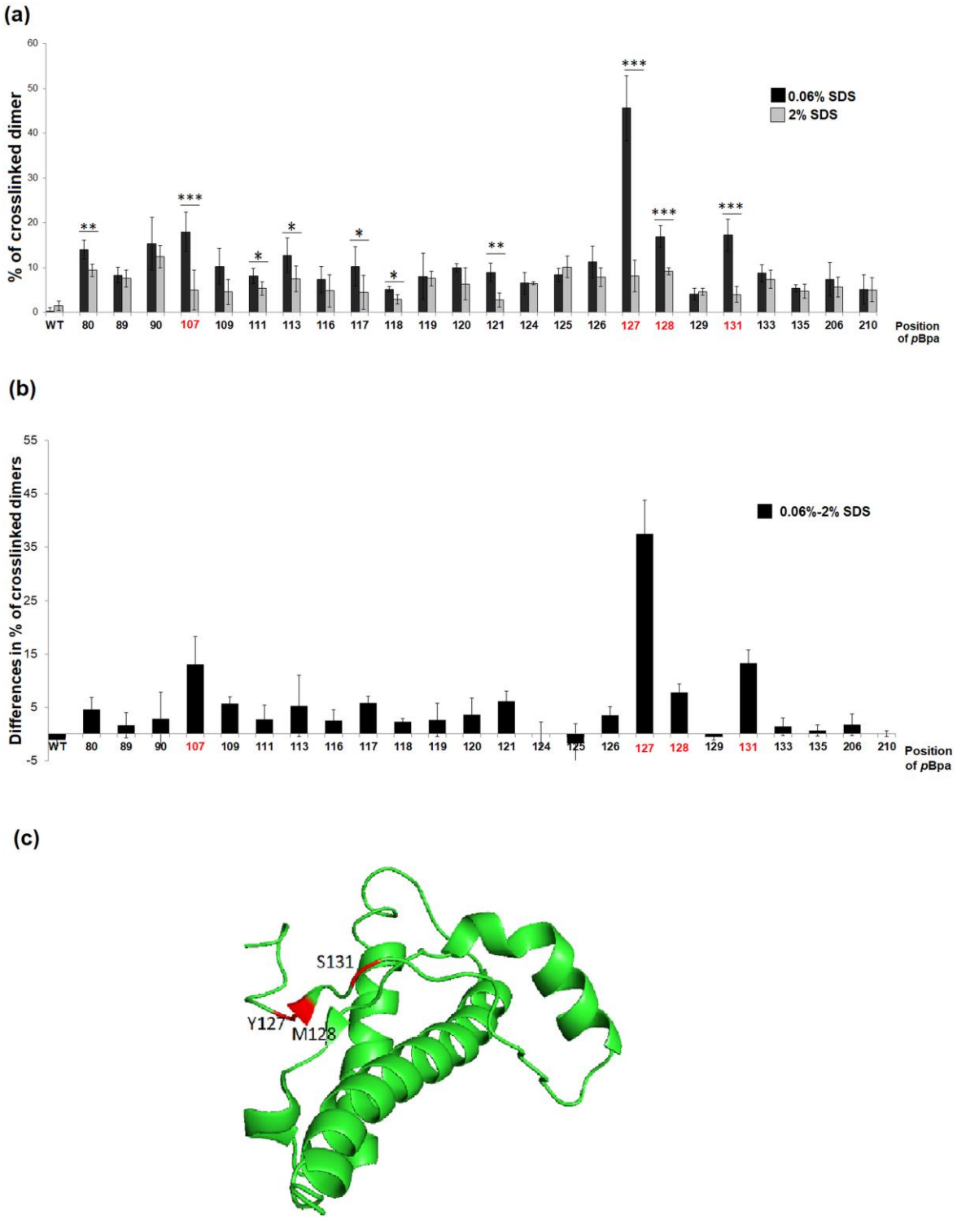

Figure 10. Dimer-crosslinking efficiencies of the various positional *p*Bpa-mutant variants of prion-mCherry proteins. The percentages of crosslinked dimers **(a)** obtained after gel-densitometry analysis of irradiated samples under conditions that favor dimerization (0.06% SDS, black bars) and monomeric state (2% SDS, grey bars) are shown. Calculations were done as described in the Experimental methods. Error bars represent the standard deviations.The efficiency of crosslinking **(b)** is calculated as the difference in values obtained

in dimer-specific and monomeric conditions (0.06% SDS and 2% SDS) for each protein. Significance test was performed by using Student's t-test. Levels of significance obtained are presented on panel **(a)** by asterisks, denoting as follows. *: $p<0.05$, **: $p<0.01$, ***: $p<0.001$. The three dimensional ribbon diagram of the mPrP, for the available sequence region 120-230 aa., **(c)** is shown with highlighting the most significant dimer-crosslinker positions (127, 128, 131) along the sequence on the 3D fold. Position 107 has significant dimer crosslinking efficiency as well, but it is outside of this fold.

4.1.5. Untagged prion protein mutants with site specific insertions of pBpa crosslink dimeric complexes efficiently under dimer formation conditions

After successfully optimizing the expression of *p*Bpa-containing tagged prion protein variants, we wanted to verify if the presence of mCherry tag had any effect on the dimerization of the prion proteins, therefore, we engineered a selected set of 14 pRSET-B expression plasmids for mPrPs with an amber codon-mutation, as described in Methods. The positions 80, 90, 107, 111, 113, 116, 119, 120, 121, 124, 127, 128, 129, 131, 206 and 210, were chosen for amber codon placement based on the results of Figure 10, representing both efficient and inefficient dimer-crosslinking. We produced the untagged proteins in *E. coli*, similarly to the mPrP-mCh proteins. The purified recombinant untagged wild type and *p*Bpa-mutant prion proteins display single bands on reducing SDS-PAGE gels at the expected molecular weights of 23 kDa (Figure 11a).

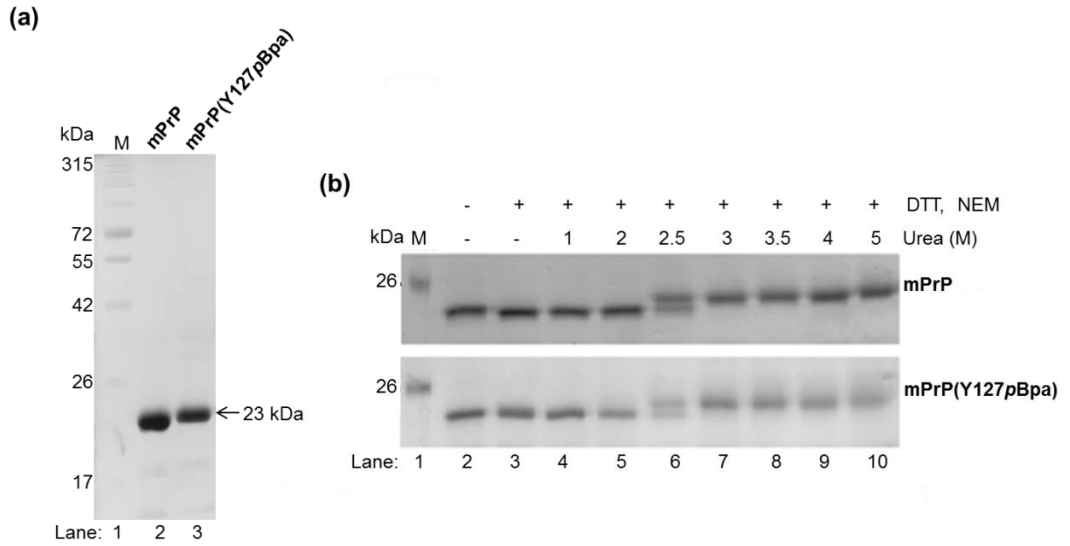

Figure 11. The conformational stabilities of untagged wild type and *p*Bpa-mutant PrPs aresimilar. Representative gel pictures of the untagged wild-type and *p*Bpa mutant mPrPc **(a)** showing single bands for the two at ~23 kDa. The purified wild type and *p*Bpa-

mutant(mPrPY127*p*Bpa) proteins are compared in the urea gradient assay **(b)**. Gels are 12% PA-SDS gels.

We used urea gradient assay to examine the stabilities of the untagged wild type and *p*Bpa-mutant prion proteins in the same way we tested the stabilities of mCherry-tagged variants. When comparing the wild type and the mPrP(Y127*p*Bpa) mutant, we found that both proteins possess same transition regions for folded to unfolded states, of between 2 to 3 M urea, and same transition midpoint at around 2.5 M (Figure 11b).

The untagged wild type and *p*Bpa-mutant PrPs were crosslinked in the same conditions as the mCherry-tagged versions of the proteins: at 0.06% and 2% SDS (in PBS, pH 7.4), to favor dimer and monomer formation of PrP, respectively, and were examined similarly on reducing SDS-gels. After irradiation, a crosslinked population of *p*Bpa-mutant protein samples can be observed at the expected molecular weight of a dimer (Figure 12a), at ~46 kDa. Higher molecular weight bands can also be detected, indicating low quantities of trimeric and tetrameric complexes of ~69 and ~92 kDa, respectively. There are no detectable dimers observed in the control samples that were kept at dark, in parallel with the samples (Figure 12b).

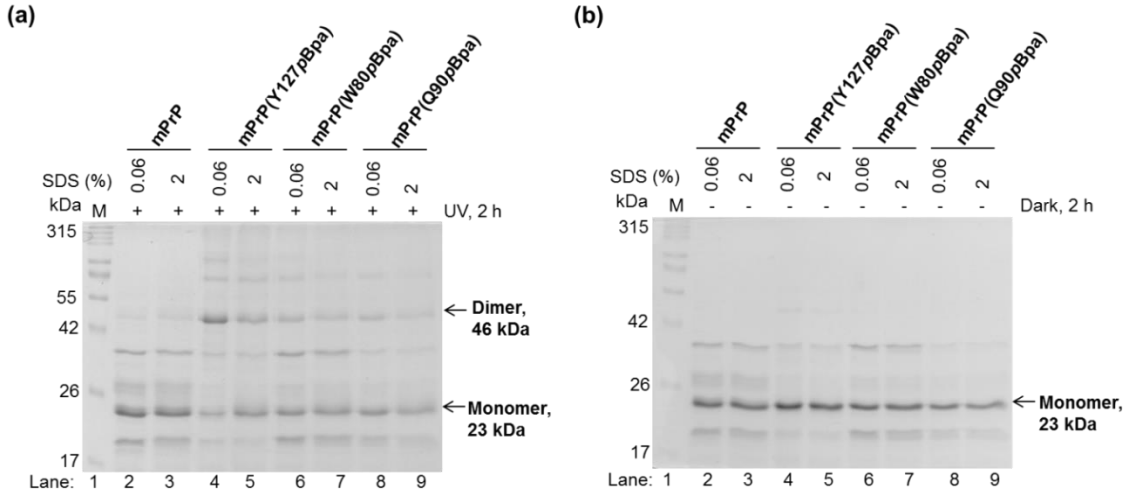

Figure 12. Detection of crosslinked dimers. Images of reducing 12% polyacrylamide gels of selected proteins with *p*Bpa-mutations irradiated at 365 nm for 2 h **(a)** and non-irradiated samples **(b)** incubated at dark in the same conditions. Proteins (6 μM) are crosslinked side-by-side in conditions of 0.06% and 2% SDS (in PBS, pH 7.4). The additional *p*Bpa-mutants tested are presented on Figure IV-5, Appendix IV.

Dimer percentages were calculated as described in the Experimental methods, and the obtained results presented on Figure 13.

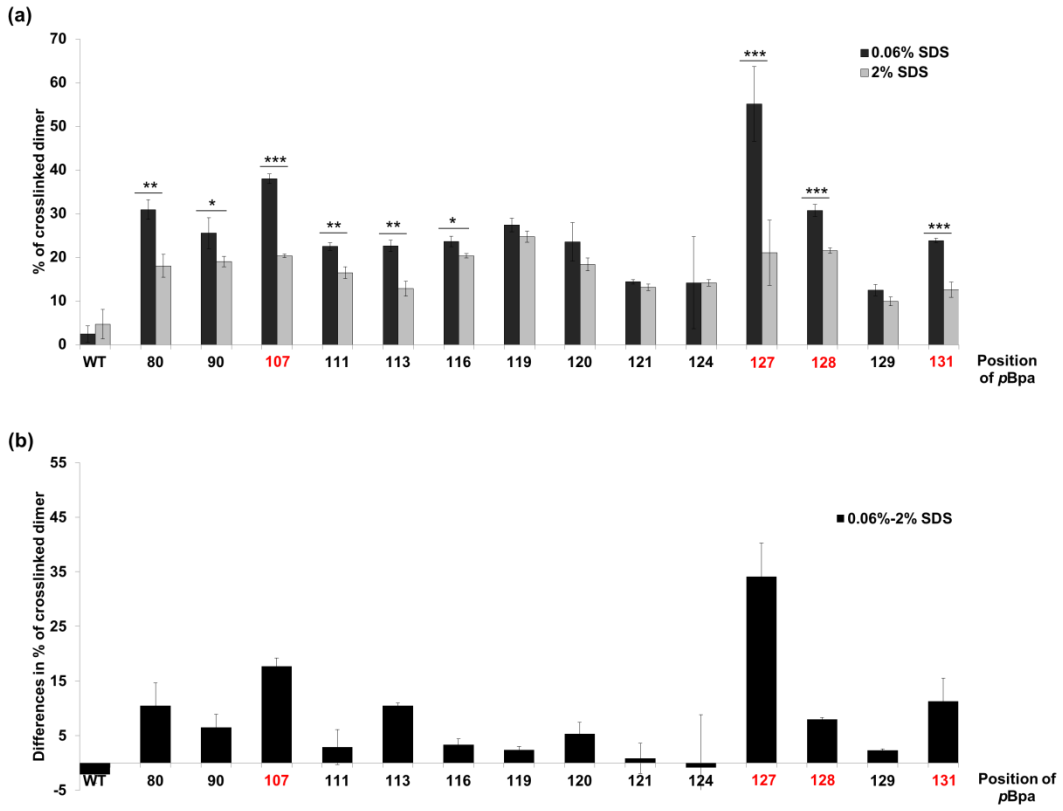

Figure 13. Dimer-crosslinking efficiencies of the various positional *p*Bpa-mutant variants of untagged mPrP proteins. Crosslinked dimer-percentages **(a)** obtained for *p*Bpa-mutants under conditions that favor dimerization (0.06% SDS, black bars) and in monomeric state (2% SDS, grey bars) are shown. Efficiencies of crosslinking **(b)** are calculated by the difference between the values obtained 0.06% SDS an 2% SDS. Bars representaverages of at least 4 repetitions of the experiment, and the error bars are standard deviations. Significance is determined by Student's t-test and the obtained levels of significance are shown on (a) by asterisks as follows *: $p<0.05$, **: $p<0.01$, ***: $p<0.001$.

The highest amounts of dimers could be crosslinked when *p*Bpa is inserted at position 127, yielding almost 40% crosslinked dimers above the unspecific control 2% SDS condition, similarly as was found in the case mCherry-tagged set of proteins. Also, as with the mCherry tagged proteins, the positional *p*Bpa-mutants 107, 128 and 131 exhibit high efficiencies. In total, nine out of the 14 mutants examined yielded significant amounts of crosslinked dimers.

These results show that the same positional *p*Bpa-mutants provide efficient dimer-crosslinking in both tagged and untagged forms and that the *p*Bpa-mutants have generally similar ranking whether tagged by mCherry or untagged.

We also investigated the secondary structural element rearrangements of the untagged wild type and the mutant proteins under monomeric and dimeric conditions, by recording and analyzing their far-UV CD spectra (Figure 14). We found that the *p*Bpa-mutations have no major effect on the native secondary structure of the proteins (Figure 14a), which confirm our

earlier results on the protein stabilities obtained by urea-stability assay (Figures 7 and 11b). We also found that there are only little alterations in the CD spectra of the prion proteins when comparing them in monomeric conditions and in dimer favoring conditions after crosslinking (Figure 14 a and b). When performing a detailed evaluation of the secondary structural element composition of these spectra by using the BestSel program, and comparing the structural elements such as regular helix (Helix1), distorted helix (Helix2), left-twisted anti-parallel β-sheet (Anti1), relaxed anti-parallel β-sheet (Anti2), right-twisted anti-parallel β-sheet (Anti3), parallel β-sheet, turn and other structural elements (Figure 14c), or when analyzing only the major secondary structural elements such as: total helix, total anti-parallel β-sheet, parallel β-sheet, turn and other structural elements (Figure 14d), we could not detect significant changes between monomeric-, dimeric crosslinked (+UV)-, and dimeric non-irradiated (-UV) samples. These indicate that PrP retains its overall helical fold when in dimer form, as previously had also been reported [91,92].

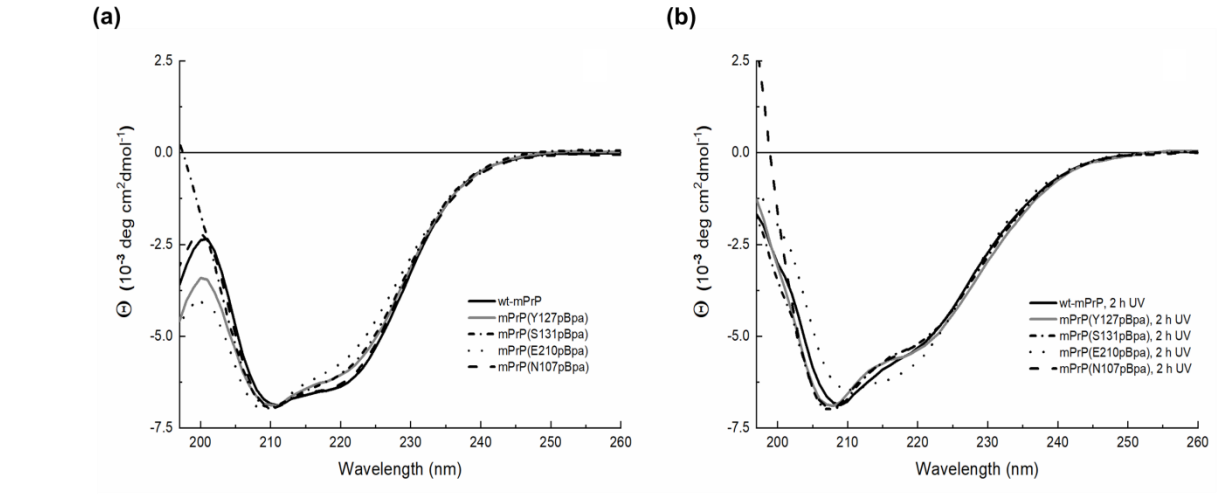
(a)
(b)
Θ (10⁻³ deg cm²dmol⁻¹)
Wavelength (nm)
wt-mPrP
mPrP(Y127pBpa)
mPrP(S131pBpa)
mPrP(E210pBpa)
mPrP(N107pBpa)
wt-mPrP, 2 h UV
mPrP(Y127pBpa), 2 h UV
mPrP(S131pBpa), 2 h UV
mPrP(E210pBpa), 2 h UV
mPrP(N107pBpa), 2 h UV

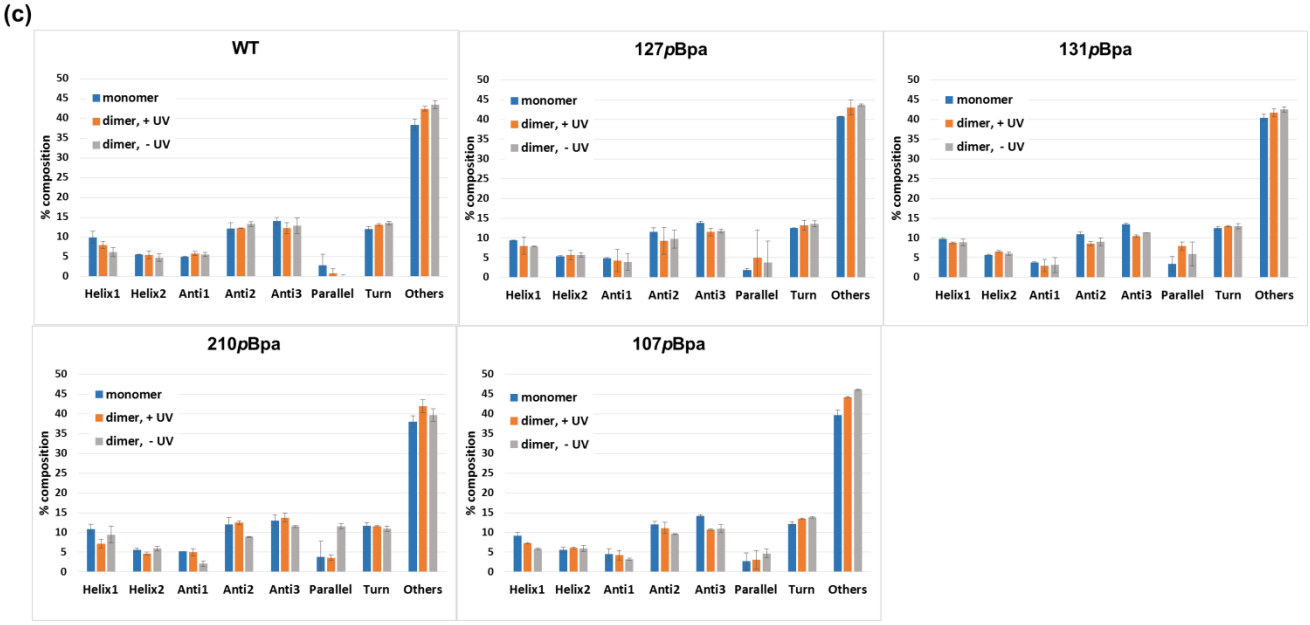
(c)
WT
127pBpa
131pBpa
210pBpa
107pBpa
% composition
monomer
dimer, + UV
dimer, - UV
Helix1
Helix2
Anti1
Anti2
Anti3
Parallel
Turn
Others

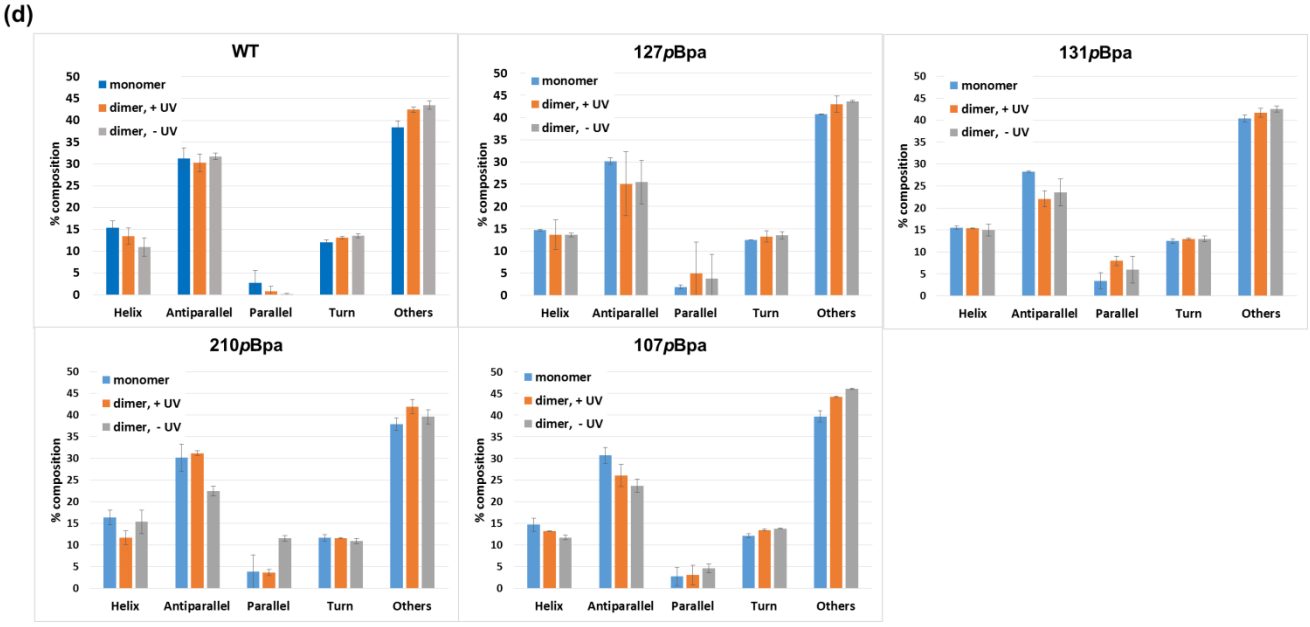
(d)
WT
127pBpa
131pBpa
210pBpa
107pBpa
% composition
monomer
dimer, + UV
dimer, - UV
Helix
Antiparallel
Parallel
Turn
Others

Figure 14. Secondary structural characteristics of wild-type untagged mPrP and its selected *p*Bpa-mutant variants in monomeric and dimeric conditions. Far-UV circular dichroism spectra of the purified proteins in water **(a)** and after bringing the samples into dimeric-state-favoring condition (0.06% SDS, PBS pH 7.2) and crosslinking by applying 2 h UV irradiation **(b)**. Panel **(c)** and **(d)** show the secondary structure evaluation of the spectra between 200 to 240 nm using the algorithm BeStSel [79] of the selected proteins, wild type and 127*p*Bpa-, 131*p*Bpa-, 210*p*Bpa-, 107*p*Bpa–mutant mPrPs. Bars represent average percentages derived from two to three independent crosslinking experiments. Error bars are the standard deviations from the mean. The colors represent the following conditions: monomeric state (blue), after crosslinking in dimeric-state (orange), without crosslinking, at dark, in dimeric-state (gray). The panels on **(c)** show a more detailed compositional evaluation for α– and β-strands based on the algorithm used (Helix1: regular helix, Helix2: distorted helix, Anti1: left-twisted anti-parallel beta sheet, Anti2: relaxed anti-parallel β-sheet, Anti3: right-twisted anti-parallel β-sheet, Parallel: parallel β-sheet, Turns, and Others: other structural elements) whereas the panels on **(d)** show the compiled data for the major secondary elements.

4.2. The study of the effect of G126V mutation on the dimerization of mouse prion protein

4.2.1. Mouse prion protein variants with site specific insertions of pBpa can be used to investigate heterodimerization

After successful study of the dimer interface of recombinant mPrP via genetic incorporation of the unnatural amino acid, *p*Bpa, we set forward to use this system to investigate the effect of the G126V mutation (the mouse equivalent of the human G127V mutation) on the dimerization of the pritein. For these studies we incorporated the *p*Bpa into the sequence of the untagged mPrP, either the wild type or the G126V mutant, using three different positions: 127, 128 and 131, for individual insertions of *p*Bpa, positions that gave the highest dimer-crosslinking efficiencies earlier in our dimer-interface studies presented above. To specifically monitor heterodimerization, we used these in pairs with mCherry-tagged mPrPs (wild type and/or G126V mutant) to easily distinguish the interacting proteins by SDS-PAGE (Figure 15).

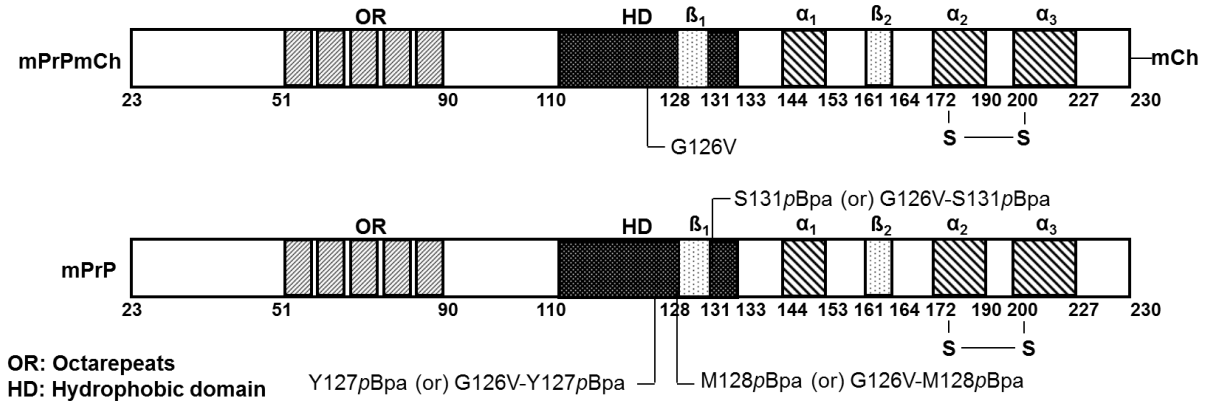

Figure 15. Schematic representation of the recombinant prion proteins generated to study the hetero- and homodimerization of mPrP. Top scheme depicts the primary structure of the mouse prion protein tagged with an mCherry (mCh), mPrP-mCh, with the location of the G126V mutation and of the mCh tag indicated. Lower scheme depicts the sequence of untagged mPrP, with the mutations indicated that were used: *p*Bpa incorporation at position 127 or 128 or 131 and/or G126V.

We designed the study as effectuating the experiments according to the steps presented on Figure 16.

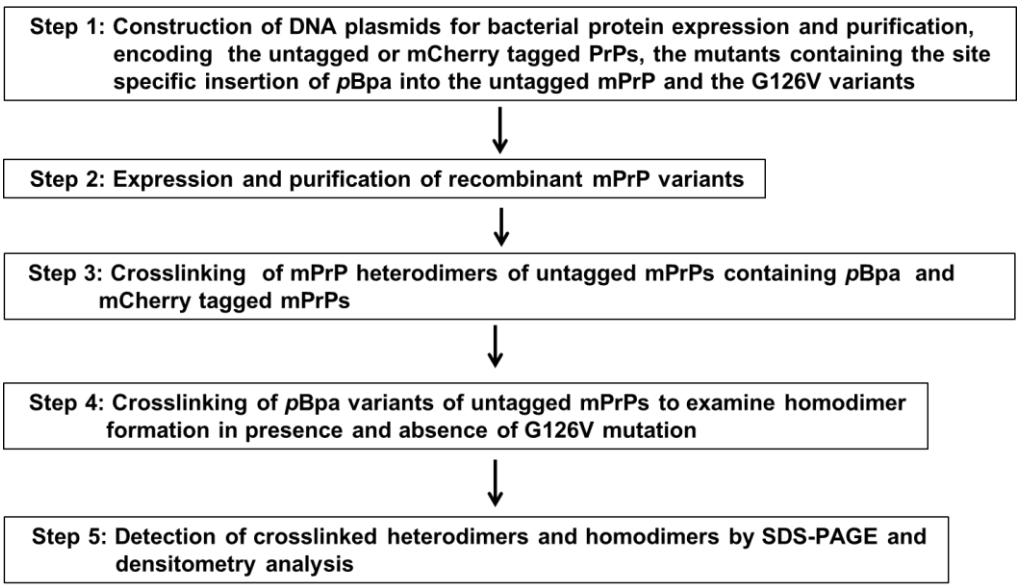

Figure 16. The major steps of the procedure employed to investigate the effect of G126V mutation on the heterodimerization and homodimerization of mPrP in *in vitro* conditions. DNA plasmids were generated for *E. coli* expression of wild type, G126V and *p*Bpa mutants mPrPs with or without fusion with mCherry (Step 1). The purified proteins (Step 2) were selected in pairs, one with mCherry tag and another with a *p*Bpa insertion, to be mixed for the studies of heterodimer formation by crosslinking (Step 3). Single protein variants with *p*Bpa were also selected to investigate homodimer formation (Step 4). SDS-

PAGE and densitometry analysis were used to evaluate the crosslinked hetero- and homodimers (Step 5).

The combination in which the *p*Bpa is incorporated into the mPrP-mCh fusion protein was not used because upon UV irradiation a band appeared on the SDS-gel at the expected position of a heterodimer in the case of the control sample containing only mPrP(Y127*p*Bpa)-mCherry with no untagged mPrP as interacting partner.

4.2.2. The G126V mutation has a diminishing effect on the dimerization of the mouse prion protein

First we tested whether the mCherry-tagged and untagged proteins with their wild-type aa. G126, can form heterodimers. For this purpose we chose the most efficient dimer-crosslinker *p*Bpa-mutant from our previous studies, the 127*p*Bpa variant of mPrP Crosslinking the selected proteins, we found that when the position 126 contains the wild type Gly residue, the mPrP(Y127*p*Bpa) effectively crosslinks mPrP-mCh (Figures 17 and 18). Next, we tested the heterodimerization of the prteins when they possessed a Val mutation in position 126, in combinations when either one of the interacting partners possessed 126Val or when both proteins at the same time possessed G126V. In each of these cases we found a reduction in the amount of heterodimers detected after crosslinking, implying an inhibition upon heterodimer formation (Figures 17 and 18). Performing similar experiments with the other two positional mutants: mPrP(M128*p*Bpa) or mPrP(S131*p*Bpa) with wild type G126 sequences and using the same experimental setup, *p*Bpa in the 128th position displayed no significant crosslinking with mPrP-mCh, whereas, *p*Bpa in the 131st position mediated significant, but less efficient heterodimer crosslinking compared to the 127*p*Bpa positional mutant (Figures IV-6 and -7, Appendix IV). Nevertheless, when the disease-protective mutation G126V was introduced in either the untagged mPrPs or the mPrP-mCh, it diminished the amount of detectable heterodimers in case of both 128*p*Bpa- and 131*p*Bpa-mutants (Figure 18 and Figure IV-7, Appendix IV).

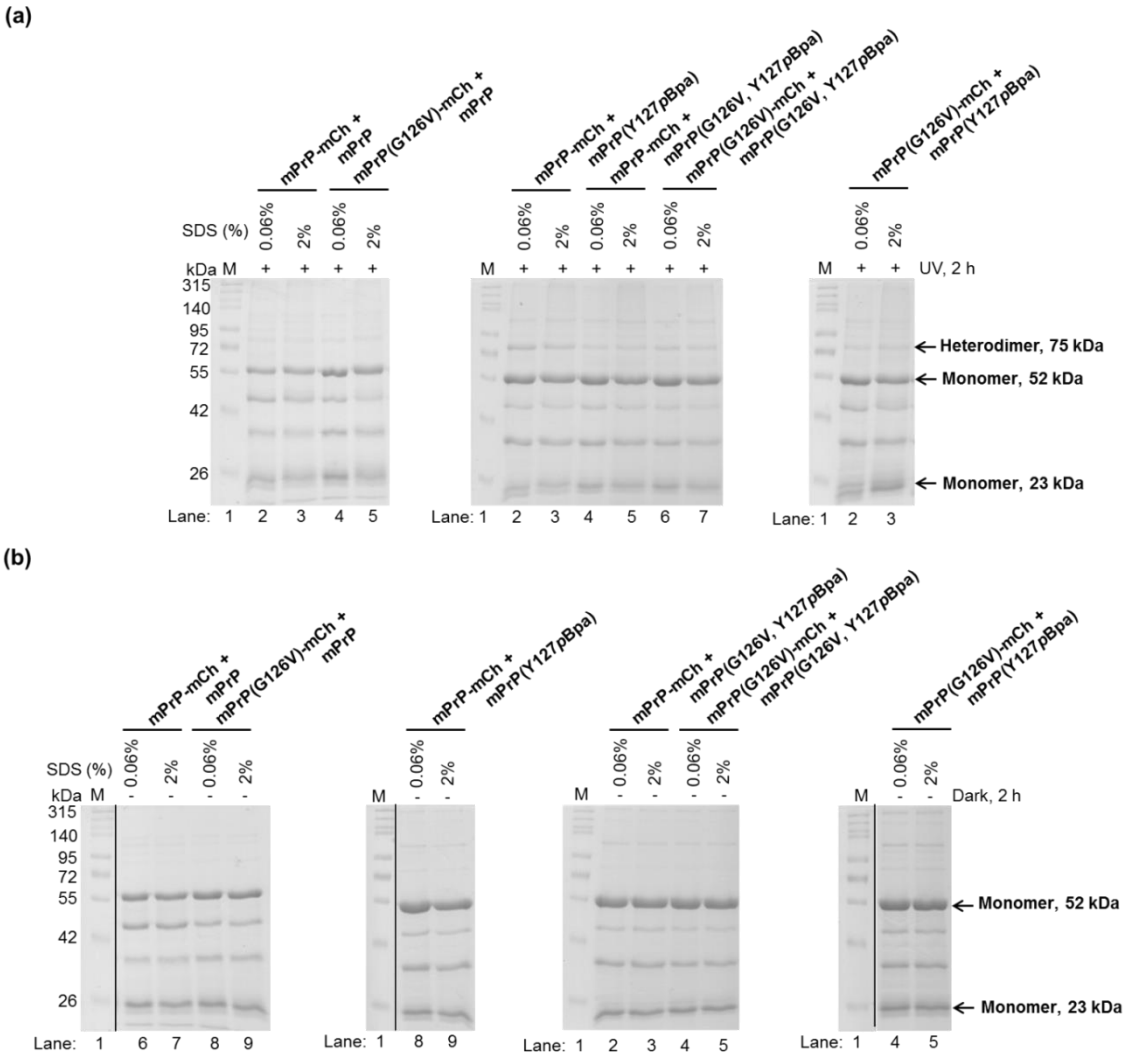

Figure 17. Effect of G126V on the amount of heterodimers crosslinked for untagged and mCherry tagged mPrPs. Photocrosslinked reaction mixtures of various mPrPs ("UV irradiated", + UV) **(a)** and their control, non-irradiated ("Non-irradiated controls", Dark) **(b)** counterparts on SDS-PAGE gels. In all of the reaction-mixtures illustrated, *p*Bpa is present at the position 127 in the untagged mPrP, (Y127*p*Bpa). In each case the partner protein is a mPrP-mCh fusion protein with or without a G126V mutation in the prion sequence. The expected position of the monomer and heterodimer is marked on the figure. The vertical black lines delineate the cropping positions on the gel images, from where lanes unrelated to the figure were eliminated. The images of the full-length gels are presented on Figure IV-8, Appendix IV.

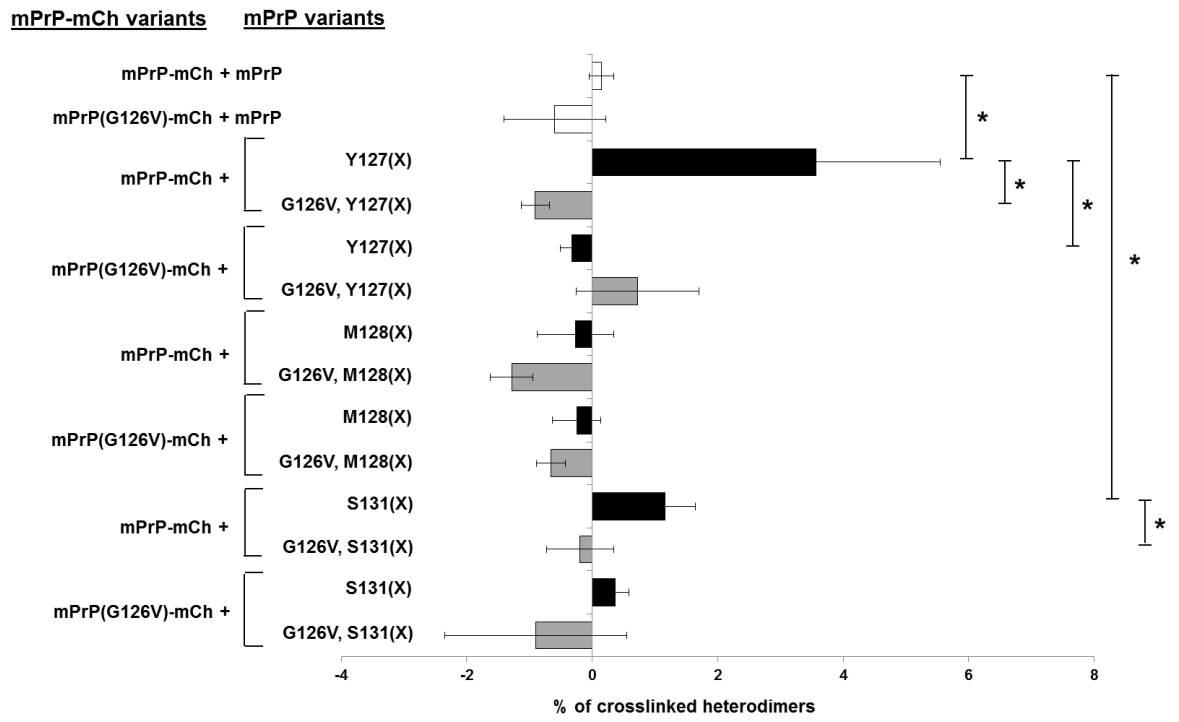

Figure 18. The G126V mutation in mPrP diminishes the formation of heterodimers. The X-axis shows the percentage of heterodimers. The crosslinked heterodimers is evaluated for the indicated mCherry-tagged and untagged prion protein mixtures, using three different positions for the *p*Bpa (denoted as "(X)" on the figure) substitution (Y127*p*Bpa, M128*p*Bpa and S131*p*Bpa) in untagged mPrP. The percentages are calculated based on gel densitometry analysis as described in the Experimental methods. White bars represent values obtained in the absence of *p*Bpa-insertion, i.e. for control samples. Black and grey color bars represent the % of heterodimers without and with Val mutation at position 126, respectively, in either untagged or mCh-tagged proteins. Statistical significances of the differences were determined by unpaired Student's t-test. Significantly different pairs are marked on the graph, and significance levels are represented by stars, *: $p \leq 0.05$. In the notation of Y-axis category names, "(X)" refers to *p*Bpa.

We also investigated the effect of the G126V mutation on the homodimerization of mPrP by crosslinking and evaluation of the homodimers in case of the three untagged *p*Bpa mutants,Y127*p*Bpa, M128*p*Bpa and S131*p*Bpa of mPrP, with or without the presence of the disease protective G126V mutation (Figure 19 and Figures IV-6, -7 and -8, Appendix IV).

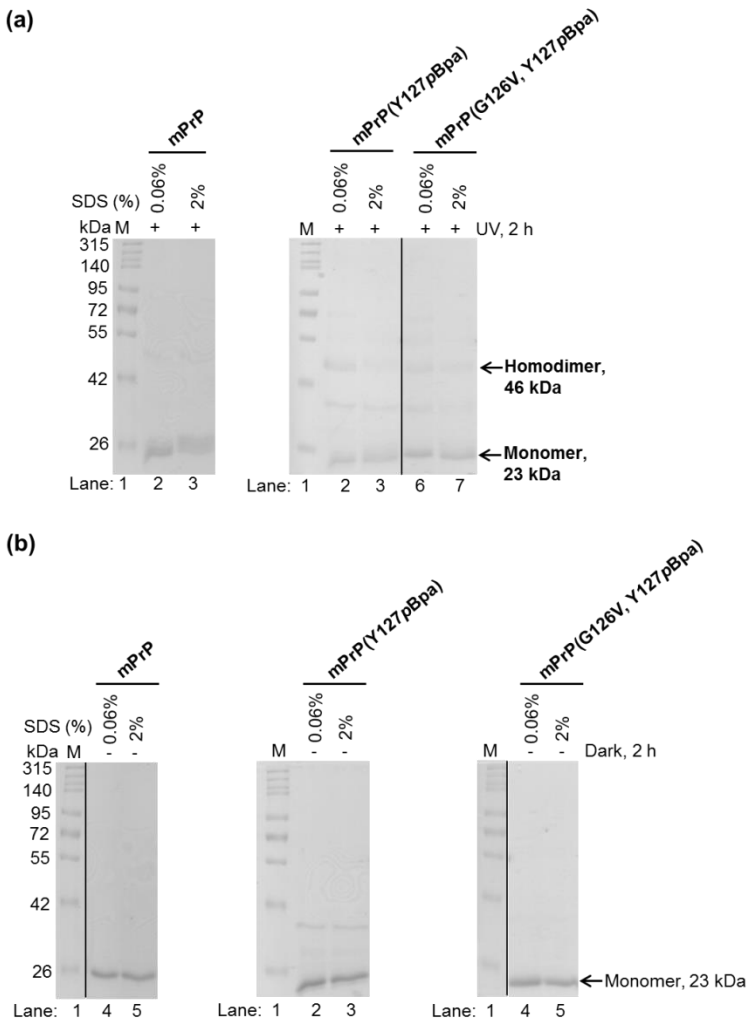

Figure 19. G126V mutation affects the amount of crosslinked homodimers for mPrP. Representative SDS-PAGE gel images of crosslinked ("UV irradiated", +UV) **(a)** and their corresponding non-irradiated control ("Non-irradiated controls", Dark) **(b)** samples of single proteins. The homodimers formed in the absence or presence of a G126V mutation were crosslinked using untagged mPrPs with *p*Bpa mutation at position 127. The expected positions of monomers and homodimers are indicated. The vertical black lines on some of the gels delineate the position of cropping of images, in order to omit lanes unrelated to the content discussed. Proteins (6 μM) are UV irradiated or incubated at dark, side-by-side in the presence of either 0.06% or 2% SDS (in PBS, pH 7.4), which favors either dimerization or the monomeric form of the prion protein, respectively. The images of the full-length gels are provided on Figure IV-8, Appendix IV).

Evaluating the gels by densitometry in a similar manner as for the dimer-interface studies and representing the results side-by-side for the 126G wild-type and for the 126V protective mutant, we can observe a decreased amounts of homodimers for the valine mutant (Figure 20).

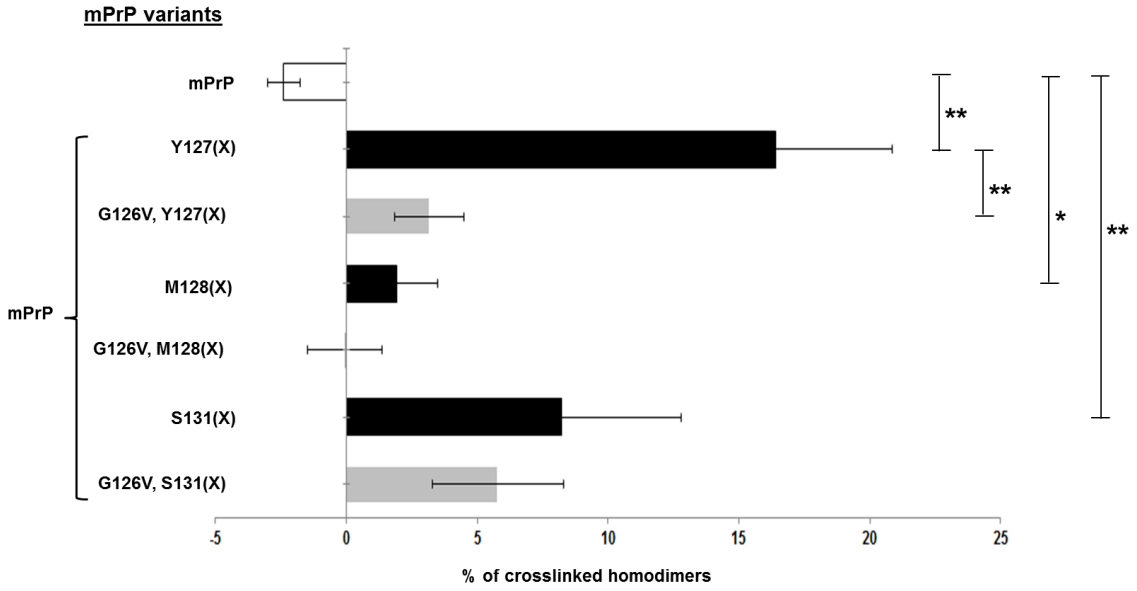

Figure 20. The G126V mutation diminishes the formation of homodimers of mPrP. On the X-axis, the percentage of crosslinked homodimers is represented for the indicated PrP variants as categories on the vertical axis. Efficiencies of homodimers were assessed after photocrosslinking for single-type *p*Bpa-mutant mPrPs: mPrP(Y127*p*Bpa), mPrP(M128*p*Bpa) or mPrP(S131*p*Bpa), either comprising a G126V mutation (grey color bars) or not (black bars). As a negative control, mPrP without *p*Bpa was used (white bar). Percentages were calculated using gel densitometry analysis as described in the Experimental methods. Unpaired Student's t-test was used to determine the statistical significance of differences. Significantly different pairs and the level of significance are indicated by stars and correspond to **: $p \leq 0.01$. In the notation of Y-axis category names, "(X)" denotes *p*Bpa, referring to the *p*Bpa-mutation at the stated positions.

However, given the relative size of the scatter of the data from 3 parallel experiments, the diminishing effect of G126V on homodimeric PrP formation reached a statistically significant level only in case of crosslinking of the mPrP(Y127*p*Bpa) variant.

4.2.3. The disease protective mutation G127V does not interfere with dimerization of mPrP in cellulo

Further, in a collaborative work with Prof. Jörg Tatzelt (Institute of Biochemistry and Pathobiochemistry, Ruhr-University Bochum, Bochum, Germany), we have investigated whether the G126V mutation has a similar effect on the dimerization of mPrP in *in cellulo* conditions, using a model cellular system. These experiments had been performed by the Laboratory of Prof. Tatzelt, therefore, the results obtained are only summarized here, to aid a better understanding of our findings and their discussion. These results are presented in detail in our joint publication, Sangeetham et al., 2021 [93].

To accomplish this aim, a similar approach was used as previously developed by the Tatzelt group [94] for studying dimerization of mPrP in a cellular environment. This employs in parallel cysteine mutants (S132C) of mPrP to identify the dimers through disulphide bond stabilization, and native co-immunoprecipitation of the wild type (with Ser at 132nd position) proteins, while these are transiently expressed by cells. To test the effect of the disease protective mutation G127V (human numbering), the corresponding pointmutation (G126V in the mouse sequece) was introduced into the mPrP sequence (hereafter reffered to as the G127V mutant). DNA constructs were made encoding: wild type or G127V mutants, with and without 132Cys mutation, and hemagglutinin (HA) - or V5 fusion tags, respectively. The introduced cysteine can form intermolecular disulphide bond between dimers of PrP, while the fusion tags serve for immunoprecipitation and Western blot identification of the protein partners. The plasmids, encoding G127V mutant and/or corresponding wild type, were transiently transfected or co-transfected into HeLa cells. Immunofluoroscence and Western blot analysis revealed that G127VPrP variant, is localized at the plasma membrane, forms homodimers and is complex glycosylated similarly to wild type PrP. Western blot analysis was used to detect homo- or heterodimers, in reducing and non-reducing conditions, of the Cystein mutants with either HA or V5 tags, in cell lysates of cells expressing these proteins. The dimer formation assessed by densitometry analysis of the Western blots revealed that the G127V mutant variant forms disulfide bond-linked homodimers and also heterodimers with the wild type protein, and that the mutation does not have an effect on these interactions. Native co-immunoprecipitation experiments yieded similar result in case of the S132 proteins for the G127V mutant. All together, these results show that contrary to *in vitro* results, there is no measurable effect of the G127V mutation on the dimerization *in cellulo*.

5. DISCUSSION

Previous studies using recombinant hamster PrP (aa. 90–231) indicated that the dimer form of PrP possesses predominantly α-helical structure and it had been proposed that the dimeric form may act as an intermediate on the putative pathway of transition of PrP^C to the pathogenic form [76,95]. These studies were conducted with the argument that recombinant hamster PrP (aa. 90–231), represents the amino acid sequence of infectious prion rods or PrP 27–30, containing only the globular, rigid part of the structure. To elucidate more precisely the structure of the dimer formed by the normal, healthy prion protein, we used the full length

recombinant mPrP (aa. 23-230) in order to better approximate the physiological fold of the protein, and studied both in untagged and tagged forms where we placed an mCherry fusion protein at the mPrP's C-terminal end. In contrast to previous investigations, we used a site-specific approach by incorporating a *p*Bpa, as a non-cannonical amino acid at desired positions of the sequence of mPrP. *p*Bpa is photoreactive and can act as a site-specific crosslinker, which upon UV irradiation reacts with nearby C-H groups of protein backbones and side chains if they are within 3.1 Å from the carbonyl oxygen of *p*Bpa. However, when flexible parts of a complex are crosslinked and a nearby methionine is present, it may mediate efficient crosslinking up to a distance of 13 Å, a phenomenon known as the magnet effect of methionine [96]. The 90-135 aa. segment of PrP is known to possess flexibility in PrP's monomeric and dimeric states, whereas, the 124-135 region appears as structured in the solution NMR studies. Thus, many of the positions that we selected for *p*Bpa substitutions in our studies lie in the 90-135 flexible region, which also harbors two methionines. However, the flexible 23-124 fragment lacks methionine, which significanctly decreases the likelihood of such an unspecific methionine "magnet effect" [96].

In this study we generated mPrP variants with substitutions of specific residues with *p*Bpa along the sequence of the protein. These variants enabled us to investigate the dimerization interface of PrP. *p*Bpa confers highest propensity for crosslinking the dimer when placed at the beginning of the structured domain of PrP, aa. positions 126-131(with 127 *p*Bpa being the most efficient), implying that this region is either part of or adjacent to the dimer interface. Previous investigations have reported that a Cys131 mutant of overexpressed mouse PrP^{C} forms disulfide-bonded dimer in the membrane of SH-SY5Y human neuroblastoma cells, indicating that position 131 is part of or close to the homodimeric interface [37]. Our results corroborate these findings , supporting the notion that PrP^{C} dimers formed in the cell membrane of mammalian cells under more physiological condition and those formed *in vitro*, in 0.06% SDS conditions, share structural similarities.

The incorporation of *p*Bpa in numerous positions of flexible N-terminal of PrP, between aa. 80 to 126, mediates dimer crosslinking to a lesser but significant extent. Aa. positions 107, 111 and 113 yielding high specificity crosslinking are at the beginning of the HD region (aa. 111-134) of PrP. The highest crosslinking efficiencies are obtained in case of the positiona *p*Bpa variants 127, 128 and 131, which are part of the second aprt of the HD. By contrast, some positions within the HD region, exhibit lesser amounts of dimer crosslinked for the mCherry-tagged mPrP, and five of the aa. positions (119, 120, 121, 124 and 129) examined with the untagged protein exhibit no specific crosslinkings. Because the *p*Bpa mutation in

position at the dimer-interface might interfere with the binding, more efficient *p*Bpa crosslinkings might occur at regions nearby the actual binding site. Thus, this observation is consistent with a model in which the HD region participates in dimer formation by forming a homodimeric interface. Strikingly, the Tatzel's lab reported that in the absence of the HD region, a disulfide-bonded dimer of PrP involving Cys131 did not form, highlighting the importance of the HD region in dimer formation [37].

In addition to the protein segment involving the HD region, we also investigated PrP variants possessing *p*Bpa at either position 89 or 90. The results of specific crosslinking with both variants support previous works from the Riesner group using similar experimental conditions (0.06% SDS, pH 7.2), but recombinant hamster recPrP(90-231), in which the N-terminal amino group of Gly90 is crosslinked to Glu152, or Glu196 or Asp202 in both the dimer and monomeric protein [76,95]. The specificity of the interactions towards just three out of the several other acidic side chains present in the protein, indicates that the this region of the N-terminal domain of the recombinant protein is constrained to at least one side of the PrP fold, while, the very N-terminal parts retain some conformational freedom. Molecular modeling using some of these experimental constrains resulted in a structure in which the 90-124 aa. tail acquires stabile structural features and folds back along the 128-152 aa. segment, forming the dimer's homodimeric interface [76,95]. Our results showing the presence of interaction sites along the enitre 90-125 aa. segment is consistent with this structure and establishes a link between the dimers observed with prion proteins anchored to the plasma membrane of mammalian cells and the dimers observed with the recombinant prion protein *in vitro* in 0.06% SDS. The *p*Bpa-containing PrP variants and the methods established here, among other approaches, may potentially aid direct testing of whether the dimer observed here is on the pathways of oligomerization, fibrillization and possibly of the formation of PrP^{Sc}, via triggering the process from the covalently crosslinked dimer forms.

Our photocrosslinking results indicate that the N-terminal flexible tail, approximately between 90 and 124 aa. of PrP, acquires some stabile, structurally constrained conformations in the dimer formed at low SDS concentration *in vitro* and, similarly to the dimer formed in the mammalian cell membrane, likely forms a homodimeric interface involving at least parts of the HD. The methodology developed here allows for easy access to ncAA-containing PrP variants and, when combined with mass spectrometry analysis, could also aid in mapping the interface of PrP molecules in PrP^{Sc} and in amyloid PrP preparations. Furthermore, the study demonstrates that the dimerization of full length mPrP, is mediated by its N-terminal region

and the approach we developed here holds promis for elucidating the structure of the protease resistant PrP^{Sc} form.

Previous NMR structural studies on wild type HuPrP (aa. 91–231) and *in silico* findings suggest that Tyr128 plays a key role in dimer formation, and altering the Gly127 to Val changes the orientation of this Tyr128 side chain, while diminishing PrP dimerization [58]. Here we used full length mPrP and site-specific photocrosslinking via *p*Bpa127-mutant of mPrP, mPrP(Tyr127*p*Bpa), to investigate the effect of G126V mutation corresponding to HuPrP(G127V) disease-protective mutation on homo- and heterodimerization of the protein. In both homo- and heterodimerization experiments with an mCherry tagged variant of mPrP, we found that the presence of G126V diminishes homo- and homodimer formation under *in vitro* conditions. When we studied earlier the dimerization interface of mPrP using this *p*Bpa-mutant, Tyr127*p*Bpa, we obtained the highest dimer-crosslinking among 24 single *p*Bpa-mutant variants, of different positions of *p*Bpa. This confirmed that position 127 has a prominent role in the formation of mPrP dimer interface, and also indicated that a Tyr to *p*Bpa mutation has no detrimental effect on dimer formation. Since this *p*Bpa substitution is exactly in the aforementioned position, of the *in silico* studies, the G126V mutation in the mPrP(Tyr127*p*Bpa) protein may affect directly the orientation of the *p*Bpa residue and thus its crosslinking, without affecting the dimerization itself. However, in the crosslinking experiments of mPrP(Y127*p*Bpa) with mPrP(G126V)-mCh, where the G126V mutation lies in the partner protein and can not directly affect the orientation of the *p*Bpa side chain, the effect of G126V is apparent, significantly lowering the percentage of crosslinkable dimers. We also employed a mammalian cell culture system, to study the effect of the protective G127V mutation on homo- and heterodimerization of the mouse prion protein. Using HeLa cells overexpressing the mutat and wild type mPrPs, we found that the G127V mutation (G126V mPrP) forms homodimers and also heterodimers with wild type mPrP under physiological conditions, as well as that contrary to the *in vitro* findings, the mutation did not exhibit diminishing effect on mPrP dimer formation.

Previous studies on the full-length prion protein revealed that in *in vitro* and in mammalian cell culture experiments at physiological conditions the protein formes dimers with similar features [37,76]. Here the two systems confer contrasting results. While the presence of G126V reduces dimer formation *in vitro*, this proclivity of the G126V mutation is not detected in cell culture experiments. The observed disparity may be attributed to the confinement of the GPI-anchored prion protein to a two-dimensional membrane surface in the

cell culture experiments, as opposed to the recombinant protein, which moves freely in a solution in the test tube. Indeed, transgenic mouse models demonstrated that the C-terminal GPI anchor has a significant impact on PrP^{C} folding [97]. Generation of transgenic mice expressing cellular prion protein (PrP^{C}) with stop codon mutant (S231X), lacking the GPI anchor, revealed that this form of PrP causes neurodegeneration [97,98]. Furthermore, brain extracts from both human patients expressing stop codon mutants, Y226X and mice expressing S231X contain infectious prions and are capable of transmitting disease. These findings suggest that the absence of the GPI anchor/membrane attachment promotes spontaneous conversion of the protein into infectious and neurotoxic conformers that may also be a consequence of more flexibility in the absence of the anchor.

Latest findings provided a mechanistic explanation on mutant HuPrP(G127V) (aa. 119-231, PrP fragment devoid of 23-118 region) inhibiting prion propagation, arguing that the G127V mutation alters the backbone conformation preceding the ß-sheet of the protein enhancing the intermolecular hydrogen bonding, which facilitates stablization of PrP dimers, inhibiting in turn the prion propagation [99]. *In vitro* studies demonstrated that flexible and unstructured N-terminal regions of PrP have an intrinsic tendency to form homodimers and are involved in dimerization interface of PrP [76,100]. In the lack of these interactions mediated by the 23-118 N-terminal tail, the destabilizing effects of G127V mutation are not evident in the *in vitro* experiments [99]. In contrast, the N-terminal PrP fragment has been reported to be involved in interactions with cellular partners,which may restrict its conformation and thus may be responsible also for the apparent absence of the destabilizing effect of the V127 mutation on PrP dimers *in cellulo*. Furthermore, *in cellulo* studies clearly show that the effect of the G126V mutation on dimerization of the full length mPrP as demonstrated by *in vitro*, molecular dynamics and NMR studies, is not becoming apparent within the complexity of the cellular context.

Overall our findings are in accordance with NMR structural and *in silico* studies showing that the G127V mutation inhibits the formation of PrP dimers, and our study emphasizes the important role of the flexible N-terminal in the conformational (mis)folding of PrP. It also draws attention upon the differences that may result from different approaches and of using *in vitro* anchorless vs. cellularly expressed full length PrP.

6. CONCLUSIONS

In this work, we produced a set of 44 variants of recombinant full length mouse prion protein, mPrP, majority of which possessed a site-specific insertion of one non-canonical amino acid, *p*Bpa, in order to permit covalent photocrosslinking and the study of interactions and interaction sites of mPrP. We proved the usefulness of this approach and of the set of proteins created as a tool, in two studies. First, we used this system to interrogate the dimerization interface of the full length mPrP. Second, we used this approach to test the effect of the prion disease-refractive mutation G126V (equivalent to G127V in HuPrP) on the homo- and heterodimerization of mPrP. Our major findings include the following.

1. Insertion of the photocrosslinkable ncAA *p*Bpa as a point mutation into the sequence of the mPrP using *E. coli* system was efficient. The presence of the *p*Bpa at the chosen positions did not disturb the stability of the protein, and provided efficient crosslinking in order to study the dimerization of mPrP by SDS-PAGE and densitometry analysis. Proving also that the developed system can be used as a site-specific tool to interrogate the interaction surfaces of PrP.
2. Using this system, we found that the N-terminal part of the prion protein, specifically the regions around position 127 and 107, is integral part of the dimerization interface of the full length mPrP, and that the formed dimers are alpha helical.
3. By using selected proteins from the set of *p*Bpa-mutant variants, and by creating targeted additional mutants, we studied the effect of the prion disease-refractive mutant G126V of mPrP on the homo- and heterodimerization of the protein, and found that this mutation has a diminishing effect on dimerization of the protein *in vitro*. These results are in agreement with previous NMR and MD simulation studies. However, our results obtained in a collaborative work in corresponding experiments using cell culture systems showed no major effects of this mutation on dimerization *in cellulo*, indicating a more complex nature for the mechanism of effect of G126V in protecting against disease at cellular level.

Taken together, the system we developed and the large set of *p*Bpa-variants of mPrP that we created, proved to be a useful tool in the study of the dimerization interactions and the interaction surfaces of the mPrP. Thus, it may also prove useful in studies of other interactions of the prion protein, such as, it may facilitate to gain in depth site-specific

structural insights into its oligomeric and fibrillar species, including the pathological variants of prion, helping this way to uncover details on the mechanisms of prion disease.

REFERENCES

[1] S.B. Prusiner, Prions, Proc. Natl. Acad. Sci. U. S. A. 95 (1998) 13363–13383. doi:10.1073/pnas.95.23.13363.

[2] A. Aguzzi, F. Baumann, J. Bremer, The Prion's Elusive Reason for Being, Annu. Rev. Neurosci. 31 (2008) 439–477. doi:10.1146/annurev.neuro.31.060407.125620.

[3] J. Collinge, Prion diseases of humans and animals: their causes and molecular basis., Annu. Rev. Neurosci. 24 (2001) 519–550. doi:10.1146/annurev.neuro.24.1.519.

[4] S.B. Prusiner, M.R. Scott, S.J. DeArmond, F.E. Cohen, Prion protein biology, Cell. (1998). doi:10.1016/S0092-8674(00)81163-0.

[5] S. Mead, M.P.H. Stumpf, J. Whitfield, J.A. Beck, M. Poulter, T. Campbell, J.B. Uphill, D. Goldstein, M. Alpers, E.M.C. Fisher, J. Collinge, Balancing selection at the prion protein gene consistent with prehistoric Kurulike epidemics, Science (80-.). (2003). doi:10.1126/science.1083320.

[6] C. Chen, X.P. Dong, Epidemiological characteristics of human prion diseases, Infect. Dis. Poverty. (2016). doi:10.1186/s40249-016-0143-8.

[7] S.B. Prusiner, Molecular biology of prion diseases, Science (80-.). 252 (1991) 1515–1522. doi:10.1126/science.1675487.

[8] T.E. Eckland, R.A. Shikiya, J.C. Bartz, Independent amplification of co-infected long incubation period low conversion efficiency prion strains, PLoS Pathog. (2018). doi:10.1371/journal.ppat.1007323.

[9] M.P. Murphy, H. Levine, Alzheimer's disease and the amyloid-β peptide, J. Alzheimer's Dis. (2010). doi:10.3233/JAD-2010-1221.

[10] K.A. Jellinger, Neuropathology of sporadic Parkinson's disease: Evaluation and changes of concepts, Mov. Disord. (2012). doi:10.1002/mds.23795.

[11] J. Labbadia, R.I. Morimoto, Huntington's disease: Underlying molecular mechanisms and emerging concepts, Trends Biochem. Sci. (2013). doi:10.1016/j.tibs.2013.05.003.

[12] I. Ramasamy, M. Law, S. Collins, F. Brooke, Organ distribution of prion proteins in variant Creutzfeldt-Jakob disease, Lancet Infect. Dis. (2003). doi:10.1016/S1473-3099(03)00578-4.

[13] F. Wopfner, G. Weidenhöfer, R. Schneider, A. Von Brunn, S. Gilch, T.F. Schwarz, T. Werner, H.M. Schätzl, Analysis of 27 mammalian and 9 avian PrPs reveals high conservation of flexible regions of the prion protein, J. Mol. Biol. (1999).

doi:10.1006/jmbi.1999.2831.

[14] A.R. Castle, A.C. Gill, Physiological functions of the cellular prion protein, Front. Mol. Biosci. (2017). doi:10.3389/fmolb.2017.00019.

[15] S. Yoon, G. Go, Y.M. Yoon, J.H. Lim, G. Lee, S.H. Lee, Harnessing the physiological functions of cellular prion protein in the kidneys: Applications for treating renal diseases, Biomolecules. 11 (2021). doi:10.3390/biom11060784.

[16] N. Singh, D. Das, A. Singh, M.L. Mohan, Prion protein and metal interaction: Physiological and pathological implications, Curr. Issues Mol. Biol. (2010). doi:10.21775/9781912530076.04.

[17] A. Aguzzi, M. Heikenwalder, Pathogenesis of prion diseases: Current status and future outlook, Nat. Rev. Microbiol. 4 (2006) 765–775. doi:10.1038/nrmicro1492.

[18] F.F. Damberger, B. Christen, D.R. Peŕez, S. Hornemann, K. Wuẗhrich, Cellular prion protein conformation and function, Proc. Natl. Acad. Sci. U. S. A. (2011). doi:10.1073/pnas.1106325108.

[19] R. Riek, S. Hornemann, G. Wider, M. Billeter, R. Glockshuber, K. Wuthrich, NMR structure of the mouse prion protein domain PrP(121-231), Nature. (1996). doi:10.1038/382180a0.

[20] K. Wüthrich, R. Riek, Three-dimensional structures of prion proteins, Adv. Protein Chem. (2001). doi:10.1016/S0065-3233(01)57018-7.

[21] C. Acevedo-Morantes, H. Wille, The Structure of Human Prions: From Biology to Structural Models — Considerations and Pitfalls., Viruses. 6 (2014) 3875–3892. doi:10.3390/v6103875.

[22] H. Büeler, M. Fischer, Y. Lang, H. Bluethmann, H.P. Lipp, S.J. Dearmond, S.B. Prusiner, M. Aguet, C. Weissmann, Normal development and behaviour of mice lacking the neuronal cell-surface PrP protein, Nature. 356 (1992) 577–582. doi:10.1038/356577a0.

[23] J.A. Richt, P. Kasinathan, A.N. Hamir, J. Castilla, T. Sathiyaseelan, F. Vargas, J. Sathiyaseelan, H. Wu, H. Matsushita, J. Koster, S. Kato, I. Ishida, C. Soto, J.M. Robl, Y. Kuroiwa, Production of cattle lacking prion protein, Nat. Biotechnol. 25 (2007) 132–138. doi:10.1038/nbt1271.

[24] S.L. Benestad, L. Austbø, M.A. Tranulis, A. Espenes, I. Olsaker, Healthy goats naturally devoid of prion protein, Vet. Res. 43 (2012). doi:10.1186/1297-9716-43-87.

[25] Y.R. Li, Q. Li, J.M. Yang, X.M. Zhou, X.M. Yin, D.M. Zhao, Expression patterns of Doppel gene in golden hamster: Quantification using real-time RT-PCR, Mol. Cell.

Probes. 22 (2008) 255–258. doi:10.1016/j.mcp.2008.04.004.

[26] A. Behrens, N. Genoud, H. Naumann, T. Rülicke, F. Janett, F.L. Heppner, B. Ledermann, A. Aguzzi, Absence of the prion protein homologue Doppel causes male sterility, EMBO J. 21 (2002) 3652–3658. doi:10.1093/emboj/cdf386.

[27] M. Premzl, L. Sangiorgio, B. Strumbo, J.A. Marshall Graves, T. Simonic, J.E. Gready, Shadoo, a new protein highly conserved from fish to mammals and with similarity to prion protein, Gene. 314 (2003) 89–102. doi:10.1016/S0378-1119(03)00707-8.

[28] V. Sakthivelu, R.P. Seidel, K.F. Winklhofer, J. Tatzelt, Conserved stress-protective activity between prion protein and Shadoo, J. Biol. Chem. (2011). doi:10.1074/jbc.M110.185470.

[29] J.C. Watts, B. Drisaldi, V. Ng, J. Yang, B. Strome, P. Horne, M.S. Sy, L. Yoong, R. Young, P. Mastrangelo, C. Bergeron, P.E. Fraser, G.A. Carlson, H.T.J. Mount, G. Schmitt-Ulms, D. Westaway, The CNS glycoprotein Shadoo has PrPC-like protective properties and displays reduced levels in prion infections, EMBO J. (2007). doi:10.1038/sj.emboj.7601830.

[30] D. Westaway, S. Genovesi, N. Daude, R. Brown, A. Lau, I. Lee, C.E. Mays, J. Coomaraswamy, B. Canine, R. Pitstick, A. Herbst, J. Yang, K.W.S. Ko, G. Schmitt-Ulms, S.J. DeArmond, D. McKenzie, L. Hood, G.A. Carlson, Down-regulation of shadoo in prion infections traces a pre-clinical event inversely related to PrP sc accumulation, PLoS Pathog. 7 (2011). doi:10.1371/journal.ppat.1002391.

[31] K.M. Pan, M. Baldwin, J. Nguyen, M. Gasset, A. Serban, D. Groth, I. Mehlhorn, Z. Huang, R.J. Fletterick, F.E. Cohen, S.B. Prusiner, Conversion of α-helices into β-sheets features in the formation of the scrapie prion proteins, Proc. Natl. Acad. Sci. U. S. A. (1993). doi:10.1073/pnas.90.23.10962.

[32] H. Zhang, J. Stockel, I. Mehlhorn, D. Groth, M.A. Baldwin, S.B. Prusiner, T.L. James, F.E. Cohen, Physical studies of conformational plasticity in a recombinant prion protein., Biochemistry. 36 (1997) 3543–53. doi:10.1021/bi961965r.

[33] M. Horiuchi, S.A. Priola, J. Chabry, B. Caughey, Interactions between heterologous forms of prion protein: Binding, inhibition of conversion, and species barriers, Proc. Natl. Acad. Sci. 97 (2000) 5836–5841. doi:10.1073/pnas.110523897.

[34] E. Welker, W.J. Wedemeyer, H.A. Scheraga, A role for intermolecular disulfide bonds in prion diseases?, Proc. Natl. Acad. Sci. U. S. A. (2001). doi:10.1073/pnas.071066598.

[35] S.B. Prusiner, M. Scott, D. Foster, K.M. Pan, D. Groth, C. Mirenda, M. Torchia, S.L.

Yang, D. Serban, G.A. Carlson, P.C. Hoppe, D. Westaway, S.J. DeArmond, Transgenetic studies implicate interactions between homologous PrP isoforms in scrapie prion replication, Cell. (1990). doi:10.1016/0092-8674(90)90134-Z.

[36] J. Hardy, Prion dimers: a deadly duo, Trends Neurosci. (1991). doi:10.1016/0166-2236(91)90038-V.

[37] A.S. Rambold, V. Müller, U. Ron, N. Ben-Tal, K.F. Winklhofer, J. Tatzelt, Stress-protective signalling of prion protein is corrupted by scrapie prions, EMBO J. 27 (2008) 1974–1984. doi:10.1038/emboj.2008.122.

[38] J. Warwicker, P.J. Gane, A model for prion protein dimerisation based on alpha-helical packing, Biochem. Biophys. Res. Commun. (1996).

[39] J. Warwicker, Species barriers in a model for specific prion protein dimerisation, Biochem. Biophys. Res. Commun. (1997). doi:10.1006/bbrc.1997.6325.

[40] J. Warwicker, Modeling a prion protein dimer: Predictions for fibril formation, Biochem. Biophys. Res. Commun. (2000). doi:10.1006/bbrc.2000.3829.

[41] P.M. Harrison, H.S. Chan, S.B. Prusiner, F.E. Cohen, Thermodynamics of model prions and its implications for the problem of prion protein folding, J. Mol. Biol. (1999). doi:10.1006/jmbi.1998.2497.

[42] P.E. Bendheim, D.C. Bolton, A 54-kDa normal cellular protein may be the precursor of the scrapie agent protease-resistant protein, Proc. Natl. Acad. Sci. U. S. A. (1986). doi:10.1073/pnas.83.7.2214.

[43] G.C. Telling, M. Scott, J. Mastrianni, R. Gabizon, M. Torchia, F.E. Cohen, S.J. DeArmond, S.B. Prusiner, Prion propagation in mice expressing human and chimeric PrP transgenes implicates the interaction of cellular PrP with another protein, Cell. (1995). doi:10.1016/0092-8674(95)90236-8.

[44] K. Kaneko, L. Zulianello, M. Scott, C.M. Cooper, A.C. Wallace, T.L. James, F.E. Cohen, S.B. Prusiner, Evidence for protein X binding to a discontinuous epitope on the cellular prion protein during scrapie prion propagation, Proc. Natl. Acad. Sci. U. S. A. (1997). doi:10.1073/pnas.94.19.10069.

[45] R.K. Meyer, A. Lustig, B. Oesch, R. Fatzer, A. Zurbriggen, M. Vandevelde, A monomer-dimer equilibrium of a cellular prion protein (PrP(C)) not observed with recombinant PrP, J. Biol. Chem. (2000). doi:10.1074/jbc.M007114200.

[46] T.L. James, H. Liu, N.B. Ulyanov, S. Farr-Jones, H. Zhang, D.G. Donne, K. Kaneko, D. Groth, I. Mehlhorn, S.B. Prusiner, F.E. Cohen, Solution structure of a 142-residue recombinant prion protein corresponding to the infectious fragment of the scrapie

isoform., Proc. Natl. Acad. Sci. U. S. A. 94 (1997) 10086–91. doi:10.1073/pnas.94.19.10086.

[47] K.J. Knaus, M. Morillas, W. Swietnicki, M. Malone, W.K. Surewicz, V.C. Yee, Crystal structure of the human prion protein reveals a mechanism for oligomerization, Nat. Struct. Biol. (2001). doi:10.1038/nsb0901-770.

[48] S.A. Priola, B. Caughey, K. Wehrly, B. Chesebro, A 60-kDa prion protein (PrP) with properties of both the normal and scrapie-associated forms of PrP, J. Biol. Chem. 270 (1995) 3299–3305. doi:10.1074/jbc.270.7.3299.

[49] D. a Kocisko, J.H. Come, S. a Priola, B. Chesebro, G.J. Raymond, P.T. Lansbury, B. Caughey, Cell-free formation of protease-resistant prion protein., Nature. 370 (1994) 471–474. doi:10.1038/370471a0.

[50] E. Turk, D.B. Teplow, L.E. Hood, S.B. Prusiner, Purification and properties of the cellular and scrapie hamster prion proteins, Eur. J. Biochem. 176 (1988) 21–30. doi:10.1111/j.1432-1033.1988.tb14246.x.

[51] A.D. Engelke, A. Gonsberg, S. Thapa, S. Jung, S. Ulbrich, R. Seidel, S. Basu, G. Multhaup, M. Baier, M. Engelhard, H.M. Schätzl, K.F. Winklhofer, X. Jörg Tatzelt, Dimerization of the cellular prion protein inhibits propagation of scrapie prions, J. Biol. Chem. (2018). doi:10.1074/jbc.RA117.000990.

[52] D.C. Gajdusek, V. Zigas, Degenerative disease of the central nervous system in New Guinea; the, N. Engl. J. Med. 257 (1957) 974–978. doi:10.1056/NEJM195711142572005.

[53] J. Collinge, J. Whitfield, E. McKintosh, J. Beck, S. Mead, D.J. Thomas, M.P. Alpers, Kuru in the 21st century-an acquired human prion disease with very long incubation periods, Lancet. 367 (2006) 2068–2074. doi:10.1016/S0140-6736(06)68930-7.

[54] S. Mead, J. Whitfield, M. Poulter, P. Shah, J. Uphill, T. Campbell, H. Al-Dujaily, H. Hummerich, J. Beck, C.A. Mein, C. Verzilli, J. Whittaker, M.P. Alpers, J. Collinge, A novel protective prion protein variant that colocalizes with kuru exposure, N. Engl. J. Med. 361 (2009) 2056–2065. doi:10.1056/NEJMoa0809716.

[55] T. Jour, E.A. Asante, M. Smidak, A. Grimshaw, R. Houghton, A. Tomlinson, A. Jeelani, T. Jakubcova, S. Hamdan, A. Richard-Londt, J.M. Linehan, S. Brandner, M. Alpers, J. Whitfield, S. Mead, J.D.F. Wadsworth, J. Collinge, A naturally occurring variant of the human prion protein completely prevents prion disease, Nature. (2015). doi:10.1038/nature14510.A.

[56] A.T. Sabareesan, J.B. Udgaonkar, The G126V Mutation in the Mouse Prion Protein

Hinders Nucleation-Dependent Fibril Formation by Slowing Initial Fibril Growth and by Increasing the Critical Concentration, Biochemistry. 56 (2017) 5931–5942. doi:10.1021/acs.biochem.7b00894.

[57] S. Zhou, D. Shi, X. Liu, H. Liu, X. Yao, Protective V127 prion variant prevents prion disease by interrupting the formation of dimer and fibril from molecular dynamics simulations, Sci. Rep. 6 (2016). doi:10.1038/srep21804.

[58] Z. Zheng, M. Zhang, Y. Wang, R. Ma, C. Guo, L. Feng, J. Wu, H. Yao, D. Lin, Structural basis for the complete resistance of the human prion protein mutant G127V to prion disease, Sci. Rep. 8 (2018). doi:10.1038/s41598-018-31394-6.

[59] Q. Wang, A.R. Parrish, L. Wang, Expanding the Genetic Code for Biological Studies, Chem. Biol. (2009). doi:10.1016/j.chembiol.2009.03.001.

[60] L. Wang, P.G. Schultz, Expanding the genetic code, Chem. Commun. (2002). doi:10.1039/b108185n.

[61] K. Lang, L. Davis, S. Wallace, M. Mahesh, D.J. Cox, M.L. Blackman, J.M. Fox, J.W. Chin, Genetic encoding of bicyclononynes and trans-cyclooctenes for site-specific protein labeling in vitro and in live mammalian cells via rapid fluorogenic diels-alder reactions, J. Am. Chem. Soc. (2012). doi:10.1021/ja302832g.

[62] A. Dumas, L. Lercher, C.D. Spicer, B.G. Davis, Designing logical codon reassignment-Expanding the chemistry in biology, Chem. Sci. (2015). doi:10.1039/c4sc01534g.

[63] A. Wittelsberger, D.F. Mierke, M. Rosenblatt, Mapping ligand-receptor interfaces: Approaching the resolution limit of benzophenone-based photoaffinity scanning, Chem. Biol. Drug Des. (2008). doi:10.1111/j.1747-0285.2008.00646.x.

[64] G. Dormán, G.D. Prestwich, Benzophenone Photophores in Biochemistry, Biochemistry. (1994). doi:10.1021/bi00185a001.

[65] R. Atarashi, V.L. Sim, N. Nishida, B. Caughey, S. Katamine, Prion Strain-Dependent Differences in Conversion of Mutant Prion Proteins in Cell Culture, J. Virol. 80 (2006) 7854–7862. doi:10.1128/JVI.00424-06.

[66] S. Hornemann, C. Korth, B. Oesch, R. Riek, G. Wider, K. Wüthrich, R. Glockshuber, Recombinant full-length murine prion protein, mPrP(23-231): Purification and spectroscopic characterization, FEBS Lett. 413 (1997) 277–281. doi:10.1016/S0014-5793(97)00921-6.

[67] I.S. Farrell, R. Toroney, J.L. Hazen, R.A. Mehl, J.W. Chin, Photo-cross-linking interacting proteins with a genetically encoded benzophenone., Nat. Methods. 2 (2005) 377–384. doi:10.1038/nmeth0505-377.

[68] T.S. Young, I. Ahmad, J.A. Yin, P.G. Schultz, An Enhanced System for Unnatural Amino Acid Mutagenesis in E. coli, J. Mol. Biol. 395 (2010) 361–374. doi:10.1016/j.jmb.2009.10.030.

[69] J. F. Sambrook and D.W. Russell, Molecular cloning: A Laboratory Manual.3rd Ed. Vol.1., Cold Spring Harb. Lab. Press. New York, USA. (2001).

[70] B.Y. Lu, P.J. Beck, J.Y. Chang, Oxidative folding of murine prion mPrP(23-231), Eur. J. Biochem. 268 (2001) 3767–3773.

[71] M.M. Lyles, H.F. Gilbert, Catalysis of the oxidative folding of ribonuclease A by protein disulfide isomerase: dependence of the rate on the composition of the redox buffer., Biochemistry. 30 (1991) 613–619. doi:10.1021/bi00217a005.

[72] M.M. Bradford, A rapid and sensitive method for the quantitation of microgram quantities of protein utilizing the principle of protein-dye binding, Anal. Biochem. 72 (1976) 248–254. doi:10.1016/0003-2697(76)90527-3.

[73] G. Xu, M. Narayan, E. Welker, H.A. Scheraga, A novel method to determine thermal transition curves of disulfide-containing proteins and their structured folding intermediates, Biochem. Biophys. Res. Commun. 311 (2003) 514–517. doi:10.1016/j.bbrc.2003.10.039.

[74] H. Yasumitsu, Y. Ozeki, S.M.A. Kawsar, Y. Fujii, M. Sakagami, Y. Matuo, T. Toda, H. Katsuno, RAMA stain: A fast, sensitive and less protein-modifying CBB R250 stain, Electrophoresis. 31 (2010) 1913–1917. doi:10.1002/elps.200900524.

[75] R. Ahrends, J. Kosinski, D. Kirsch, L. Manelyte, L. Giron-Monzon, L. Hummerich, O. Schulz, B. Spengler, P. Friedhoff, Identifying an interaction site between MutH and the C-terminal domain of MutL by crosslinking, affinity purification, chemical coding and mass spectrometry, Nucleic Acids Res. 34 (2006) 3169–3180. doi:10.1093/nar/gkl407.

[76] T. Kaimann, S. Metzger, K. Kuhlmann, B. Brandt, E. Birkmann, H.D. Höltje, D. Riesner, Molecular Model of an α-Helical Prion Protein Dimer and Its Monomeric Subunits as Derived from Chemical Cross-linking and Molecular Modeling Calculations, J. Mol. Biol. 376 (2008) 582–596. doi:10.1016/j.jmb.2007.11.035.

[77] W. Rasband, ImageJ [Software], U. S. Natl. Institutes Heal. Bethesda, Maryland, USA. (2015) //imagej.nih.gov/ij/.

[78] L.A. Gross, G.S. Baird, R.C. Hoffman, K.K. Baldridge, R.Y. Tsien, The structure of the chromophore within DsRed, a red fluorescent protein from coral, Proc. Natl. Acad. Sci. 97 (2000) 11990–11995. doi:10.1073/pnas.97.22.11990.

[79] A. Micsonai, F. Wien, L. Kernya, Y.H. Lee, Y. Goto, M. Refregiers, J. Kardos,

Accurate secondary structure prediction and fold recognition for circular dichroism spectroscopy, PNAS. 112 (2015) E3095–E3103. doi:10.1073/pnas.1500851112.

[80] Y. Ryu, P.G. Schultz, Efficient incorporation of unnatural amino acids into proteins in Escherichia coli., Nat. Methods. 3 (2006) 263–5. doi:10.1038/nmeth864.

[81] E. Biasini, L. Tapella, E. Restelli, M. Pozzoli, T. Massignan, R. Chiesa, The hydrophobic core region governs mutant prion protein aggregation and intracellular retention., Biochem. J. 430 (2010) 477–486. doi:10.1042/BJ20100615.

[82] A. Li, H.M. Christensen, L.R. Stewart, K. a Roth, R. Chiesa, D. a Harris, Neonatal lethality in transgenic mice expressing prion protein with a deletion of residues 105-125., EMBO J. 26 (2007) 548–58. doi:10.1038/sj.emboj.7601507.

[83] D. Peretz, R. a Williamson, Y. Matsunaga, H. Serban, C. Pinilla, R.B. Bastidas, R. Rozenshteyn, T.L. James, R. a Houghten, F.E. Cohen, S.B. Prusiner, D.R. Burton, A conformational transition at the N terminus of the prion protein features in formation of the scrapie isoform., J. Mol. Biol. 273 (1997) 614–622. doi:10.1006/jmbi.1997.1328.

[84] R. Linden, V.R. Martins, M. a M. Prado, M. Cammarota, I. Izquierdo, R.R. Brentani, A. Aguzzi, A.M. Calella, B. Chesebro, A. Aguzzi, M. Polymenidou, S.B. Prusiner, J. Collinge, Prions: protein aggregation and infectious diseases., Physiol. Rev. 88 (2008) 673–728. doi:10.1152/physrev.00006.2009.

[85] L. Calzolai, D.A. Lysek, P. Guntert, C. von Schroetter, R. Riek, R. Zahn, K. Wüthrich, NMR structures of three single-residue variants of the human prion protein., Proc. Natl. Acad. Sci. U. S. A. 97 (2000) 8340–5. doi:10.1073/pnas.97.15.8340.

[86] J. Singh, H. Kumar, A.T. Sabareesan, J.B. Udgaonkar, Rational stabilization of helix 2 of the prion protein prevents its misfolding and oligomerization, J. Am. Chem. Soc. 136 (2014) 16704–16707. doi:10.1021/ja510964t.

[87] I. V. Baskakov, G. Legname, M.A. Baldwin, S.B. Prusiner, F.E. Cohen, Pathway complexity of prion protein assembly into amyloid, J. Biol. Chem. 277 (2002) 21140–21148. doi:10.1074/jbc.M111402200.

[88] F. Eghiaian, T. Daubenfeld, Y. Quenet, M. van Audenhaege, A.-P.P. Bouin, G. van der Rest, J. Grosclaude, H. Rezaei, Diversity in prion protein oligomerization pathways results from domain expansion as revealed by hydrogen/deuterium exchange and disulfide linkage., Proc. Natl. Acad. Sci. U. S. A. 104 (2007) 7414–7419. doi:10.1073/pnas.0607745104.

[89] F. Sokolowski, A.J. Modler, R. Masuch, D. Zirwer, M. Baier, G. Lutsch, D.A. Moss, K. Gast, D. Naumann, Formation of Critical Oligomers Is a Key Event during

Conformational Transition of Recombinant Syrian Hamster Prion Protein, J. Biol. Chem. 278 (2003) 40481–40492. doi:10.1074/jbc.M304391200.

[90] K.W. Leffers, J. Schell, K. Jansen, R. Lucassen, T. Kaimann, L. Nagel-Steger, J. Tatzelt, D. Riesner, The structural transition of the prion protein into its pathogenic conformation is induced by unmasking hydrophobic sites, J. Mol. Biol. 344 (2004) 839–853. doi:10.1016/j.jmb.2004.09.071.

[91] M. Beland, J. Motard, A. Barbarin, X. Roucou, PrPC Homodimerization Stimulates the Production of PrPC Cleaved Fragments PrPN1 and PrPC1, J. Neurosci. 32 (2012) 13255–13263. doi:10.1523/JNEUROSCI.2236-12.2012.

[92] M. Béland, X. Roucou, Homodimerization as a molecular switch between low and high efficiency PrP C cell surface delivery and neuroprotective activity., Prion. 7 (2013) 170–4. doi:10.4161/pri.23583.

[93] S.B. Sangeetham, A.D. Engelke, E. Fodor, S.L. Krausz, J. Tatzelt, E. Welker, The G127V variant of the prion protein interferes with dimer formation in vitro but not in cellulo, Sci. Rep. 11 (2021) 1–13. doi:10.1038/s41598-021-82647-w.

[94] A.D. Engelke, A. Gonsberg, S. Thapa, S. Jung, S. Ulbrich, R. Seidel, S. Basu, G. Multhaup, M. Baier, M. Engelhard, H.M. Schätzl, K.F. Winklhofer, X. Jörg Tatzelt, Dimerization of the cellular prion protein inhibits propagation of scrapie prions, J. Biol. Chem. 293 (2018) 8020–8031. doi:10.1074/jbc.RA117.000990.

[95] K. Jansen, O. Schäfer, E. Birkmann, K. Post, H. Serban, S.B. Prusiner, D. Riesner, Structural intermediates in the putative pathway from the cellular prion protein to the pathogenic form, Biol. Chem. 382 (2001) 683–691. doi:10.1515/BC.2001.081.

[96] A. Wittelsberger, B.E. Thomas, D.F. Mierke, M. Rosenblatt, Methionine acts as a “magnet” in photoaffinity crosslinking experiments, FEBS Lett. 580 (2006) 1872–1876. doi:10.1016/j.febslet.2006.02.050.

[97] J. Stöhr, J.C. Watts, G. Legname, A. Oehler, A. Lemus, H.O.B. Nguyen, J. Sussman, H. Wille, S.J. DeArmond, S.B. Prusiner, K. Giles, Spontaneous generation of anchorless prions in transgenic mice, Proc. Natl. Acad. Sci. U. S. A. 108 (2011) 21223–21228. doi:10.1073/pnas.1117827108.

[98] B. Race, K. Williams, A.G. Hughson, C. Jansen, P. Parchi, A.J.M. Rozemuller, B. Chesebro, Familial human prion diseases associated with prion protein mutations Y226X and G131V are transmissible to transgenic mice expressing human prion protein, Acta Neuropathol. Commun. 6 (2018) 13. doi:10.1186/s40478-018-0516-2.

[99] L.L.P. Hosszu, R. Conners, D. Sangar, M. Batchelor, E.B. Sawyer, S. Fisher, M.J.

Cliff, A.M. Hounslow, K. McAuley, R. Leo Brady, G.S. Jackson, J. Bieschke, J.P. Waltho, J. Collinge, Structural effects of the highly protective V127 polymorphism on human prion protein, Commun. Biol. 3 (2020). doi:10.1038/s42003-020-01126-6.

[100] S.B. Sangeetham, K. Huszár, P. Bencsura, A. Nyeste, É. Hunyadi-Gulyás, E. Fodor, E. Welker, Interrogating the Dimerization Interface of the Prion Protein Via Site-Specific Mutations to p-Benzoyl-L-Phenylalanine, J. Mol. Biol. 430 (2018) 2784–2801. doi:10.1016/j.jmb.2018.05.027.

APPENDIX I

The nucleic acid sequences of the protein coding regions of bacterial expression plasmids, pRSET-B-mPrP and pRSET-B-mPrP-mCh, generated for the expression of the wild type proteins, mPrP and mPrP-mCh.

DNA sequence of the coding region for mPrP of the *pRSET-B-PrP* plasmid:

gatctcgatcccgcgaaattaatacgactcactatagggagaccacaacggtttccctctagaaataattttgtttaactttaagaaggagatatacatat
gaaaaagcggccaaagcctggagggtggaacaccggtggaagccggtatcccgggcagggaagccctggaggcaaccgttacccacctcagg
gtggcacctgggggcagccccacggtggtggctggggacaaccccatgggggcagctggggacaacctcatggtggtagttggggtcagcccc
atggcggtggatggggccaaggaggggggtacccataatcagtggaacaagcccagcaaaccaaaaaccaaccttaagcatgtggcaggggctg
cggcagccggcgctgtagtgggggggccttggtggctacatgctggggagcgctatgagcaggcccatgatccattttggcaacgactgggagga
ccgctactaccgtgaaaacatgtaccgctaccctaaccaagtgtactacaggccagtggatcagtacagcaaccagaacaacttcgtgcacgactg
cgtcaatatcaccatcaagcagcacacggtcaccaccaccaccaaggggagaacttcaccgagaccgatgtgaagatgatggagcgcgtggtg
gagcagatgtgcgtcacccagtaccagaaggagtcccaggcctattacgacgggagaagatcctgttgaagcttgatccggctgctaacaaagcc
cgaaaggaagctgagttggctgctgccaccgctgagcaataactagcataaccccttggggcctctaaacgggtcttgaggggttttttgctgaaag
gaggaactatatccggatctggcgtaatagcgaagaggcccgcaccgatcgcccttcccaacagttgcgcagcctgaatggcgaatgggacgcg
ccctgtagcggcgcattaagcgcggcgggtgtggtggttacgcgcagcgtgaccgctacacttgccagcgccctagcgcccgctcctttcgctttct
tcccttcctttctcgccacgttcgccgcctttccccgtcaagctctaaatcgggggctccctttagggttccgatttagtgctttacggcacctcgacccc
aaaaaacttgattagggtgatggttcacgtagtgggccatcgccctgatagacggtttttcgcccctttgacgttggagtccacgttctttaatagtggact
cttgttccaaactggaacaacactcaaccctatctcggtctattcttttgatttataagggattttgccgatttcggcctattggttaaaaaatgagctgattt
aacaaaaatttaacgcgaattttaacaaaatattaacgcttacaatttaggtggcacttttcggggaaatgtgcgcggaaccccctatttgtttatttttctaa
atacattcaaatatgtatccgctcatgagacaataaccctgataaatgcttcaataatattgaaaaaggaagagtatgagtattcaacatttccgtgtcgc
ccttattcccttttttgcggcattttgccttcctgtttttgctcacccagaaacgctggtgaaagtaaaagatgctgaagatcagttgggtgcacgagtgg
gttacatcgaactggatctcaacagcggtaagatccttgagagttttcgccccgaagaacgttttccaatgatgagcacttttaaagttctgctatgtggc
gcggtattatcccgtattgacgccgggcaagagcaactcggtcgccgcatacactattctcagaatgacttggttgagtactcaccagtcacagaaaa
gcatcttacggatggcatgacagtaagagaattatgcagtgctgccataaccatgagtgataacactgcggccaacttacttctgacaacgatcggag
gaccgaaggagctaaccgcttttttgcacaacatgggggatcatgtaactcgccttgatcgttgggaaccggagctgaatgaagccataccaaacga
cgagcgtgacaccacgatgcctgtagcaatggcaacaacgttgcgcaaactattaactggcgaactacttactctagcttcccggcaacaattaatag
actggatggaggcggataaagttgcaggaccacttctgcgctcggcccttccggctggctggtttattgctgataaatctggagccggtgagcgtgg
gtctcgcggtatcattgcagcactggggccagatggtaagccctcccgtatcgtagttatctacacgacggggagtcaggcaactatggatgaacga
aatagacagatcgctgagataggtgcctcactgattaagcattggtaactgtcagaccaagtttactcatatatactttagattgatttaaaacttcatttta
atttaaaaggatctaggtgaagatccttttgataatctcatgaccaaaatcccttaacgtgagttttcgttccactgagcgtcagaccccgtagaaaaga
tcaaaggatcttcttgagatcctttttttctgcgcgtaatctgctgcttgcaaacaaaaaaaccaccgctaccagcggtggtttgtttgccggatcaagag
ctaccaactctttttccgaaggtaactggcttcagcagagcgcagataccaaatactgttcttctagtgtagccgtagttaggccaccacttcaagaact
ctgtagcaccgcctacatacctcgctctgctaatcctgttaccagtggctgctgccagtggcgataagtcgtgtcttaccgggttggactcaagacgat
agttaccggataaggcgcagcggtcgggctgaacgggggggttcgtgcacacagcccagcttggagcgaacgacctacaccgaactgagatacct
acagcgtgagctatgagaaagcgccacgcttcccgaagggagaaaggcggacaggtatccggtaagcggcagggtcggaacaggagagcgc
acgagggagcttccagggggaaacgcctggtatctttatagtcctgtcgggtttcgccacctctgacttgagcgtcgatttttgtgatgctcgtcaggg
gggcggagcctatggaaaaacgccagcaacgcggccttttacggttcctggccttttgctggccttttgctcacatgttctttcctgcgttatcccctga
ttctgtggataaccgtattaccgcctttgagtgagctgataccgctcgccgcagccgaacgaccgagcgcagcgagtcagtgagcgaggaagcgg
aagagcgcccaatacgcaaaccgcctctccccgcgcgttggccgattcattaatgcag

DNA sequence of the coding region for mPrP-mCh of the *pRSET-B-PrP-mCh plasmid:*

gatctcgatcccgcgaaattaatacgactcactatagggagaccacaacggtttccctctagaaataattttgtttaactttaagaaggagatatacatat
gaaaaagcggccaaagcctggagggtggaacaccggtggaagccggtatcccgggcagggaagccctggaggcaaccgttacccacctcagg
gtggcacctgggggcagccccacggtggtggctggggacaaccccatgggggcagctggggacaacctcatggtggtagttggggtcagcccc
atggcggtggatggggccaaggaggggtacccataatcagtggaacaagcccagcaaaccaaaaaccaacctcaagcatgtggcaggggctg
cggcagctggggcagtagtgggggccttggtggctacatgctggggagcgccatgagcaggcccatgatccattttggcaacgactgggagga
ccgctactaccgtgaaaacatgtaccgctaccctaaccaagtgtactacaggccagtggatcagtacagcaaccagaacaacttcgtgcacgactg
cgtcaatatcaccatcaagcagcacacggtcaccaccaccaccaaggggagaacttcaccgagaccgatgtgaagatgatggagcgcgtggtg
gagcagatgtgcgtcacccagtaccagaaggagtcccaggcctattacgacgggagaagatccagggatcccgccaccatggtgagcaagggc
gaggaggataacatggccatcatcaaggagttcatgcgcttcaaggtgcacatggagggctccgtgaacggccacgagttcgagatcgagggcg
agggcgagggccgcccctacgagggcacccagaccgccaagctgaaggtgaccaagggtggccccctgcccttcgcctgggacatcctgtccc
ctcagttcatgtacggctccaaggcctacgtgaagcaccccgccgacatccccgactacttgaagctgtccttccccgagggcttcaagtgggagc
gcgtgatgaacttcgaggacggcggcgtggtgaccgtgacccaggactcctccctgcaggacggcgagttcatctacaaggtgaagctgcgcgg
caccaacttcccctccgacggccccgtaatgcagaagaagaccatgggctgggaggcctcctccgagcggatgtaccccgaggacggcgccct
gaagggcgagatcaagcagaggctgaagctgaaggacggcggccactacgacgctgaggtcaagaccacctacaaggccaagaagcccgtg
cagctgcccggcgcctacaacgtcaacatcaagttggacatcacctcccacaacgaggactacaccatcgtggaacagtacgaacgcgccgagg
gccgccactccaccggcggcatggacgagctgtacaagcaccatcatcaccaccattgttgaagcttgatccggctgctaacaaagcccgaaagg
aagctgagttggctgctgccaccgctgagcaataactagcataacccctttggggcctctaaacgggtcttgaggggttttttgctgaaaggaggaact
atatccggatctggcgtaatagcgaagaggcccgcaccgatcgcccttcccaacagttgcgcagcctgaatggcgaatgggacgcgccctgtagc
ggcgcattaagcgcggcgggtgtggtggttacgcgcagcgtgaccgctacacttgccagcgccctagcgcccgctcctttcgctttcttcccttcctttt
ctcgccacgttcgccggctttccccgtcaagctctaaatcgggggctcccctttagggttccgatttagtgctttacggcacctcgaccccaaaaaactt
gattagggtgatggttcacgtagtgggccatcgccctgatagacggtttttcgcccttgacgttggagtccacgttctttaatagtggactcttgttccaa
actggaacaacactcaaccctatctcggtctattcttttgatttataagggattttgccgatttcggcctattggttaaaaaatgagctgatttaacaaaaatt
taacgcgaatttaacaaaatattaacgcttacaatttaggtggcacttttcggggaaatgtgcgcggaacccctatttgtttatttttctaaatacattcaaa
tatgtatccgctcatgagacaataaccctgataaatgcttcaataatattgaaaaaggaagagtatgagtattcaacatttccgtgtcgcccttattcccttt
tttgcggcattttgccttcctgtttttgctcacccagaaacgctggtgaaagtaaaagatgctgaagatcagttgggtgcacgagtgggttacatcgaac
tggatctcaacagcggtaagatccttgagagttttcgccccgaagaacgttttccaatgatgagcacttttaaagttctgctatgtggcgcggtattatcc
cgtattgacgccgggcaagagcaactcggtcgccgcatacactattctcagaatgacttggttgagtactcaccagtcacagaaaagcatcttacgg
atggcatgacagtaagagaattatgcagtgctgccataaccatgagtgataacactgcggccaacttacttctgacaacgatcggaggaccgaagg
agctaaccgcttttttgcacaacatgggggatcatgtaactcgccttgatcgttgggaaccggagctgaatgaagccataccaaacgacgagcgtga
caccacgatgcctgtagcaatggcaacaacgttgcgcaaactattaactggcgaactacttactctagcttcccggcaacaattaatagactggatgg
aggcggataaagttgcaggaccacttctgcgctcggcccttccggctggctggtttattgctgataaatctggagccggtgagcgtgggtctcgcgg
tatcattgcagcactggggccagatggtaagccctcccgtatcgtagttatctacacgacggggagtcaggcaactatggatgaacgaaatagaca
gatcgctgagataggtgcctcactgattaagcattggtaactgtcagaccaagtttactcatatatactttagattgatttaaaacttcatttttaatttaaaa
ggatctaggtgaagatccttttgataatctcatgaccaaaatcccttaacgtgagttttcgttccactgagcgtcagaccccgtagaaaagatcaaagg
atcttcttgagatcctttttttctgcgcgtaatctgctgcttgcaaacaaaaaaaccaccgctaccagcggtggtttgtttgccggatcaagagctaccaa
ctctttttccgaaggtaactggcttcagcagagcgcagataccaaatactgttcttctagtgtagccgtagttaggccaccacttcaagaactctgtagc
accgcctacatacctcgctctgctaatcctgttaccagtggctgctgccagtggcgataagtcgtgtcttaccgggttggactcaagacgatagttacc
ggataaggcgcagcggtcgggctgaacgggggttcgtgcacacagcccagcttggagcgaacgacctacaccgaactgagatacctacagcg
tgagctatgagaaagcgccacgcttcccgaagggagaaaggcggacaggtatccggtaagcggcagggtcggaacaggagagcgcacgagg
gagcttccagggggaaacgcctggtatctttatagtcctgtcgggtttcgccacctctgacttgagcgtcgatttttgtgatgctcgtcaggggggcgg
agcctatggaaaaacgccagcaacgcggccttttacggttcctggccttttgctggccttttgctcacatgttctttcctgcgttatcccctgattctgtgg
ataaccgtattaccgcctttgagtgagctgataccgctcgccgcagccgaacgaccgagcgcagcgagtcagtgagcgaggaagcggaagagc
gcccaatacgcaaaccgcctctccccgcgcgttggccgattcattaatgcag

APPENDIX II

The amino acid sequences of the proteins encoded by *pRSET-B-PrP* and *pRSET-B-PrP-mCh* plasmids.

Amino acid sequences

mPrP expressed from the plasmid pRSET-B-PrP:

MKKRPKPGGWNTGGSRYPGQGSPGGNRYPPQGGTWGQPHGGGWGQPHGGSWGQPHGGS
WGQPHGGGWGQGGGTHNQWNKPSKPKTNLKHVAGAAAAGAVVGGLGGYMLGSAMSRP
MIHFGNDWEDRYYRENMYRYPNQVYYRPVDQYSNQNNFVHDCVNITIKQHTVTTTTKGENF
TETDVKMMERVVEQMCVTQYQKESQAYYDGRRSC

mPrP tagged with mCherry expressed from the plasmid pRSET-B-PrP-mCh:

MKKRPKPGGWNTGGSRYPGQGSPGGNRYPPQGGTWGQPHGGGWGQPHGGSWGQPHGGS
WGQPHGGGWGQGGGTHNQWNKPSKPKTNLKHVAGAAAAGAVVGGLGGYMLGSAMSRP
MIHFGNDWEDRYYRENMYRYPNQVYYRPVDQYSNQNNFVHDCVNITIKQHTVTTTTKGENF
TETDVKMMERVVEQMCVTQYQKESQAYYDGRRSRDPATMVSKGEEDNMAIIKEFMRFKVH
MEGSVNGHEFEIEGEGEGRPYEGTQTAKLKVTKGGPLPFAWDILSPQFMYGSKAYVKHPADI
PDYLKLSFPEGFKWERVMNFEDGGVVTVTQDSSLQDGEFIYKVKLRGTNFPSDGPVMQKKT
MGWEASSERMYPEDGALKGEIKQRLKLKDGGHYDAEVKTTYKAKKPVQLPGAYNVNIKLDI
TSHNEDYTIVEQYERAEGRHSTGGMDELYKHHHHHHC

APPENDIX III

Table III-1. DNA oligonucleotides used for the mutagenesis and linker generation for the cloning procedures[*].

Oligonucleotide	**Sequence**
EagIfwd	CTAACCAAGTGTACTAC**CGGCCG**GTGGATCAGTACAGC
EagIrev	GCTGTACTGATCCAC**CGGCCG**GTAGTACACTTGGTTAG
BsmBIfwd	GGAGAACTTCACC**GAGACG**GATGTGAAGATGATGGAGC
BsmBIrev	GCTCCATCATCTTCACATC**CGTCTC**GGTGAAGTTCTCC
MluIfwd	CGATGTGAAGATGATGGA**ACGCGT**GGTGGAGCAGATG
MluIrev	CATCTGCTCCACC**ACGCGT**TCCATCATCTTCACATCG
mPrPS131Ambfwd	CTACATGCTGGGATAGGCCATGAGCAGG
mPrPS131Ambrev	CCTGCTCATGGCCTATCCCAGCATGTAG
PrP-E206X-fw	CGATGTGAAGATGATGTAGCGTGTGGTGGAGCAGATGT
PrP-E206X-rev	ACATCTGCTCCACCACACGCTACATCATCTTCACATCG
PrP-E210X-fw	GATGATGGAGCGCGTGGTCTAGCAGATGTGCGTCACCC
PrP-E210X-rev	GGGTGACGCACATCTGCTAGACCACGCGCTCCATCATC
mPrPW80Xwt1fwd	*TCA*AGGTGGCACCTGGGGGCAGCCCCACGGTGGTGGCTGG*GGAC AACCC*
mPrPW80Xwt1rev	CCAGCCACCACCGTGGGGCTGCCCCCAGGTGCCACCT
mPrPW80Xwt2fwd	CATGGGGGCAGCTGGGGACAACCTCAT
mPrPW80Xwt2rev	*ACTACCACC*ATGAGGTTGTCCCCAGCTGCCCCCATG*GGGTTGTCC*
mPrPW80Xmutfwd	*GGTGGTAGT*TAGGGTCAGCCCCATGGCGGTGGATGGGGCCAAGG AGGGG
mPrPW80Xmutrev	*GTAC*CCCCTCCTTGGCCCCATCCACCGCCATGGGGCTGACCCTA
mPrPG89Xmutfwd	*GGTGGTAGT*TGGGGTCAGCCCCATGGCGGTGGATGGTAGCAAGG AGGGG
mPrPG89Xmutrev	*GTAC*CCCCTCCTTGCTACCATCCACCGCCATGGGGCTGACCCCA

mPrPQ90Xmutfwd	*GGTGGTAGT*TGGGGTCAGCCCCATGGCGGTGGATGGGGCTAGGG AGGGG
mPrPQ90Xmutrev	*GTAC*CCCCTCCCTAGCCCCATCCACCGCCATGGGGCTGACCCCA
mPrPN107Xfwd	GCATAATCAGTGGAACAAGCCCAGCAAACCAAAAACCTAGC
mPrPN107Xrev	*TTAA*GCTAGGTTTTTGGTTTGCTGGGCTTGTTCCACTGATTATGC*G TAC*
mPrPK109Xafwd	GCATAATCAGTGGAACAAGCCCAGCAAACCA
mPrPK109Xbfwd	*AAAACCAAC*CTTTAGCATGTGGCAGGGGCTGCGGCAG
mPrPK109Xarev	*GTTGGTTTT*TGGTTTGCTGGGCTTGTTCCACTGATTATGC*GTAC*
mPrPK109Xbrev	*CCGG*CTGCCGCAGCCCCTGCCACATGCTAAAG
PrP-V111X-fw2	*TTAA*ACATTAGGCAGGGGCTGCGGCAG
PrP-V111X-rev2	*CCGG*CTGCCGCAGCCCCTGCCTAATGT
PrP-G113X-fw3	*TTAA*ACATGTGGCATAGGCTGCGGCAG
PrP-G113X-rev2	*CCGG*CTGCCGCAGCCTATGCCACATGT
A116Xmfwd	*TTAA*ACATGTGGCAGGGGCTGCGTAGG
A116Xmrev	*CCGG*CCTACGCAGCCCCTGCCACATGT
mPrPA117Xafwd	*TTAA*GCATGTGGCAGGGGCTGCGGCATAGGGC
mPrPA117Xamutrev	*CACTACAGC*GCCCTATGCCGCAGCCCCTGCCACATGC
mPrPA117Xbfwd	*GCTGTAGTG*GGGGGCCTTGGTGGCTACATGCTGGGGAGT
mPrPA117Xbwtrev	ACTCCCCAGCATGTAGCCACCAAGGCCCCC
mPrPG118Xfwd	*TTAA*GCATGTGGCAGGGGCTGCGGCAGCCTAG
mPrPG118Xrev	*CACTACAGC*CTAGGCTGCCGCAGCCCCTGCCACATGC
A119Xmfwd	*CCGG*CTAGGTAGTGGGGGGCCTTGGTGGCTACATGCTGGGGAGT
A119Xmrev	ACTCCCCAGCATGTAGCCACCAAGGCCCCCCACTACCTAG
mPrPV120Xfwd	*CCGG*CGCTTAGGTGGGGGGCCTTGGTGGCTACATGCTGGGGAGT
mPrPV120Xrev	ACTCCCCAGCATGTAGCCACCAAGGCCCCCCACCTAAGCG
PrP-V121X-fw2	*CCGG*AGCATAGGTGGGGGGCCTTGGTGGCTACATGCTGGGGAGC
PrP-V121X-rev2	GCTCCCCAGCATGTAGCCACCAAGGCCCCCCACCTATGCT

PrP-L124X-fw2	*CCGG*AGCAGTAGTGGGGGGCTAGGGTGGCTACATGCTGGGGAGC
PrP-L124X-rev2	GCTCCCCAGCATGTAGCCACCCTAGCCCCCCACTACTGCT
mPrPG125Xfwd	*CCGG*CGCTGTAGTGGGGGGCCTTTAGGGCTACATGCTGGGGAGT
mPrPG125Xrev	ACTCCCCAGCATGTAGCCCTAAAGGCCCCCCACTACAGCG
mPrPG126Xfwd	*CCGG*CGCTGTAGTGGGGGGCCTTGGTTAGTACATGCTGGGGAGT
mPrPG126Xrev	ACTCCCCAGCATGTACTAACCAAGGCCCCCCACTACAGCG
PrP-Y127X-fw2	*CCGG*AGCAGTAGTGGGGGGCCTTGGTGGCTAGATGCTGGGGAGC
PrP-Y127X-rev2	GCTCCCCAGCATCTAGCCACCAAGGCCCCCCACTACTGCT
mPrPM128Xfwd	*CCGG*CGCTGTAGTGGGGGGCCTTGGTGGCTACTAGCTGGGGAGT
mPrPM128Xrev	ACTCCCCAGCTAGTAGCCACCAAGGCCCCCCACTACAGCG
PrP-L129X-fw2	*CCGG*AGCAGTAGTGGGGGGCCTTGGTGGCTACATGTAGGGGAGC
PrP-L129X-rev2	GCTCCCCTACATGTAGCCACCAAGGCCCCCCACTACTGCT
mPrPM133Xamutfwd	GCATAGAGCAGGCCCATGATCCATTTTGGC*AACGACTGG*
mPrPM133Xamutrev	GCCAAAATGGATCATGGGCCTGCTCTATGC
mPrPM133Xbwtfwd	GAGGACCGCTACTACCGTGAA*AACATGTAC*
mPrPM133Xbwtrev	TTCACGGTAGTAGCGGTCCTC*CCAGTCGTT*
mPrPM133Xcwtfwd	CGCTACCCTAACCAAGTGTACTACC
mPrPM133Xcwtrev	*GGCC*GGTAGTACACTTGGTTAGGGTAGCG*GTACATGTT*
mPrPR135Xamutrev	GCCAAAATGGATCATGGGCTAGCTCATTGC
mPrPR135Xamutfwd	GCAATGAGCTAGCCCATGATCCATTTTGGC*AACGACTGG*

* Restriction sites are bolded, inserted Amber (X) codons are underlined, overhangs are italicized.

Table III-2. The DNA linkers used for the specific amber mutations in the prion protein** [3].

Amber mutation	**restriction sites**	**linker1**	**linker2**	**linker3**	**removed restriction site**
W80X	**Eco81I-Acc65I**	mPrPW80Xwt1fwd	mPrPW80Xwt2fwd	mPrPW80Xmutfwd	**Eco81I**
		mPrPW80Xwt1rev	mPrPW80Xwt2rev	mPrPW80Xmutrev	

G89X	**Eco81I-Acc65I**	mPrPW80Xwt1fwd	mPrPW80Xwt2fwd	mPrPG89Xmutfwd	**Eco81I**
		mPrPW80Xwt1rev	mPrPW80Xwt2rev	mPrPG89Xmutrev	
Q90X	**Eco81I-Acc65I**	mPrPW80Xwt1fwd	mPrPW80Xwt2fwd	mPrPQ90Xmutfwd	**Eco81I**
		mPrPW80Xwt1rev	mPrPW80Xwt2rev	mPrPQ90Xmutrev	
N107X	**KpnI-AflII**	mPrPN107Xfwd	-	-	**KpnI**
		mPrPN107Xrev	-	-	
K109X	**KpnI-NgoMIV**	mPrPK109Xafwd	mPrPK109Xbfwd	-	**KpnI**
		mPrPK109Xarev	mPrPK109Xbrev	-	
V111X	**AflII-NgoMIV**	PrP-V111X-fw2	-	-	**AflII**
		PrP-V111X-rev2	-	-	
G113X	**AflII-NgoMIV**	PrP-G113X-fw3	-	-	**AflII**
		PrP-G113X-rev2	-	-	
A116X	**AflII-NgoMIV**	A116Xmfwd	-	-	**AflII**
		A116Xmrev	-	-	
A117X	**AflII-AfeI**	mPrPA117Xafwd	mPrPA117Xbfwd	-	**AfeI**
		mPrPA117Xamutrev	mPrPA117Xbwtrev	-	
G118X	**AflII-AfeI**	mPrPG118Xfwd	mPrPA117Xbfwd	-	**AfeI**
		mPrPG118Xrev	mPrPA117Xbwtrev	-	
A119X	**NgoMIV-AfeI**	A119Xmfwd	-	-	**AfeI**
		A119Xmrev	-	-	
V120X	**NgoMIV-AfeI**	mPrPV120Xfwd	-	-	**AfeI**
		mPrPV120Xrev	-	-	
V121X	**NgoMIV-AfeI**	PrP-V121X-fw2	-	-	**NgoMIV**
		PrP-V121X-rev2	-	-	
L124X	**NgoMIV-AfeI**	PrP-L124X-fw2	-	-	**NgoMIV**
		PrP-L124X-rev2	-	-	
G125X	**NgoMIV-**	mPrPG125Xfwd	-	-	**AfeI**

	AfeI	mPrPG125Xrev	-	-	
G126X	**NgoMIV-AfeI**	mPrPG126Xfwd	-	-	**AfeI**
		mPrPG126Xrev	-	-	
Y127X	**NgoMIV-AfeI**	PrP-Y127X-fw2	-	-	**AfeI**
		PrP-Y127X-rev2	-	-	
M128X	**NgoMIV-AfeI**	mPrPM128Xfwd	-	-	**AfeI**
		mPrPM128Xrev	-	-	
L129X	**NgoMIV-AfeI**	PrP-L129X-fw2	-	-	**AfeI**
		PrP-L129X-rev2	-	-	
M133X	**AfeI-EagI**	mPrPM133Xamutfwd	mPrPM133Xbwtfwd	mPrPM133Xcwtfwd	**AfeI**
		mPrPM133Xamutrev	mPrPM133Xbwtrev	mPrPM133Xcwtrev	
R135X	**AfeI-EagI**	mPrPR135Xamutfwd	mPrPM133Xbwtfwd	mPrPM133Xcwtfwd	**AfeI**
		mPrPR135Xamutrev	mPrPM133Xbwtrev	mPrPM133Xcwtrev	

**: The linkers containing the Amber stop codon are marked as red color.

Table III-3. Oligonucleotides used for the construction of the mPrP variants with G126V mutations.

mPrP variant	**Oligonucleotides used**
G126V, 127X	1: CCGGTGCTGTAGTGGGGGGCCTTGGTGTGTAGATGCTGGGGAGT
	2: ACTCCCCAGCATCTACACACCAAGGCCCCCCACTACAGCA
G126V, 128X	1: CCGGTGCTGTAGTGGGGGGCCTTGGTGTGTACTAGCTGGGGAGT
	2: ACTCCCCAGCTAGTACACACCAAGGCCCCCCACTACAGCA
G126V, 131X	1: CCGGTGCTGTAGTGGGGGGCCTTGGTGTGTACATGCTGGGGTAG
	2: CTACCCCAGCATGTACACACCAAGGCCCCCCACTACAGCA
G126V	1: CCGGTGCTGTAGTGGGGGGCCTTGGTGTGTACATGCTGGGGAGT
	2: ACTCCCCAGCATGTACACACCAAGGCCCCCCACTACAGCA

APPENDIX IV

1. Optimization of the crosslinking conditions:the gel pictures of the protein samples: mPrP(Y127*p*Bpa)-mCherry mutant and control, wild type mPrP-mCherry, used for optimization of conditions of crosslinking in the study of the dimerization interface of mPrP - a complementation to the Results, section 4.1.3.

Figure IV-1. The optimal SDS conditions for mPrPmCherry proteins to form dimers

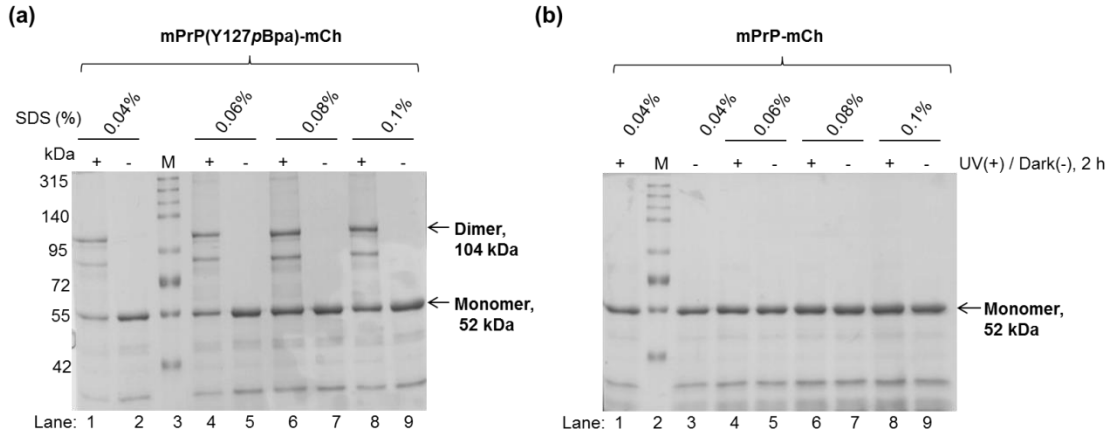

Figure IV-1. Best conditions that favor dimer formation of mPrP-mCherry proteins. Proteins, mPrP(Y127*p*Bpa)-mCherry mutant **(a)** and control, wild type mPrP-mCherry **(b)** crosslinked at different SDS %, in PBS, as indicated. The condition corresponding to 0.06% SDS was chosen in the further experiments to crosslink dimers of mPrP.

Figure IV-2. The amount of dimers crosslinked is affected by the UV irradiation time.

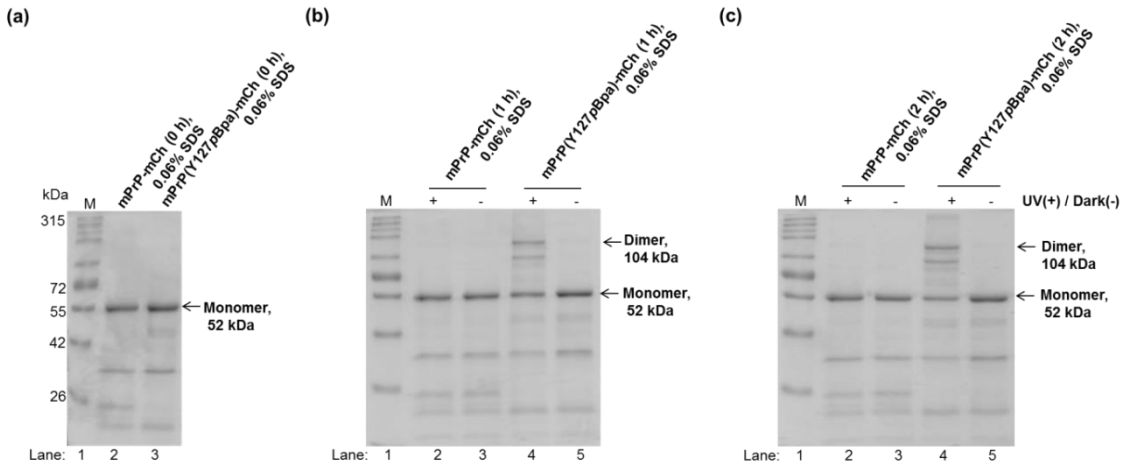

Figure IV-2. Effect of irradiation time on the amount of dimers crosslinked. Representative gel pictures of mPrP-Ch and mPrP(Y127*p*Bpa)-mCh samples irradiated for different times: 0 h **(a)**, 1 h **(b)**, 2 h **(c)**, or kept at dark (- UV). Monomers and dimers are marked by arrows. 2 h irradiation time proved to be a good chice for obtaining efficient crosslinking.

Figure IV-3. Determining the amount of nonspecific dimers crosslinked.

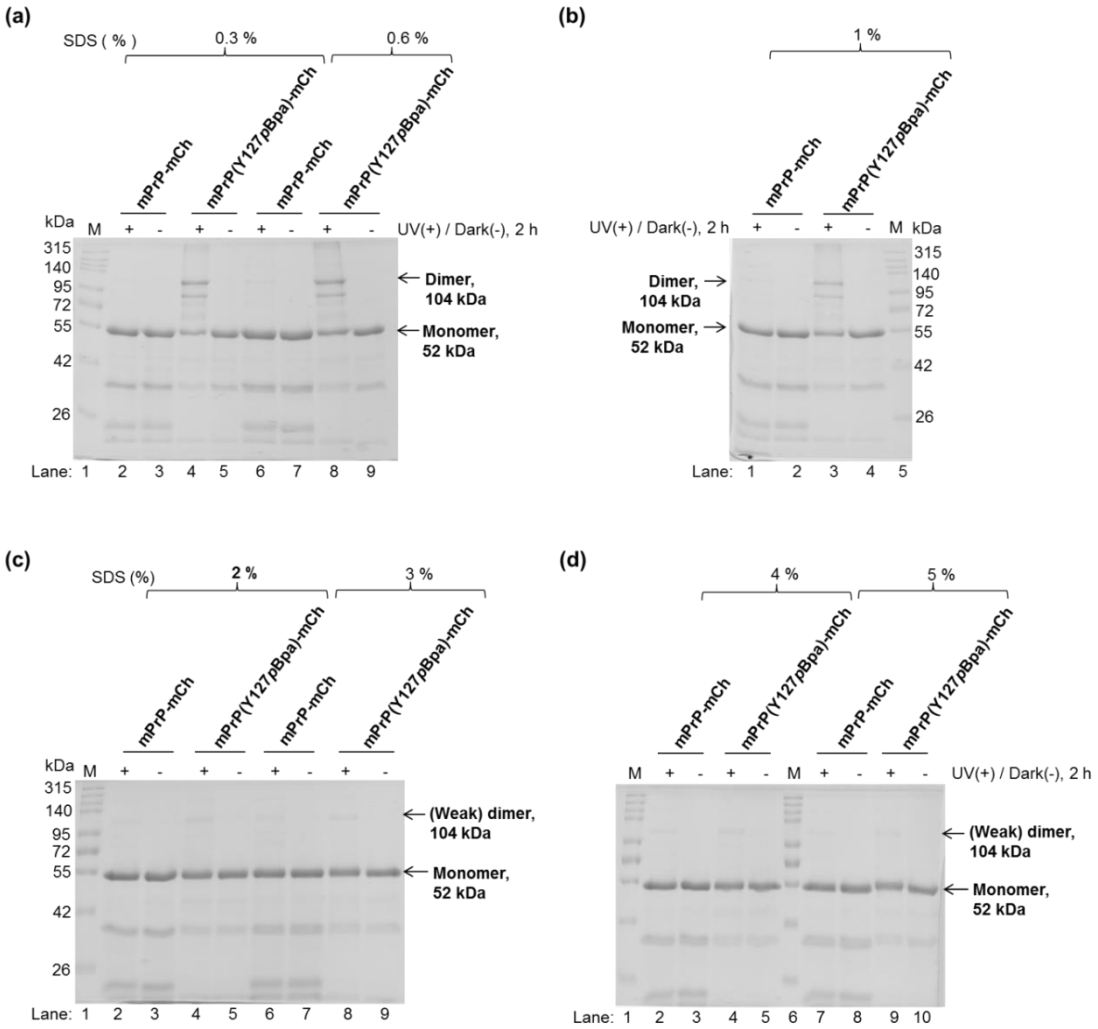

Figure IV-3. Assessing the amount of nonspecific dimers crosslinked. Representative gel pictures of crosslinked samples of *p*Bpa-mutant mPrP(Y127*p*Bpa)-mCherry while shifting conditions towards monomeric state by increasing SDS concentrations (0.3 - 5% SDS) as marked **(a-d)**. Crosslinking is done side-by-side with the wild type mPrP-mCherry used as control. Irradiated (+UV, 2 h) samples have their non-irradiated counterparts (-UV, 2 h) as additional controls. Above 2% SDS no further reduction in dimers was observed.

2. The additional gel pictures of the crosslinked samples used for evaluation of the homodimer percentages in the study of the dimerization interface of mPrP - a complementation to the Results, sections 4.1.3., 4.1.4., and 4.1.5..

<u>Figure IV-4: Crosslinking of mCherry tagged prion, mPrP-mCh, *p*Bpa-variants:</u>

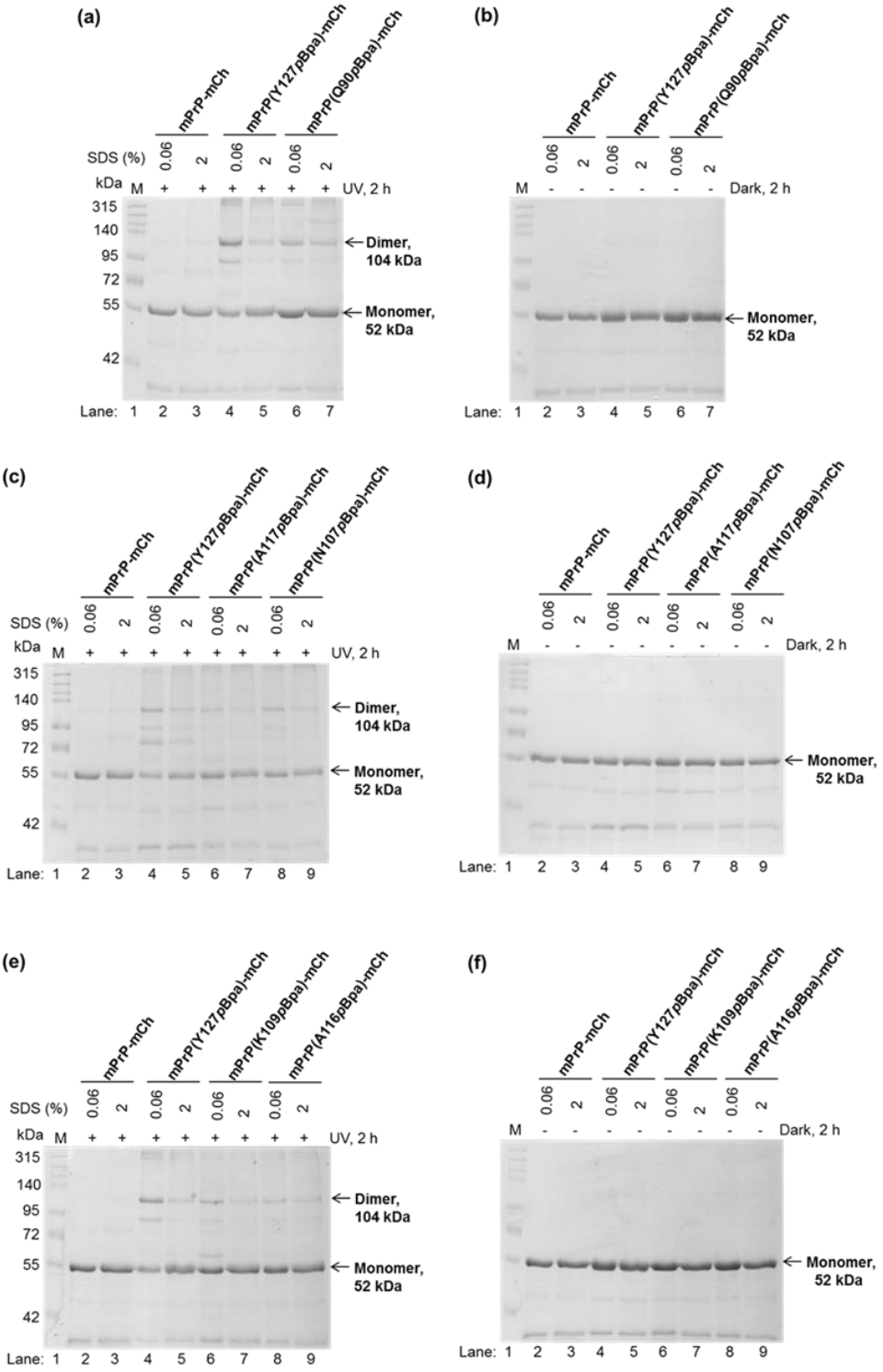

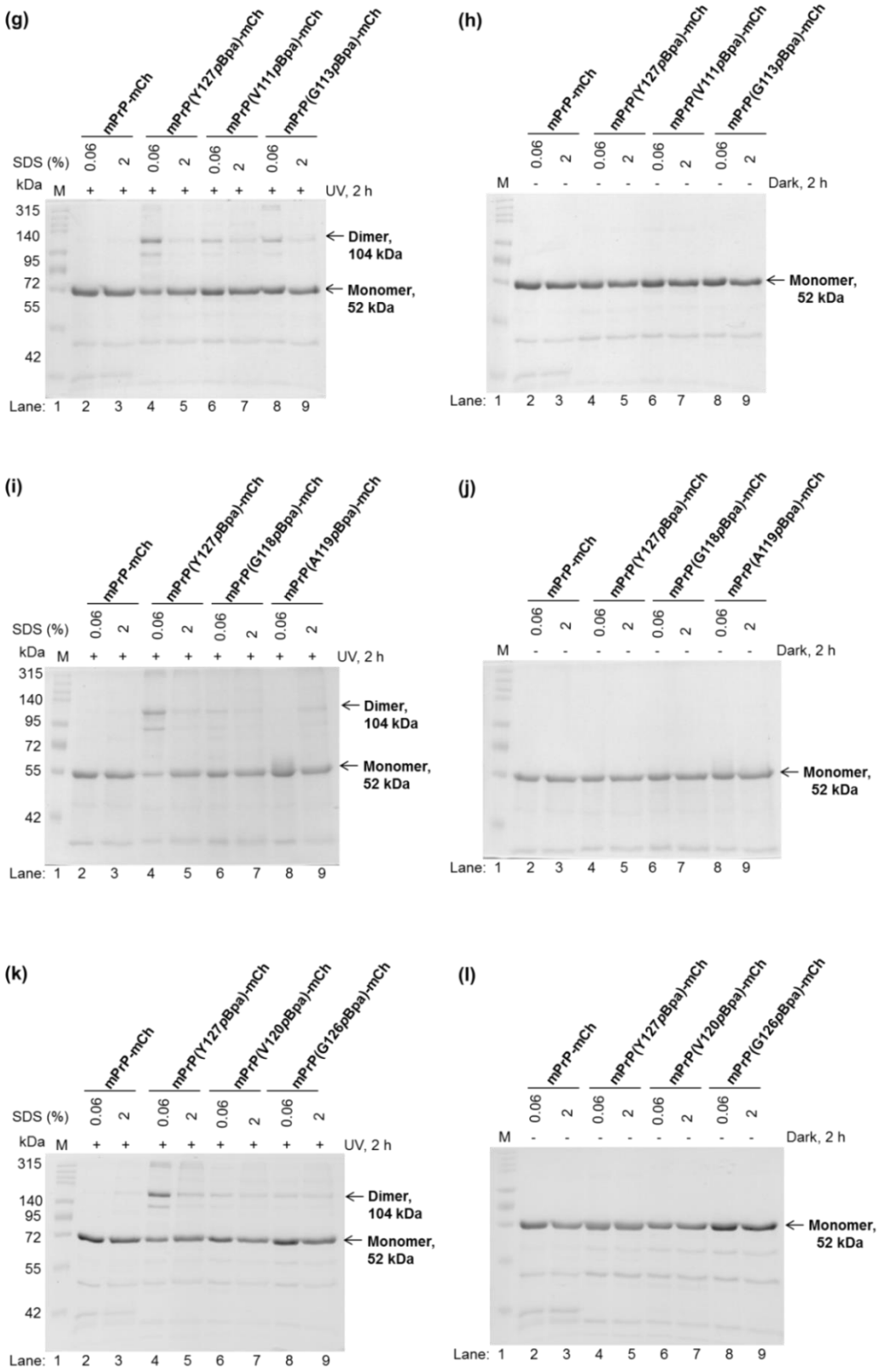
(g)
mPrP-mCh
mPrP(Y127pBpa)-mCh
mPrP(V111pBpa)-mCh
mPrP(G113pBpa)-mCh
SDS (%)
0.06
2
kDa
M
UV, 2 h
315
140
95
72
55
42
Dimer, 104 kDa
Monomer, 52 kDa
Lane: 1 2 3 4 5 6 7 8 9
(h)
Dark, 2 h
(i)
mPrP(G118pBpa)-mCh
mPrP(A119pBpa)-mCh
(j)
(k)
mPrP(V120pBpa)-mCh
mPrP(G126pBpa)-mCh
(l)

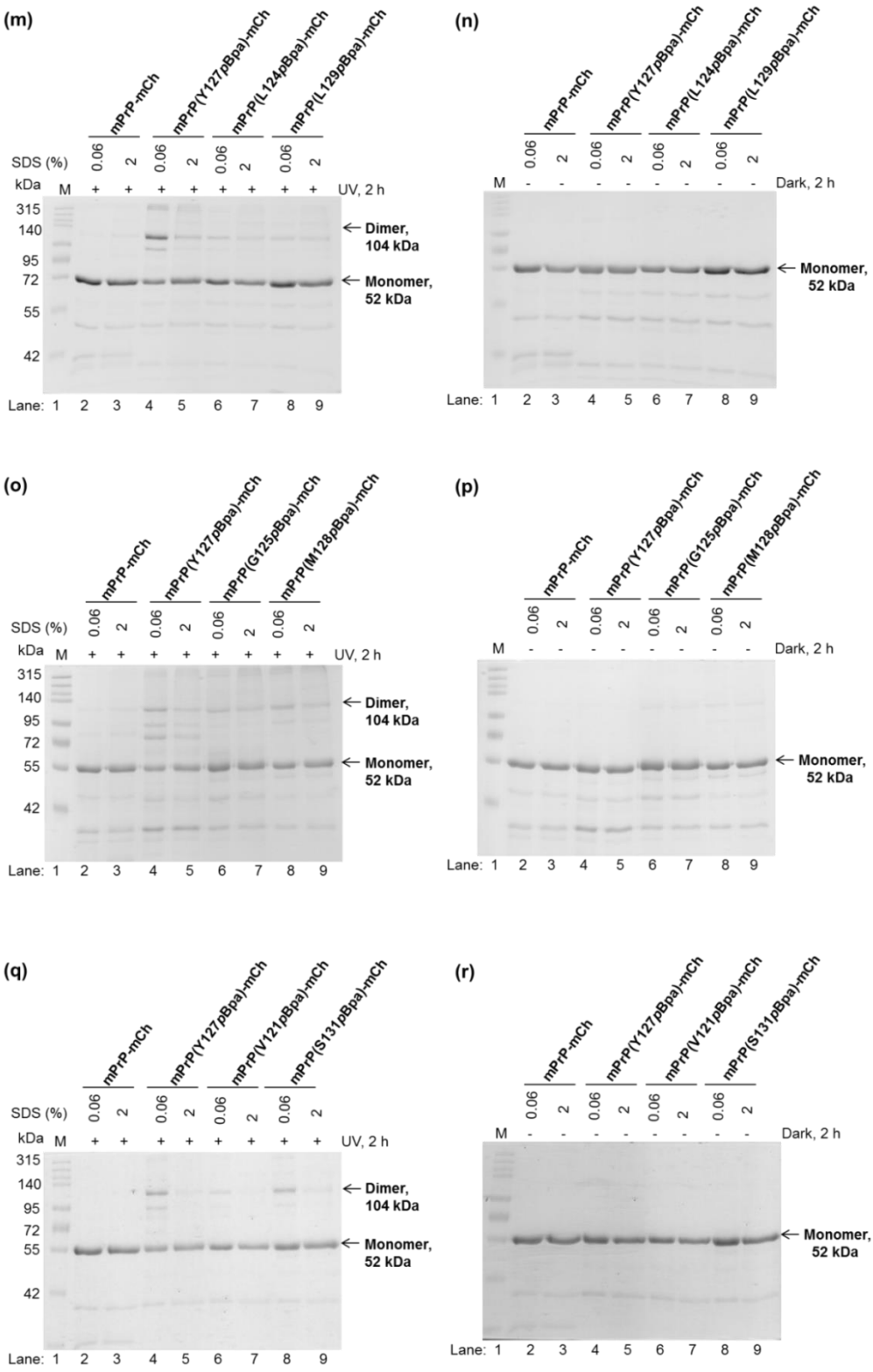
(m)
mPrP-mCh
mPrP(Y127pBpa)-mCh
mPrP(L124pBpa)-mCh
mPrP(L129pBpa)-mCh
SDS (%)
0.06
2
kDa
M
UV, 2 h
315
140
95
72
55
42
Dimer, 104 kDa
Monomer, 52 kDa
Lane: 1 2 3 4 5 6 7 8 9
(n)
Dark, 2 h
(o)
mPrP(G125pBpa)-mCh
mPrP(M128pBpa)-mCh
(p)
(q)
mPrP(V121pBpa)-mCh
mPrP(S131pBpa)-mCh
(r)

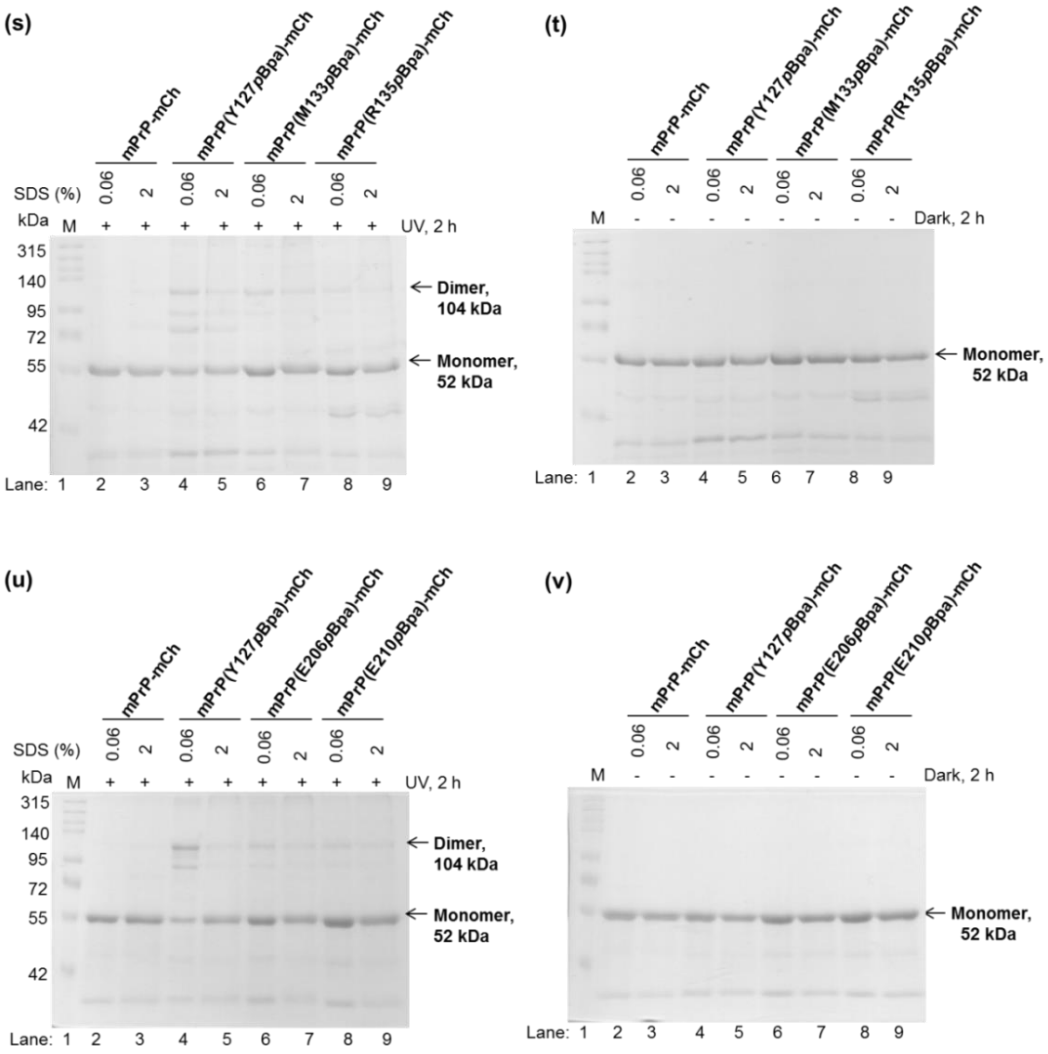

Figure IV-4. Photocrosslinking at dimer- or monomer-favoring conditions of mCherry-tagged prion protein mutants with site specifically inserted *p*Bpa at various positions along the sequence. Representative gel pictures of wild type and of the additional *p*Bpa-mutant mPrP-mCh proteins and were used in calculations of the percentage of crosslinked dimers presented on Figure 11a and b. Proteins are irradiated at 365 nm (UV, 2 h) or kept at dark (Dark, 2 h) at dimer (0.06%) and monomer (2%) favoring SDS conditions. In each experiment the wild type and the 127*p*Bpa positional mutant is present as controls. The bands corresponding to the monomeric proteins (52 kDa) and the dimers (104 kDa) are marked by arrows. Examined mutants are with *p*Bpa at positions: 90 **(a, b)**; 117, 107 **(c, d)**; 109, 116 **(e, f)**; 111, 113 **(g, h)**; 118, 119 **(i, j)**; 120, 126 **(k, l)**; 124, 129 **(m, n)**; 125, 128 **(o, p)**; 121, 131 **(q, r)**; 133, 135 **(s, t)**; 206, 210 **(u, v)**.

Figure IV-5: Crosslinking of untagged mPrP *p*Bpa-variants:

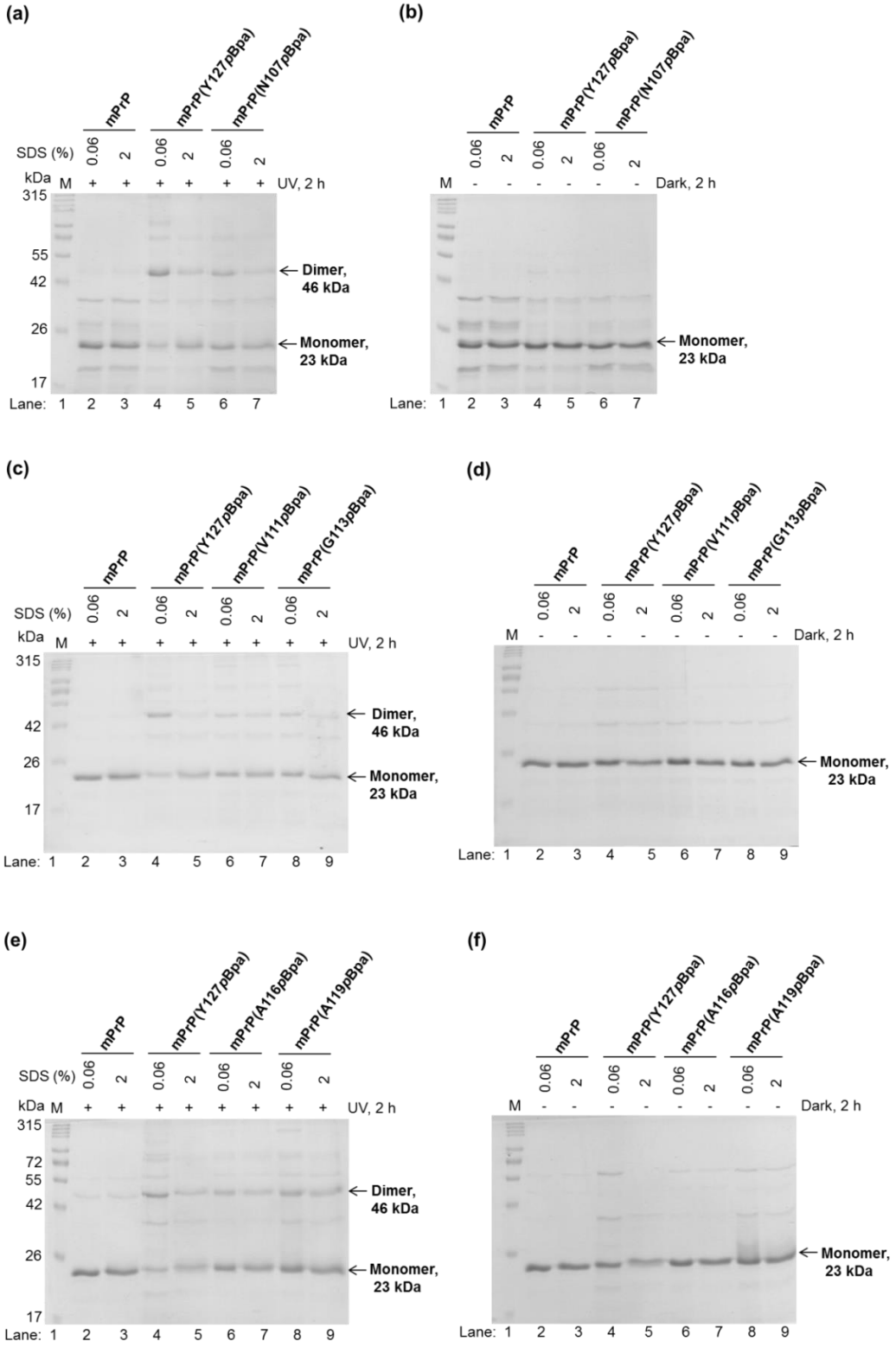

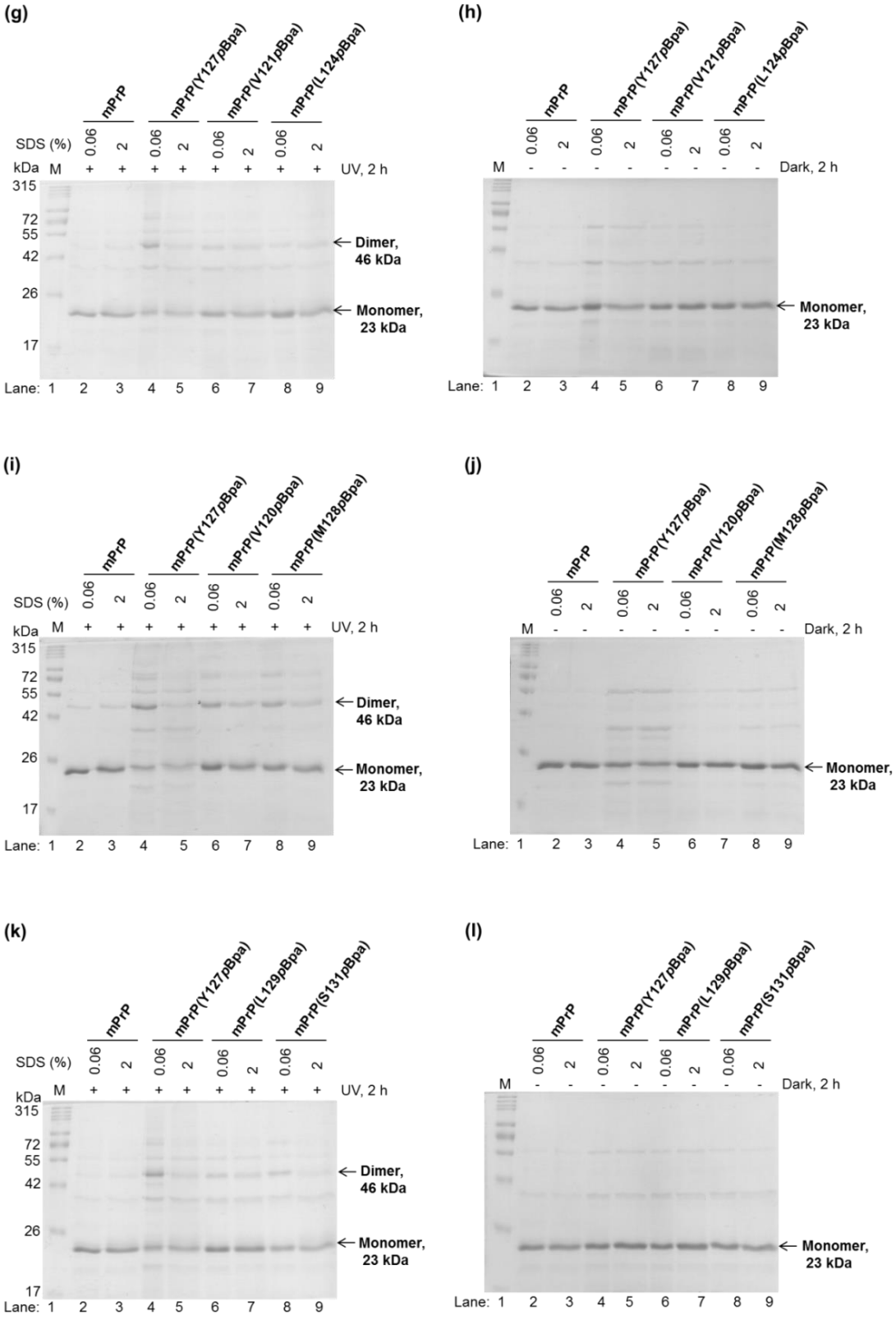

Figure IV-5. Photocrosslinking at dimer- or monomer-favoring conditions of untagged prion protein mutants with site specifically inserted *p*Bpa at various positions along the sequence. Representative gel pictures of wild type and of the additional *p*Bpa-mutant prion proteins were used in calculations of the percentage of crosslinked dimers presented on Figure 14. Proteins are irradiated at 365 nm (UV, 2 h) or kept at dark (Dark, 2 h) at dimer (0.06%)

and monomer (2%) favoring SDS conditions. In each experiment the wild type and the 127*p*Bpa positional mutant is present as controls. The bands corresponding to the monomeric proteins (23 kDa) and the dimers (46 kDa) are marked by arrows. Examined mutants are with *p*Bpa at positions: 107 **(a, b);** 111, 113 **(c, d);** 116, 119 **(e, f);** 121, 124 **(g, h);** 120, 128 **(i, j);** 129, 131 **(k, l).**

3. Additional gel pictures of the crosslinked samples used for evaluation of the hetero- and homodimer percentages in the study of the effect of G126V mutation on the dimerization of mPrP - a complementation to the Results, sections 4.2.1. and 4.2.2.

Figure IV-6: Crosslinking using the M128*p*Bpa mPrP variant:

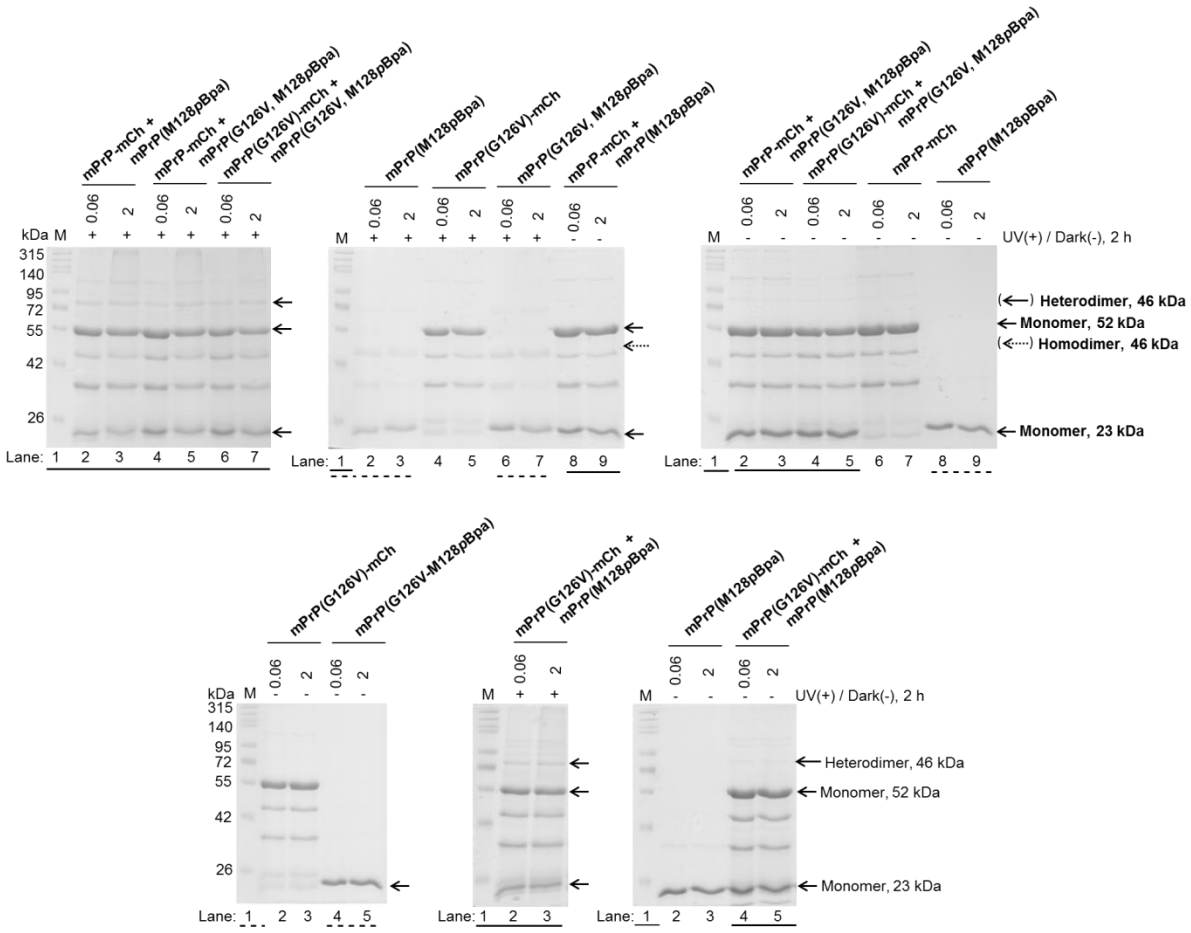

Figure IV-6. mPrP heterodimers and homodimers, as detected by crosslinking the M128*p*Bpa mPrP variant. Representative SDS-PAGE gel pictures of the photocrosslinked protein mixtures (lanes underlined by solid black lines) or single proteins (lanes underlined by dashed lines) of various mPrP ("UV irradiated", + UV) and their control, non-irradiated ("Non-irradiated controls", Dark) counterparts. *p*Bpa is present in the untagged mPrP (without mCherry) constructs with or without possessing a G126V mutation. The gels were

used in calculations of the percent heterodimer presented on Figure 18 and percent homodimer on Figure 20, corresponding to the use of mPrP(M128*p*Bpa) variant. The protein mixtures or single variants are in presence of either 0.06% or 2% SDS in order to promote dimerization in the first case and to assess the background non-specific association of the proteins in the latter case, respectively. The expected positions of the monomers (untagged mPrP and mPrP-mCh), heterodimers and homodimers are indicated on the figure by arrows. M: molecular weight marker.

Figure IV-7: Crosslinking using the S131*p*Bpa mPrP variant:

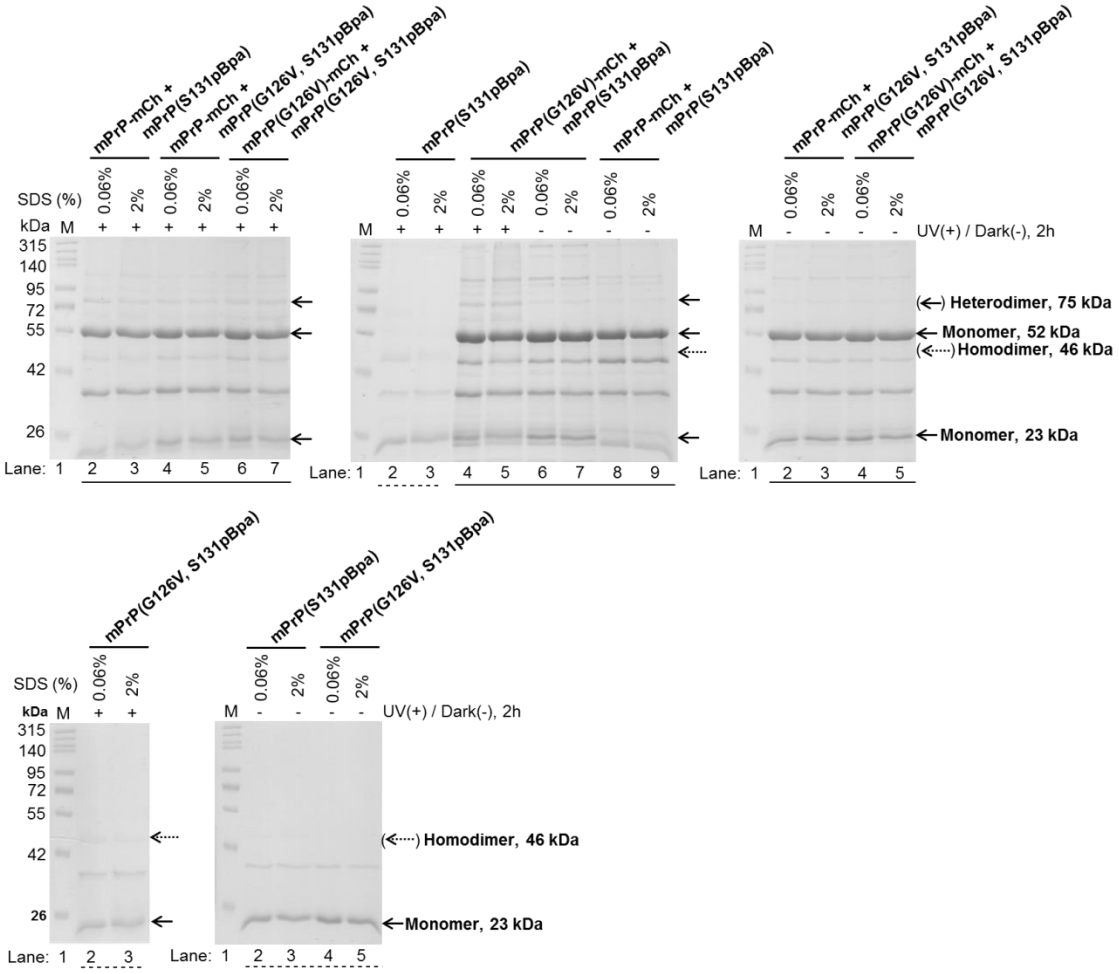

Figure IV-7. mPrP heterodimers and homodimers, as detected by crosslinking the S131*p*Bpa mPrP variant. Representative SDS-PAGE gel pictures of the photocrosslinked protein mixtures (lanes underlined by solid black lines) or single proteins (lanes underlined by dashed lines) of various mPrP ("UV irradiated", + UV) and their control, non-irradiated ("Non-irradiated controls", Dark) counterparts. *p*Bpa is present in the untagged mPrP (without mCherry) constructs with or without possessing a G126V mutation. The gels were used in calculations of the percent heterodimer presented on Figure 18 and percent homodimer on Figure 20, corresponding to the use of mPrP(S131*p*Bpa) variant.

Figure IV-8: Uncropped images of the gels presented on Figures 17b, 19a and b:

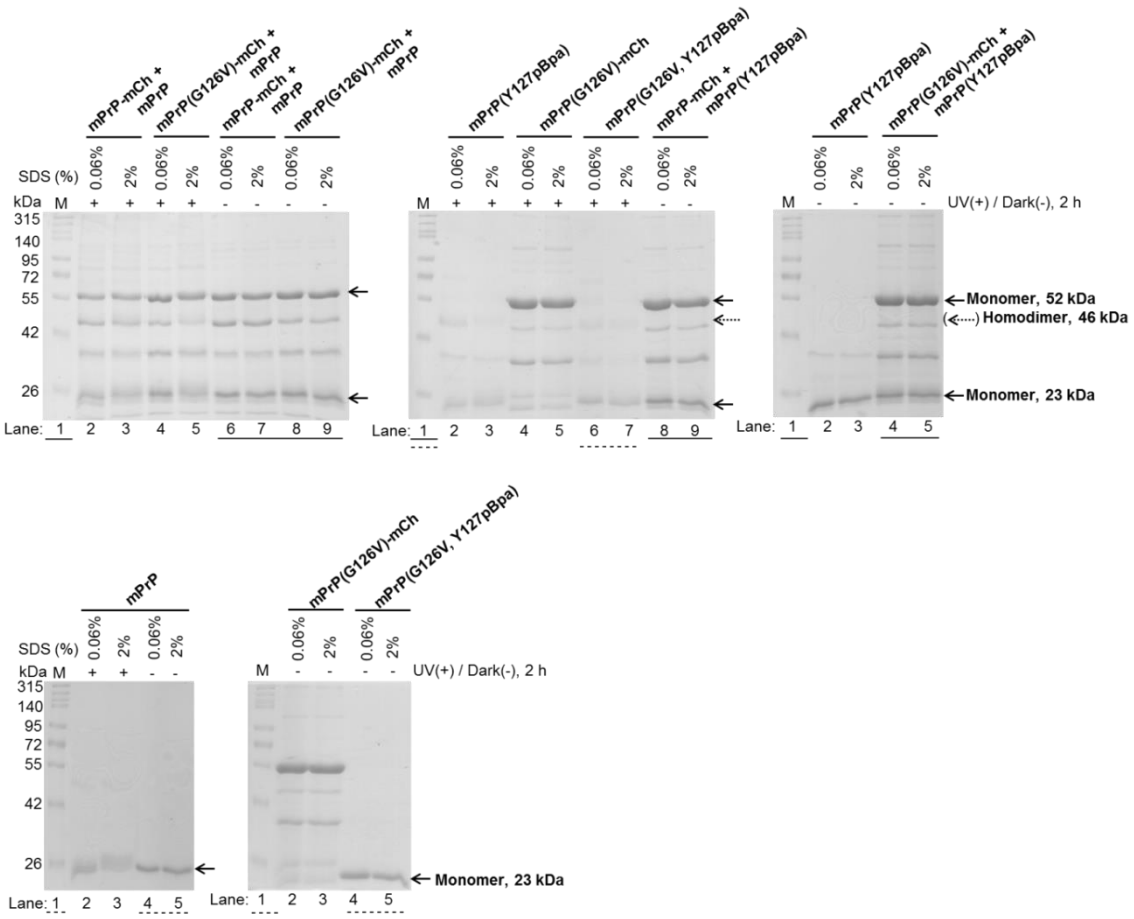

Figure IV-8. Uncropped images of the representative gels of mPrP heterodimerization and homodimerization experiments. The lanes underlined by solid lines are presented as cropped images on Figure 17b, showing the non-irradiated samples in the heterodimerization experiment. The lanes that are underlined by dashed lines were used as cropped images on Figure 19a and b, to indicate homodimerization and their non-irradiated controls, respectively. The positions of the monomeric and homodimeric proteins are indicated by arrows.